Discovery and analysis of novel microRNAs playing a role in cancer dormancy.

by

Sahra Aras

A Dissertation Submitted to the
Graduate School of Health Sciences
in Partial Fulfillment of the Requirements for
the Degree of

Master of Science

in

(Cellular and Molecular Medicine)

August, 2022

Discovery and analysis of novel microRNAs playing a role in cancer dormancy.

Koç University

Graduate School of Health Sciences

This is to certify that I have examined this copy of a master's thesis by

Sahra Aras

and have found that it is complete and satisfactory in all respects,
and that any and all revisions required by the final
examining committee have been made.

Committee Members:

Prof. Devrim Gözüaçık

Assoc. Prof. Tunahan Çakır

Assoc. Prof. Özlem Kutlu

Assoc. Prof. Gözde Korkmaz

Date: 12.08.2022

To Zeynep and my family

ABSTRACT

Discovery and analysis of novel microRNAs playing a role in cancer dormancy.

Sahra Aras

Master of Science in Cellular and Molecular Medicine

August 2022

Recurrence after cancer treatment accounts for most cancer-related deaths. Disseminated tumor cells can settle in tissues and organs in a quiescence-like state for years or even decades. These quiescent cells are called dormant cells. Dormant cells, when reactivated, form more aggressive and treatment-resistant tumors. Therefore, study of cancer dormancy is very important from a basic science and a clinical perspective. MicroRNAs (miRNAs) are non-coding RNAs playing crucial roles in gene expression regulation. miRNAs generally interact with the 3' untranslated region (UTR) of the gene their target mRNAs, and lead to their degradation or block their translation (3,4). The role of microRNAs in dormant cancer cell behavior is not clear. In our lab, a Matrigel 3D cell culture system was optimized as an *in vitro* model of cancer dormancy. To discover new players in cancer dormancy using this system, miRNA Sequencing (miR-Seq), RNA Sequencing (RNA-Seq) and proteomics analyses were performed. Comparison of miR-Seq results of actively dividing cancer cells with their dormant counterparts revealed a list of dormancy-associated novel miRNAs. As a result of the genetic manipulation of two novel dormancy microRNAs in cancer cell lines, we demonstrated the importance of the miRNAs for dormant cell behavior. Direct gene targets of the miRNAs playing a role in the dormant phenotype were discovered. Study of dormancy-associated miRNAs will allow a better understanding of molecular pathways of cancer dormancy and contribute to the development of new diagnosis, follow-up, and treatment strategies.

ÖZETÇE

Kanser dormansisinde rol oynayan yeni mikroRNA'ların keşfi ve analizi.

Sahra Aras

Hücresel ve Moleküler Tıp, Yüksek Lisans

Ağustos 2022

Kanser tedavisi sonrası nüks, kansere bağlı ölümlerin çoğundan sorumludur. Yayılmış tümör hücreleri, doku ve organlara yıllarca hatta on yıllar boyunca durgunluk benzeri bir durumda yerleşebilir. Bu sessiz hücrelere uyuyan (dormant) hücreler denir. Dormant hücreler, yeniden aktive edildiğinde daha agresif ve tedaviye dirençli tümörler oluşturur. Bu nedenle, kanser dormansisinin incelenmesi, temel bilim ve klinik açıdan çok önemlidir. MikroRNA'lar (miRNA'lar), gen ekspresyonunun düzenlenmesinde önemli roller oynayan kodlanmayan RNA'lardır. miRNA'lar genellikle hedef mRNA'ları olan genin 3' çevrilmemiş bölgesi (UTR) ile etkileşir ve bozulmalarına yol açar veya çevirilerini bloke eder. Dormant kanser hücresi davranışında mikroRNA'ların rolü henüz yeterince anlaşılmamıştır. Laboratuvarımızda, bir Matrigel 3D hücre kültürü sistemi kullanılarak, in vitro kanser dormansi modeli olarak optimize edildi. Bu sistemi kullanarak kanser dormansisinde yeni oyuncuları keşfetmek için miRNA Dizileme (miR-Seq), RNA Dizileme (RNA-Seq) ve proteomik analizleri yapıldı. Aktif olarak bölünen kanser hücrelerinin miR-Seq sonuçlarının uykudaki muadilleriyle karşılaştırılması, uyku hali ile ilişkili yeni miRNA'ların bir listesini ortaya çıkardı. Kanser hücre dizilerinde iki yeni dormansi mikroRNA'nın genetik manipülasyonunun bir sonucu olarak, miRNA'ların uyuyan hücre davranışı için önemini gösterdik. Uyuyan fenotipte rol oynayan miRNA'ların doğrudan gen hedefleri keşfedildi. Dormansi ile ilişkili miRNA'ların incelenmesi, kanser dormansinin moleküler yolaklarının daha iyi anlaşılmasını sağlayacak ve yeni tanı, takip ve tedavi stratejilerinin geliştirilmesine katkıda bulunacaktır.

AKNOWLEDGEMENTS

I would like to express my sincere appreciation to my supervisor Prof. Dr. Devrim GÖZÜAÇIK for his constant guidance, encouragement, and support during the period of my master's studies. Thanks to my supervisor, I have made great progress in my academic career, and I would like to thank him for educating me as a good scientist. He made me a person who realizes the importance of perseverance and he taught me how can handle challenges in working life.

I would like to express my gratitude to my dear friend Dr. Yunus AKKOÇ for giving me valuable advice and supporting me whenever I needed it. It cannot be imagined how much he influences me in a good way during my master's studies. Also, thanks him for his contribution to this work. His knowledge helped me become a patient and motivated person and always supported me both technically and emotionally.

I would like to express my sincere thanks to my friends and my colleagues Sıla TURGUT and Ayse Seray GUZEL. I always felt their support and love. They made my whole time much more appealing in the lab and in my life. I want to express all my thanks to current and former my lab mates, especially thanks Nesibe Peker for her contributions and support to this study. We were all passengers on the same ship and doing a good job all together.

I would like to express my sincere respect, love and gratitude to my dear parents, and my brother who have provided all kinds of support throughout my entire life and always stood behind me and made me feel their endless love and trust. I also would like to thank my sisters from another mothers, Ceren AVCILAR and Ayşenur MERAL, who have always been with me whenever I need and continue to support and love me. My words cannot be enough to express how grateful I am for the enjoyable times we shared in my life.

I would like to thank Zeynep ALPSOY for being included in my life and coloring it. She was a source of joy and always full of life. She was always an inspiration to the people around her. She has become a star in the sky and still she is shining perfectly.

I would like to thank TUBITAK for supporting my master's studies with a scholarship. This project is funded by TUBITAK-1003-Scientific and Technological Research Projects Funding Program, Project No: 216S489.

I also would like to express my thankfulness to Koc University Research Center for Translational Medicine (KUTTAM) for financially supporting my studies, and for being my second home at the Koc University Hospital during this period.

TABLE OF CONTENTS

LIST OF TABLES

LIST OF FIGURES

ABBREVIATIONS

5-FU	5-fluorouracil
AMPK	AMP-activated protein kinase
ATG	Autophagy-related genes
BMP	Bone morphogenetic proteins
BMPR2	BMP receptor 2
CDK	Cyclin-Dependent Kinase
CRISPR	Clustered Regularly Interspaced Palindromic Repeats
CTC	Circulating tumor cell
CTL	Cytotoxic T lymphocytes
DMEM	Dulbecco's modified Eagle's medium
DTC	Disseminated tumor cells,
ECM	Extracellular matrix
EMT	Epithelial-mesenchymal transition
FAK	Focal adhesion kinase
FBS	Fetal bovine serum
FPKMs	Fragments per kilobase per million mapped reads
GABARAP	γ-aminobutyric acid type A receptor-associated protein
GAPDH	Gyceraldehyde-3- phosphate dehydrogenase
GATE-16	Golgi-associated 16 kDa ATPase enhancer
GRNA	Guide RNA
HEK293T	Human embryonic kidney cells
HNSCC	Head and neck squamous cell carcinoma cell
ID1	DNA binding 1
LAMP2A	Lysosomal-associated membrane protein 2A receptor
LCC	Large cell carcinoma
MAP1LC3	Microtubule-associated protein 1 light chain 3
MAPK	Mitogen-activated kinase
MiRNA	Micro RNA
MMTV	Mouse mammary tumor virus

MRE	MiRNA response elements
MRNA	Messenger RNA
MTT	Dimethylthiazol
NR2F1	Nuclear Receptor Subfamily 2 Group F Member 1
NSCLC	Non-small cell lung cancer
PAM Sequence	Palindromic sequence-containing regions
PAS	Pre-autophagosomal structure
PE	Phosphatidylethanolamine
PFA	Paraformaldehyde
PI3K	Phosphoinositide 3-kinase
PI3P	Phosphatidyl inositol triphosphate
Plat-A	Platinum-A
RA	Retinoic acid
RGN	Regucalsin
RISC	RNA-induced silencing complex
SCF	The SKP1, CUL1, F-box protein
SCLC	Small cell lung cancer
uPAR	Urokinase plasminogen activator receptor
VPS34	Vesicular protein sortin 34

Chapter 1:
INTRODUCTION

1.1 Hallmarks of Cancer

Cancer is still one of the biggest causes of human death today. Although early diagnosis significantly increases the chance of treatment, the findings obtained in advanced technology and cancer studies are insufficient to resolve the disease completely. Various external factors such as smoking, air pollution, obesity, and cancer-causing infections increase cancer incidence. The first application in cancer treatments is usually surgical removal of the primary tumor and chemotherapy and/or radiotherapy. Many recent studies have shown that immunotherapy and targeted therapy methods are effectively in distinct patient groups. Thanks to advances in high-resolution diagnostic tools, tumor ablation techniques, drug combinations, and targeted therapies, 5-year survival rates for some types of cancer have been greatly improved. Despite all technological advances, survival rates in patients with advanced cancer are still low. Drug resistance can be counted as the leading cause of the spread of cancer cells to distant tissues and organs and the formation of metastatic lesions. In other words, metastasis is among the leading causes of cancer-related deaths.

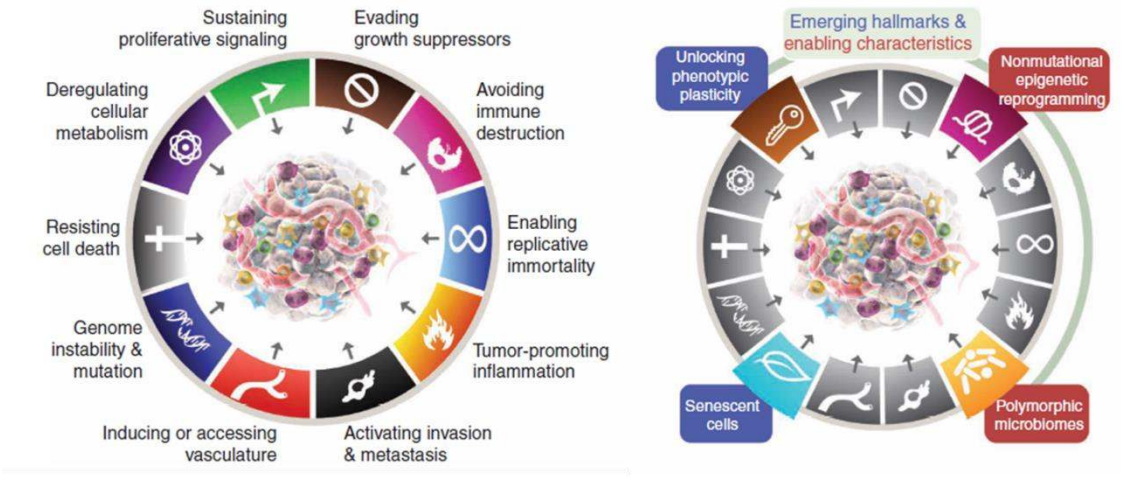

Figure 1:1 Hallmarks of Cancer.

(Hanahan 2022)

Identifying the mechanisms involved in the transformation of normal cells into malignant cells is helpful in understanding the formation and progression of cancer and why it is one of the leading causes of human death. Unlike normal cells, cancer cells produce growth signals on their own, reducing or eliminating their dependence on external stimuli. This is called self-sufficiency in growth signals. In addition, insensitivity to growth-related suppressive signals occurs in cancer cells. Antiproliferative signals are necessary to maintain homeostasis in normal tissue. Neoplastic cells overexpress growth-stimulating factors, disrupting the mechanisms of the cell cycle. Thus, they can avoid anti-proliferative signals (Hanahan and Weinberg 2000)

Programmed cell death allows cancer cells to continue to increase in number due to their ability to avoid apoptosis. Normal cells have limited growth potential, but this changes in cancer cells. This growth restriction, which is governed by telomere shortening during cell division, is lost in cancer cells. Telomerase enzyme activity is high in cancer cells so that they can have the potential to divide continuously (Hanahan and Weinberg 2000). In addition, epigenetic modifications can cause normal cells to turn into malignant cells by reprogramming the gene network.

Due to the continuous division of cells, the increased need for nutrients and oxygen is provided by the formation of new blood vessels (Hanahan and Weinberg 2000). Cancer cells release pro-angiogenic signals, triggering the formation of new blood vessels. Moreover, metastasis and invasion of cancer cells to distant organs account for the vast majority of cancer-related deaths (Hanahan and Weinberg 2000). Therefore, invasion into tissues, localization and continued tumor formation in distant organs are one of the hallmarks of cancer. Changes that promote the epithelial-mesenchymal transition (EMT) greatly contribute to the metastases of cancer cells. The integrity of normal tissues in the body is tightly regulated by cell-cell and cell-matrix interactions. During the transition from a normal cell to a cancer cell, epithelial cells lose critical epithelial markers (e.g., E-cadherin, α-catenin) and may acquire mesenchymal cell-like properties by increasing the expression of mesenchymal markers (e.g., N-cadherin and vimentin) (Dongre and Weinberg 2019). EMT is regulated by transcriptional programs (e.g., ZEB1/2, Snail, etc.) (Korpal et al. 2008; Nieto 2002). Thus, remodeling of epithelial junctions and cytoskeleton increases the motility and invasive character of cancer cells (Chaffer et al. 2016). Motile and invasive, cancer cells penetrate the tissue extracellular matrix (ECM) and spread through the blood and lymph vessels to the lymph nodes and secondary sites.

In metastatic sites, however, the establishment of this cell and metastatic growth requires the reversal of this process, that is, the mesenchymal-epithelial transition (MET).

The loss of mechanisms necessary to maintain genome integrity also allows cancer cells to reach their biological endpoint. (Hanahan and Weinberg 2011). Moreover, while normal cells use oxygen to generate energy from glucose, cancer cells can switch to aerobic glycolysis even in the presence of oxygen (Hanahan and Weinberg 2011). Cancer cells survive by avoiding cytotoxic/T cells, natural killer cells. It has been reported that certain inflammatory cells have a stimulating effect on tumor formation. It is thought that inflammation may cause additional mutations in cancer cells and cause the release of various molecules such as reactive oxygen species.

Avoidance of immune destruction is one of the distinguishing features during cancer formation (Hanahan and Weinberg 2011). Increasing cancer studies emphasize the importance of phenotypic plasticity and impaired differentiation in cancer cells in cancer development (Hanahan 2022). Terminal differentiation is associated with a permanent division arrest in normal cells. It appears to unlock the mechanism known as phenotypic plasticity so that malignant cells can escape this differentiation and continue to grow. This is essentially the mechanism by which normal cells activate to repair and regenerate tissues. Thus, cells can become inclined to proliferate. The review, also suggested that some of the various microorganisms found in the body may have protective or detrimental effects on the progression of cancer development and response to treatment (Hanahan 2022).

The process of transformation of normal cells to malignant cells requires a sequential and complex chain of events. In summary, this sequence of events includes cancer cells gaining the ability to migrate and invade due to genetic and epigenetic modifications, then pass into the circulation, survive in blood vessels and lymphatics, exit the circulation, and adapt to the new environment (Figure 1.1).

1.2 Cancer Dormancy: A New Hallmark of Cancer

Despite the development of cancer therapy over the years, cancer recurrence is still a critical problem for many cancer patients. The prolonged asymptomatic period before relapse after treatment is clinically defined as cancer dormancy. In other words, it is the state in which the disseminated cells/clusters of cells (disseminated tumor cells, DTC)

can remain in a state where death and proliferation are balanced (Holmgren, O'reilly, and Folkman 1995; Karrison, Ferguson, and Meier 1999). Recurrence of cancer usually has more aggressive and metastatic features. DTCs continue to evolve in new tumor niches and often acquire different genetic and epigenetic signatures from the primary tumor. Although the aggressive proliferation of DTCs can result in metastasis. This process has been reported to take months or even years (Hüsemann et al. 2008; Magbanua et al. 2013; Pixberg et al. 2017; Schardt et al. 2005). Studies have revealed that subgroups of pre-cancer cells, namely cancer stem cells, are responsible for the disease's evolution, progression and metastasis in many different tumor types (Bennett et al. 1978; Hager et al. 1981).

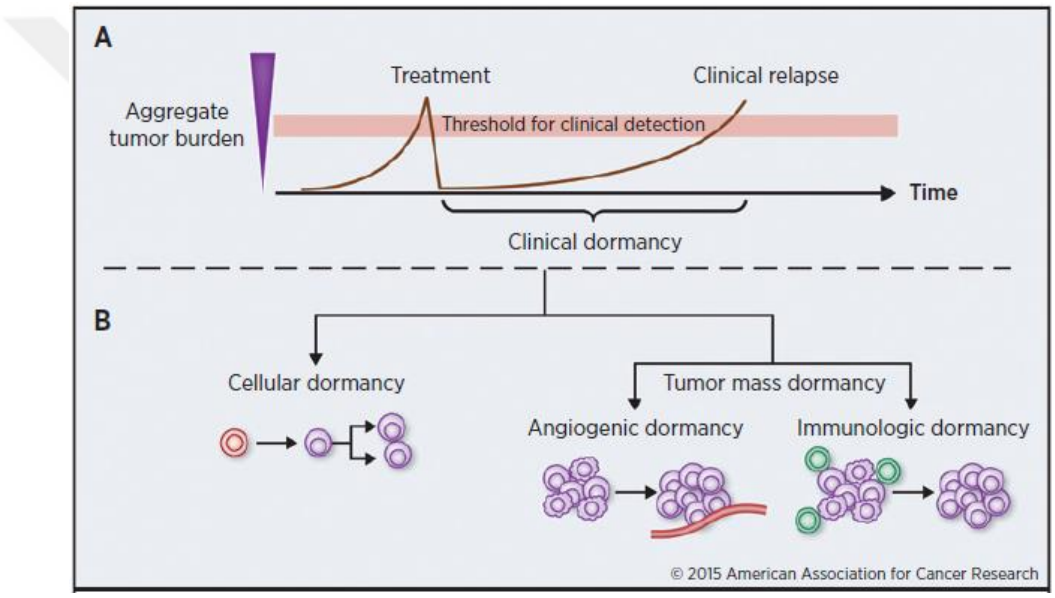

Figure 1:2 Schematic description of cancer dormancy.

Schematic description of cancer dormancy. Cancer dormancy is separated into tumor mass dormancy and cellular dormancy. In tumor mass dormancy, the tumor growth is suppressed by angiogenic factors or the immune environment. In the cellular dormancy model, one or more cells go into dormancy independent of the primary tumor. (Yeh and Ramaswamy 2015).

Dormant cells (at least some of them) can reactivate and form metastatic lesions. According to the literature, it has been observed that recurrent tumors are associated with drug resistance and aggressive behavior. Many patients with the relapse of disease show a very poor prognosis (Kobayashi et al. 2007).Therefore, cancer dormancy, as a mechanism that plays an important role in tumor recurrence, has become the focus of attention in recent years. Cancer dormancy is classified under two main headings. These are tumor mass dormancy and cellular dormancy (Figure 1.2).

1.2.1 Tumor Mass Dormancy

Tumor mass dormancy is the state of maintaining the tumor mass at a certain size by keeping the death and proliferation of cancer cells in balance. Clinically no growth is observed in the tumor mass, while some cancer cells in the tumor tissue continue to divide, some cells die on the other hand. Therefore, no enlargement is observed in the tumor mass. The balance in the growth of the tumor mass is explained by two different mechanisms: *Angiogenic Dormancy* and *Immunogenic Dormancy.*

1.2.2 Angiogenic Dormancy

The formation of new blood vessels necessary for the growth of tumors was introduced in the 1970s. As a result of many studies, the mechanism underlying angiogenesis has been clarified. When the tumor expands beyond 1-2 mm, hypoxia is induced by the increased expression of hypoxia-stimulating factor-1 (Hif-1) in the cells due to the lack of oxygen in the environment. Pro-angiogenic factors are released by the tumor. These factors trigger the formation of new vascular beds and the need for nutrients and oxygen is met (Lee, Jeong, and Jang 2021; Naumov, Akslen, and Folkman 2006; Semenza 2003). Before elucidating this regulation, an explanatory model of the clinical undetectability of angiogenic changes associated with cancer formation for many years was presented. Judah Folkman, one of the first pioneers of the model, suggested that small tumors are kept under control by preventing the supply of new blood vessels, namely angiogenic dormancy. (Folkman and Kalluri 2004). It has been shown that stained (with endothelial cell markers) small or large tumors have well-organized vascular structures in large tumors, while small tumors have few small vessels (Naumov, Bender, et al. 2006).This idea has been supported by the evolution of growing tumor masses using mouse models of angiogenic dormancy (Aguirre-Ghiso 2007; Giuriato et al. 2006; Indraccolo et al. 2006; Naumov, Akslen, et al. 2006).

1.2.3 Immunogenic Dormancy

The immune system's role in cancer development has been extensively studied recently. Its role in cancer development and progression is a three-step process. The immune system first recognizes cancer cells and eliminates, the stage is "elimination". Next is the "equilibrium" stage, where the immune system takes control. At this stage,

the growth of cancer cells cannot be eliminated entirely, only controlled. The third is "escape" at this stage cancer cells escape from immune surveillance. In other words, the message: "there's nothing wrong with this area." is given from the tumor to immune cells through the signals. Therefore, the immune system becomes insensitive to the tumor. (Dunn, Old, and Schreiber 2004; Teng et al. 2008).

Mouse studies on the elucidation of immunological dormancy have demonstrated that innate and adaptive immunity can control a growing tumor (Farrar et al. 1999; Koebel et al. 2007; Matsuzawa et al. 1991; Weinhold, Goldstein, and Frederick Wheelock 1979). In a case study, two allograft recipients who received the presumed healthy kidney of an organ donor who had been treated for melanoma 23 years ago, developed metastatic melanoma 1-2 years after transplantation (MacKie, Reid, and Junor 2003). None of the patients with declining cancer signs and symptoms and detectable anti-tumor Cytotoxic T lymphocytes (CTLs) had a recurrence up to 74 months. On the other hand, 7 of 8 patients whose antitumor CTLs undetected recurred within 2-17 months after treatment.

In conclusion, it can be said that the recurrence rate of the disease is higher in such patients when the immune system is compromised (Uhr and Pantel 2011). The regulation of the immune system at the cellular level is still unknown, as it may play both inducing and reducing roles in tumor development (Shiao et al. 2011).

1.2.4 Cellular Dormancy

Cellular dormancy is one of the most important issues that has not yet been fully elucidated. In the cellular dormant state, cells stop at a particular stage in the cell cycle, generally at G0/G1, and regulate all their signaling pathways and metabolisms to adapt to the state of dormancy. This state of dormancy is a reversible event. Dormant cells can re-enter the cell cycle and begin to divide again. It is an interesting question: if they keep their ability to proliferate, or not?

The mechanisms underlying the maintenance of dormancy state and the re-proliferation of the dormant cells after years, maybe decades, are still unclear today. In this thesis, cellular dormancy was investigated. The lack of knowledge in the literature makes the cellular dormancy more exciting and valuable. Technical inadequacies still limit knowledge of this dynamic process, and it is still challenging to demonstrate and characterize the existence of dormant cancer cells in vivo and in clinic.

In vivo Ki-67 or TUNEL staining can provide limited information. Moreover, the growth kinetics of a single cell can be studied in experimental models through live-cell imaging. In one study, in vivo video microscopy revealed that dormant cancer cells have higher survival rates. Metastasis was detected in mouse models 11 weeks after injection (Naumov et al. 2002). It has also been suggested that dormant cancer cells may resist treatment. It was determined that there was an increasing of dormant cells after chemotherapy in tumor tissue samples of patients with breast cancer after neoadjuvant chemotherapy compared to pre-treatment. Although it is not yet known whether it is induced by chemotherapy, it has been suggested that there is a direct relationship with the treatment of the disease. As a result of the isolation and characterization of tumor cells from the blood of patients, it has been shown that these cells have a limited proliferative capacity (Müller et al. 2005; Pantel, Brakenhoff, and Brandt 2008; Solakoglu et al. 2002). In another study, in the analysis performed during chemotherapy in patients with initially circulating tumor cell (CTC)-negative metastatic breast cancer; It was thought that KI-67-negative CTCs emerged. These KI-67-negative cells circulating in the blood might be resistant to treatment. In other words, the presence of KI-67 negative CTCs in these patients was associated with disease progression and increased tumor markers (Müller et al. 2005).

Detection and characterization of dormant cells or micro metastases clinically is still difficult. Limitations on detection of the dormant cells in patients complicate clinical evaluations while at the same time limiting the investigation of underlying mechanisms. Therefore, establishing in vitro models is important in revealing the fundamental mechanisms of dormancy. Moreover, we consider that this complex phenomenon plays a critical role in cancer development and disease progression and that new *in vitro/in vivo* cancer dormancy models can be established by revealing the metabolic regulations that occur at the cellular level.

1.2.5 Cellular Dormancy at Molecular Level

Cellular dormancy is defined by the arresting of cancer cell proliferation. This non-proliferating but not dying state can continue for months or even years. No matter how long the dormant state is, at least some cancer cells regain their ability to reactivate and proliferate (Hadfield 1954; Sosa, Bragado, and Aguirre-Ghiso 2014; Yeh and

Ramaswamy 2015). Therefore, cellular dormancy is defined as a reversible mechanism. It has been suggested that dormant cells are usually arrested in the G0-G1 phase of the cell cycle. Therefore, these cells in a cellular dormant state lack proliferation (e.g., Ki67), apoptosis (e.g., active caspases), and senescence (e.g., beta-galactosidase) markers (Darzynkiewicz, Juan, and Srour 2004; Marlow et al. 2013; Spiliotaki et al. 2014).

Many molecules have detected changes in dormant cells that regulate the cell cycle. For instance, cyclin-dependent kinase (CDK) inhibitors p27Kip1 and p21Cip1/WAF1 have been shown to control the non-proliferative state in hematopoietic stem cells dormancy (Zou et al. 2011). In another example, post-transcriptional regulation of Skp2, a component of the SKP1, CUL1, F-box protein (SCF) complex that includes p27Kip1 and p21Cip1/WAF1, has been reported to cause lymphoma cells to adhere to bone marrow stromal cells and enter a dormant state (Lwin et al. 2007). It has been reported that another factor responsible for the regulation of cellular dormancy state is the DREAM protein complex. The complex consists of p130 or p107 (Retinoblastoma-like pocket proteins), MuvB and E2F proteins. MuvB, a DREAM complex component, has been reported as a key molecule in the transcriptional regulation of cell cycle genes (Sadasivam and DeCaprio 2013). High levels of p130 in dormant cells have been shown to facilitate DREAM complex formation and regulate its transcriptional effects (Sadasivam and DeCaprio 2013; Schmit et al. 2007). In addition, high p107 expression levels were only observed in proliferative cells. Some regulatory kinases (eg, DYRK1A and DYRK1B) have been shown to phosphorylate LIN52, a subunit of MuvB, and regulate the DREAM complex during the transition to non-proliferative dormancy (Litovchick et al. 2011). In addition, these kinases have been reported to stabilize p27Kip1, inducing cyclin D conversion and further contributing to the non-proliferative state (Besson et al. 2006; Deng, Ewton, and Friedman 2009)

Mitogen-activated kinase (MAPK) pathway is another pathway thought to play a central role in regulating the dormancy state. Many factors associated with dormancy and their receptors have been reported to maintain cellular dormancy by affecting the balance between proliferative ERK1/2 and non-proliferative p38 MAPK. In different cancer studies, including breast, prostate and melanoma cells, it has been shown that the contribution of the p38 pathway to cancer dormancy is supported by cell cycle arrest (Adam et al. 2009; Aguirre-Ghiso et al. 2003; Khaled et al. 2005). For instance, p38 kinases stimulated by TGF-β2/TGFβRIII have been reported to promote head and neck

squamous cell carcinoma cell (HNSCC) dormancy in the bone marrow (Bragado et al. 2013)In another type of cancer TGF-β2 secreted from osteoblasts in the bone microenvironment as a paracrine factor has been found to contribute to prostate cancer dormancy through p38 activation (Yu-Lee et al. 2018). It has also been shown that dormant cells secrete high levels of TGF-β2, forming an autocrine signalling cycle in regulating dormancy. Supporting these results, TGF-β2 levels were low in proliferating cells (Yumoto et al. 2016).

The urokinase plasminogen activator receptor (uPAR) pathway has been identified as another pathway associated with cellular dormancy. In HNSCC, the status of uPAR is directly related to the cells' capacity for dormancy in vivo. In this tumor type, the interaction of uPAR with α5β1 integrin suppresses the activation of p38, resulting in the formation of insoluble fibronectin fibrils. On the other hand, decreased uPAR levels were found to be associated with a decrease in the activity of the ERK1/2 MAPK pathway (Aguirre-Ghiso et al. 2001). Furthermore, low expression of uPAR has been shown to facilitate in vivo dormancy state by inhibiting focal adhesion kinase (FAK) phosphorylation and subsequent Src activity (Aguirre Ghiso 2002; Litchfield et al. 2012).The mechanisms involved in FAK and Src have also been studied in the breast cancer dormant state, in addition to the HNSCC model. Induction of Src after CXCL2/CXCR4 signalling is associated with prolonged survival of DTC in the bone marrow microenvironment via the phosphoinositide 3-kinase (PI3K)/AKT pathway. It has been reported that this cellular dormancy induced by Src is specific to the bone marrow, and the decrease in Src expression has no effect on lung metastases (Gao et al. 2019).

Bone morphogenetic proteins (BMP) have been reported to regulate cellular dormancy through tumor-stroma interactions. Research on prostate cancer has revealed that BMP7 regulates the dormancy of prostate cancer cells by affecting the cancer stem cell population. It has been understood that this effect is due to the activation of dormancy-related signalling components such as p38, p21 and the metastasis suppressor NDRG1 following BMP receptor 2 (BMPR2) expression. Another study revealed that bidirectional communication between tumor cells and stroma is important for dormancy.

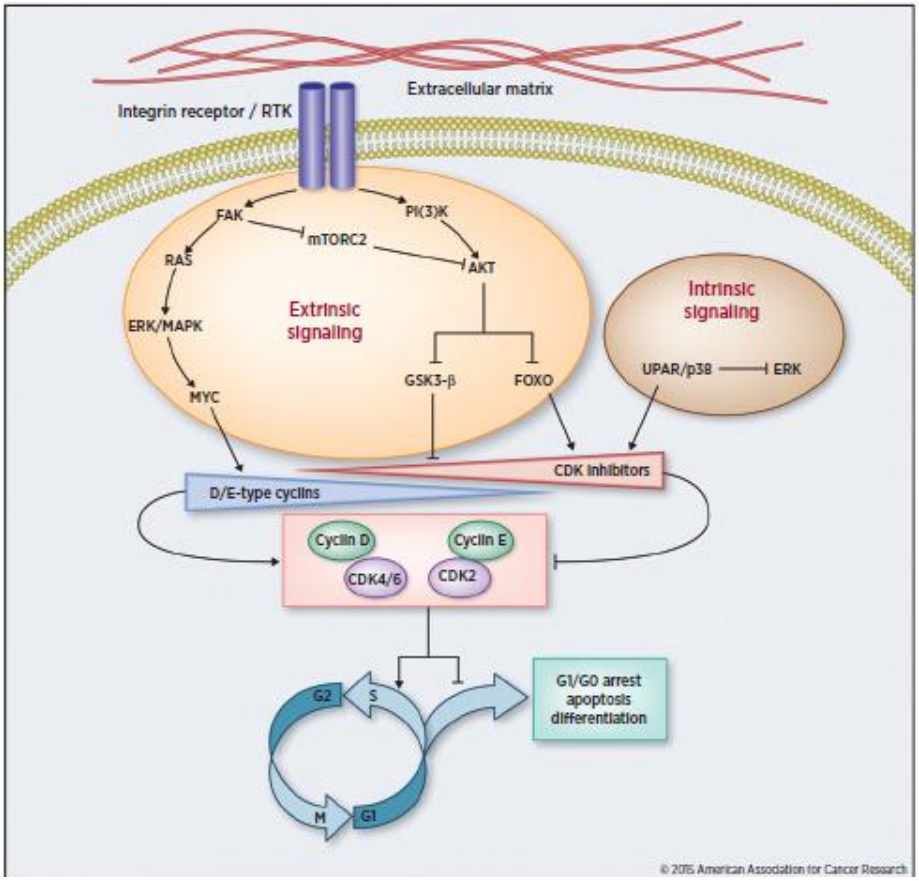

Figure 1:3 Some revealed cellular dormancy pathways.

Cellular dormancy is governed by both internal and external factors. Pathways such as RAS-ERK/MAPK, PI(3)K-AKT are directly related to the cell cycle. Integrins play a role in transmitting signals from the ECM into the cell. Signals from the ECM are critical in cellular dormancy. The uPAR/p38 pathway may play a role in the transition of the cell to dormancy through downregulation of the MAPK pathway associated with dormancy (Yeh and Ramaswamy 2015).

It has been reported that dormant prostate cancer cells secrete SPARC, a factor that contributes to maintaining the dormant phenotype by stimulating BMP7 expression in bone marrow stromal cells (Sharma et al. 2016). Another BMP protein, BMP4, has been studied in the context of breast cancer. High levels of BMP4 expression are associated with breast cancer cells entering a dormant state in the lung. Dormancy has been associated with the activation of ALK2/3 and SMAD1/5 signalling pathways (Holtzhausen et al. 2014). In the same system, DAND5, an extracellular BMP antagonist, has been shown to inhibit BMP4-assisted dormancy and promote cell proliferation (Gao et al. 2012).

Dormancy-associated signalling pathways have been reported to be involved in some gene regulatory programs. For instance, the transcription factor BHLHE41 is responsible for the p38-regulated sleep state in HNSCC (Adam et al. 2009) In another study, BHLHE41 and NR2F1 were identified as key factors promoting dormancy in ER-positive breast cancer in an in vivo xenograft mouse model (Kim et al. 2012). The importance of BHLHE41 in breast cancer dormancy was also demonstrated in a 3D bone endosteum model containing bone marrow-derived stromal cells and endothelial cells (McGrath et al. 2019). Nuclear Receptor Subfamily 2 Group F Member 1 (NR2F1) is a transcription factor belonging to the NR2F family of cancer-associated transcription factors (Litchfield et al. 2012). Dormant cancer cells have been shown to have high expression levels of NR2F1 compared to their proliferating counterparts (Gao et al. 2019; Sosa et al. 2015). In addition, elevated NR2F1 and TGF-β2 expression have been identified as a signature of dormancy in prostate cancer DTC (Sosa et al. 2015). It has been reported that the expression of SOX9, a gene regulated by p38, is directly controlled by NR2F1-binding sequences located in the promoter region. The dormancy-associated NR2F1-SOX9 axis is regulated by microenvironment-derived retinoic acid (RA) signalling and RARβ. In addition, it has been reported that NR2F1 triggers cell cycle arrest by regulating the expression of CXCL12 and its receptor CXCR4 in salivary adenoid cystic carcinoma cells (Gao et al. 2019).

Some receptor tyrosine kinases, including TYRO3, AXL, and MER, have been reported to play an essential role in dormancy in certain types of cancer. For example, stimulation of AXL or TYRO3 receptor kinases by GAS6 secreted from osteoblast cells contributed to the metastatic dormancy of prostate cancer cells in the bone marrow (Shiozawa et al. 2010; Taichman et al. 2013; Yumoto et al. 2016). In another study, the binding of GAS6 and MER in lymphoblastic leukemia cells was shown to induce dormancy (Shiozawa et al. 2010). It has been reported that the Wnt pathway is involved in controlling dormancy in a stimulus-dependent manner although it is generally thought to be a pathway involved in cancer spread and metastasis (Buczacki et al. 2018; Harper et al. 2016; Ren et al. 2019). For example, DKK1-dependent suppression of Wnt3a signalling has been shown to cause cell growth arrest and enter dormancy (Malladi et al. 2016). On the other hand, it was shown in another study that Wnt5a pathway stimulation may be responsible for the dormant state of prostate cancer cells (Ren et al. 2019).

The literature generally shows that several cytokines, growth factors, some signalling pathways, kinases, and transcription factors are associated with dormancy. In studies of cancer dormancy, breast cancer has mostly been used as a model (Ramamoorthi et al. 2022). However, studies in recent years have shown that cancer cells go into dormancy in models of head and neck cancers, ovarian, prostate, colon cancers, melanoma, osteosarcoma and blood cancers (Akkoc et al. 2021). As the knowledge about dormancy increases, it becomes clear that there are cancer-specific and metastatic target tissue-related pathways besides the main dormancy pathways.

1.2.6 Autophagy and Cancer Dormancy

Autophagy has different roles in different stages of cancer. Therefore, the relationship between them is complex. In the early stages of tumor development, autophagy suppresses cell division by preventing genomic instability, thus acting as a tumor suppressor (Gozuacik and Kimchi 2004). This suppressive effect in the early stages may change throughout the progression of the disease. The term autophagy comes from the ancient Greek autóphagos meaning "self-eating". Many of the findings at the molecular level have been made in yeast (Saccharomyces cerevisiae). 32 different autophagy-related genes (ATG) have been discovered in yeast by genetic screening. Autophagy responds to various environmental changes such as starvation and pathogen infections. Autophagy is constitutively active at a low level and contributes to intracellular homeostasis (Mizushima and Komatsu 2011). Autophagy plays a critical role in physiological events in the cell. Therefore, autophagy is associated with many diseases such as neurodegenerative diseases and cancer. (Galluzzi et al. 2017). Three different types of autophagy have been identified: macro-autophagy, micro-autophagy, and chaperone-mediated autophagy. In all three types of autophagy, Lysosome has a role in proteolytic degradation of cytosolic components.

Macroautophagy transports cytoplasmic cargos to the lysosome via a double membrane-bound vesicle called the autophagosome. As a result of the fusion of the cargo with the lysosome, an autolysosome is formed. It is the main autophagy mechanism in the cell. In micro-autophagy, cytosolic components are directly taken up into the lysosome. In chaperone-mediated autophagy, target proteins form complexes with chaperone proteins. This complex is recognized by the lysosomal-associated membrane

protein 2A receptor (LAMP-2A) located on the lysosome membrane and degradation occurs (Saftig, Beertsen, and Eskelinen 2008).

1.2.7 Mechanism of The Machinery of Autophagy

Autophagy/Macroautophagy is the fusion of autophagosomes with a bilayer membrane structure containing mainly cytoplasmic material with lysosomes (Weidberg, Shvets, and Elazar 2011). The formation of autophagosomes consists of three stages: initiation and phagophore formation; nucleation and engulfment of cytoplasmic material by the phagophore; elongation of the phagophore membrane and formation of the autophagosome (Cheng et al. 2013).

Phagophore membrane formation is known as pre-autophagosomal structure (PAS) in yeast. However, it is observed that phagophore membranes in mammalian cells are mainly in dynamic equilibrium with cytosolic membrane structures such as trans-Golgi and late endosomes and deplete the nuclear membrane under limited conditions (Axe et al. 2008; Mizushima 2007; Mizushima and Klionsky 2007).

The initiation phase of autophagosome formation begins with the assembly of the ULK1-Atg13 complex and beclin1-class III PI3K complexes. Atg1 kinase activity, which complexes with Atg13 and Atg17, is required for phagophore formation in yeast. This kinase regulates Atg9, a transmembrane protein that may function in lipid uptake into the expanding phagophore (Klionsky 2007; Kundu and Thompson 2005; Simonsen and Tooze 2009). This step is regulated by the TOR kinase, which phosphorylates Atg13, preventing its interaction with Atg1 (mammalian homologue Ulk-1). The TOR protein is a protein kinase that plays a critical role in the initiation of autophagy, which is sensitive to growth factors and nutrient availability (Díaz-Troya et al. 2008).

Insulin or similar growth factors can activate the PI3K-Akt pathway by preventing the formation of the TSC1/2 protein complex with mTOR activation (Cheng et al. 2013). Vesicular protein sortin 34 (VPS34), one of the classes III PI3Ks, is involved in various membrane sorting processes in the cell but is selectively involved in autophagy when complexed with other regulatory proteins such as Beclin-1 (Backer 2008) VPS34 is the PI3 kinase required for producing phosphatidyl inositol triphosphate (PI3P), which is required for phagophore elongation and attachment of other Atg proteins to the phagophore. The interaction of Beklin-1 with VPS34 increases its catalytic activity and increases the level of PI3P (Xie and Klionsky 2007).

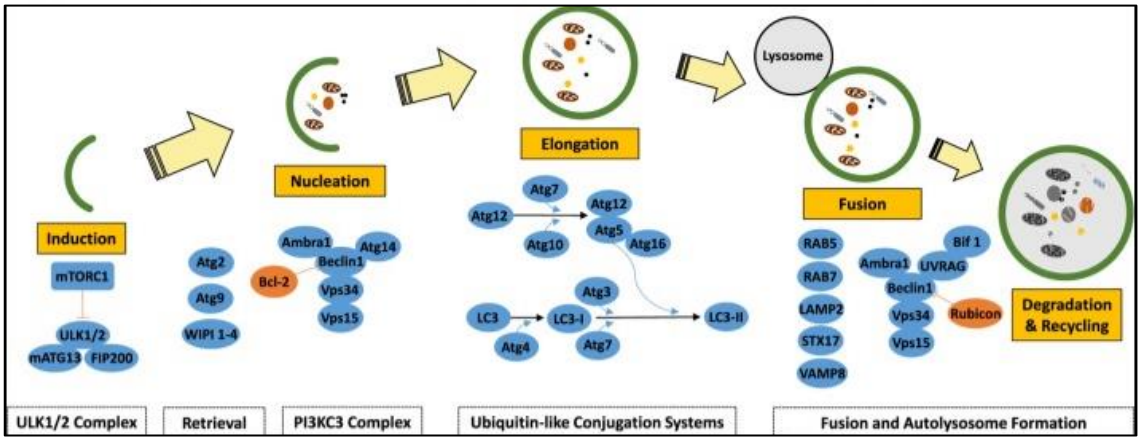

Figure 1:4 Schematic representation of autophagy mechanism

(Gozuacik et al. 2017).

Two conjugated systems are required for prolongation and closure of autophagosome formation. One of them is the processing of LC3 by Atg5-Atg12 conjugation. Atg7 binds to glycine at the carboxyl terminus of Atg12. Atg12 is activated by ATP hydrolysis and transferred to Atg10. The C-terminal glycine of Atg12 is covalently linked to the inner lysine residue of Atg5 to form the final conjugate. Atg5-Atg12 conjugates interact non-covalently with Atg16 (Mizushima, Noda, and Ohsumi 1999). The Atg12-Atg5-Atg16 complex fuses with phagophores and dissociates when autophagosome formation is complete (Yorimitsu and Klionsky 2005).

The second conjugation system includes the cleavage of Atg8 and its covalent modification with lipids (Ichimura et al. 2000). In yeast, the cysteine protease Atg4 cleaves near the glycine residue at the carboxyl terminus of Atg8. It is then activated by E1-like Atg7. The E2-like is transferred to Atg3 and finally conjugated with

phosphatidylethanolamine (PE). This complex is transported to the lysosome/vacuole and degraded along with the cargo.

Mammalian cells have at least three Atg8 homologues. These are Golgi-associated 16 kDa ATPase enhancer (GATE-16), γ-aminobutyric acid type A receptor-associated protein (GABARAP), and microtubule-associated protein 1 light chain 3 (MAP1LC3). All these proteins are modified by lipid in mammalian cells as in yeast (Kabeya et al. 2004).

LC3B undergoes proteolytic cleavage by Atg4 from the glycine residue at the carboxyl terminus to form LC3B-I upon induction of autophagy. It is activated by Atg7, dependent on ATP. Active LC3B-I is transferred to Atg3. PE is added to the carboxyl glycine to form LC3II-B. The inclusion of LC3B-II in the elongating phagophore depends on the Atg5-Atg12 complex. LC3B-II, located on the inner and outer surfaces of the autophagosome, plays a role in the hemifusion of the membranes and the selection of cargos to integrate for degradation (Barth, Glick, and Macleod 2010). Expression and processing of LC3 are increased during autophagy. Therefore, it is one of the crucial markers of autophagy (Barth et al. 2010). In addition, LC3-II remains in mature autophagosomes until fusion with lysosomes is complete. Thus, autophagosome fusion with lysosomes can be assessed by labelling LC3 and LAMP1 (Weidberg et al. 2011).

The p62/SQSTM1 complex, a ubiquitin binder, binds to LC3 via its specific sequence motif and degrades ubiquitinated proteins by the autophagic process to ensure their degradation in the lysosome (Pankiv et al. 2007). P62/SQSTM1 prominently accumulates when autophagy is suppressed. In contrast, p62/SQSTM1 is reduced when autophagy is activated; therefore, p62 is frequently used as an autophagic marker (Klionsky 2007). Protein-protein interactions with molecules associated with LC3 are thought to provide specificity in cargo selection. For example, GABARAP undergoing similar processes is localized with LC3-II in the autophagosome (Ichimura et al. 2000).

The next step in autophagy is fusion with the lysosome to form the autolysosome (Mizushima 2007). Several studies have shown that the autophagosome fusion with the early and late endosomes transports cargo before fusing with the lysosome. It also provides components of the membrane fusion machinery and lowers intravesicular pH before the delivery of lysosomal acid proteases (Eskelinen 2005).

In the autolysosome, which is formed by the autophagosome fusing with the lysosome, the cytoplasmic material is degraded by hydrolytic enzymes. Monomers

required for intracellular metabolism are given to the cytoplasm for use, while the remaining molecules are released by exocytosis to extracellular matrix (ECM) (Cheng et al. 2013).

1.2.8 Autophagy in the Context of Cancer Dormancy

Studies have shown that autophagy has important roles in cancer formation and progression, such as cell survival, drug resistance, and metastasis (Cianfanelli et al. 2015; Lazova et al. 2012; Mortensen et al. 2011; Mowers, Sharifi, and Macleod 2017; Yang et al. 2014). Therefore, autophagy is also thought to be important for cancer dormancy. However, the effects of autophagy on dormancy and the molecular mechanisms are still not well known today. Independent studies have shown that autophagy is active in non-proliferating dormant cancer cells and is in a reversible state. It has been shown that cells die when active autophagy is inhibited by chemical methods such as chloroquine (Gupta et al. 2010). In a study with gastrointestinal stromal tumor cells, it was shown that cell cycle arrest caused by the accumulation of the cell cycle inhibitor p27 causes a dormancy-like state in cells. It has been observed that autophagy is active under these conditions. Different studies revealed that the inhibition of autophagy causes the death of dormant cells. Accordingly, it shows that dormant cells are more sensitive to autophagy inhibition than proliferating cells (La Belle Flynn et al. 2019; Lu et al. 2008; Vera-Ramirez et al. 2018). DIRAS3 is a tumor suppressor whose expression level is decreased in breast and ovarian cancer. It has been demonstrated in a study that autophagy is induced when DIRAS3 is re-expressed in cancer cells (Lu et al. 2008). Interestingly, the expression of DIRAS3 in vivo has been shown to induce cancer cells into a dormancy-like phenotype. In a study in ovarian cancer xenografts, re-expression of DIRAS3 with an inducible system was found to induce autophagy and inhibit tumor growth, leading to dormancy. (O'Reilly et al. 1996; Washington et al. 2015). Studies have shown that autophagy is downregulated in proliferating metastatic cancer cells, but autophagy is required during the transition from dormant to re-proliferation (Aqbi et al. 2018; Vera-Ramirez et al. 2018).

Activation of autophagy is also regulated by AMP-activated protein kinase (AMPK). AMPK is an energy sensor for the cell; it detects the energy need of the cell according to the AMP/ATP ratio in the cell and provides various regulations according to the

environment under the conditions of the cell. AMPK activation causes activation of TSC2. TSC2 inhibits mTOR signaling by interfering with the activation of RHEB, which is necessary to activate mTORC1, thereby activating autophagy. A dormant cell has low ATP levels. Various studies have shown that AMPK is active in dormant cells. (Ornelas et al. 2016; Peart et al. 2015; Yu-Lee et al. 2018).

Lastly, when cancer cells are dormant, their mitochondria are targeted by autophagic degradation (La Belle Flynn et al. 2019; Vera-Ramirez et al. 2018). Therefore, activation of dormant autophagy may be associated with mitophagy and non-selective autophagy. However, its relationship with cancer dormancy, selective autophagy and mitophagy has not been sufficiently clarified.

1.2.9 Metastasis, Invasion and Cancer Dormancy

As mentioned in the previous sections, most cancer-related deaths are due to the spread of the disease to the whole body by passing to the metastatic stage (Luo et al. 2020). The metastatic process is multistage. Briefly, this process begins when the metastatic cancer cell enters the circulation (intravasation) due to invasion from the site of the primary tumor. CTCs can survive in the bloodstream. Moreover, these cells extravasate to the target organ and settle and proliferate to survive (Lambert, Pattabiraman, and Weinberg 2017). These cells are called DTC. In fact, a small amount of these cancer cells can migrate to distant tissues and colonize (Risson et al. 2020).

Cancer cells reach invasive and metastatic properties through the epithelial-mesenchymal transition (EMT), that is, the loss of epithelial properties and their acquisition of mesenchymal properties. Cancer cells need to release various proteases into the matrix for their intravasation. Cancer cells with invasive potential can invade surrounding tissues (Lambert et al. 2017).

Adhesion of CTCs to endothelial cells in blood vessels is the first stage of extravasation. After this migration of cancer cells, it will be found in the dormant or proliferative form. The dormant state of these cells may contribute to their survival. The dormant state of the primary tumor is the state in which the cells are quiet at the molecular level to survive. These cells can be in proliferative or quiescent state depending on environmental conditions and intracellular regulations (Crea et al. 2015; Galvao et al. 2014).

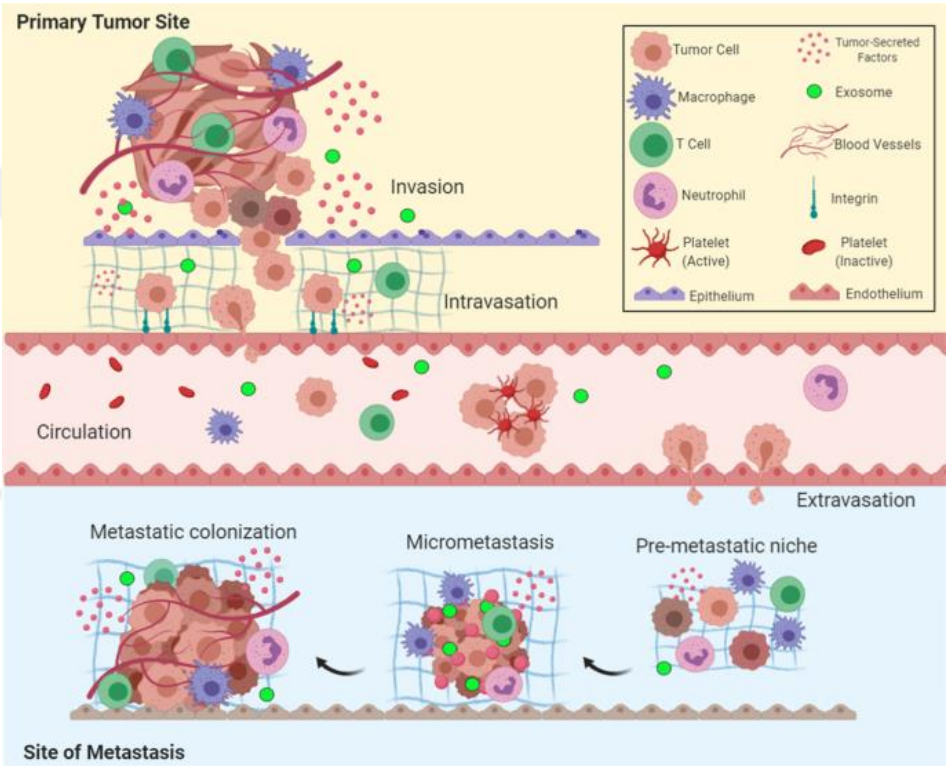

Figure 1:5 Schematic representation of the metastatic cascade.

The metastatic process is multistage that begins when the metastatic cancer cell enters the circulation (*intravasation*) due to *invasion* from the site of the primary tumor. *CTCs* can survive in the bloodstream. Moreover, these cells *extravasate* to the target organ and settle and proliferate to survive (Fares et al. 2020).

Metastatic dormancy terminology is also used in the literature. This refers to dormant DTCs while adapting to the microenvironment in the bloodstream or in the organ to which they metastasize (Risson et al. 2020). In the clinic, metastatic dormancy may be an indication of tumor recurrence. Another terminology, treatment-induced dormancy, describes the state of cancer cells entering a dormant state to evade the anticancer drugs

used to treat patients. Anticancer drugs used in the clinic mostly aim to kill cancer cells by targeting continuously dividing cells. Since the dormant cells are in the stationary phase, they can develop resistance to drugs (Damen, van Rheenen, and Scheele 2021). Breast cancer cells detected in the bone marrow after treatment have been associated with a poor disease prognosis (Braun et al. 2005; Drageset et al. 2006; Hall et al. 2012; Janni et al. 2011). Therefore, the characterization of dormant DTCs is extremely important for the follow-up and progression of the disease.

A study revealed that NR2F1 could be used as a dormancy marker. It has been reported that patients with NR2F1-high DTCs do not have bone metastases for a longer period compared to patients with NR2F1-low DTCs (Borgen et al. 2018). The small number of studies in the literature reveals the lack of knowledge in this area. The elucidation of the complex mechanisms of tumor dormancy is crucial for both basic scientists and clinicians.

1.2.10 Tumor Microenvironment and Dormancy

Integrins are a family of heterodimeric transmembrane receptors that transmit signals from the ECM into the cell. Integrins are involved in various response mechanisms such as proliferation, survival, or cell motility. In a study, it was revealed that integrin signaling plays a role in inducing cellular dormancy. (Aguirre-Ghiso, Ossowski, and Rosenbaum 2004; Barkan et al. 2008; Dey-Guha et al. 2015; Shibue and Weinberg 2009; Weaver et al. 1997; White et al. 2004). In a study, it was shown that when HMT-3522 breast cancer cells were cultured with a β-1 integrin inhibitor in the three-dimensional basement membrane, they formed acini morphology, stopped their growth, and phenotypically differentiated. It was observed that the phenotype was reversed when the given inhibitor was withdrawn (Weaver et al. 1997).

The reduction in β-1 integrin signaling appears to induce proliferative cells to transition to a quiescent state in the cell cycle. PTK2/FAK is a cytosolic tyrosine kinase, also known as focal adhesion kinase. (Weaver et al. 1997). β-1 integrin signaling relies on PTK2/FAK phosphorylation. The mouse mammary tumor virus (MMTV) transgenic mouse model is an in vivo model of human breast cancer with impaired integrin function using the Cre/LoxP1 system. As a result of the complete reduction of the β-integrin signal, it was observed that the decrease in the phosphorylation of PTK2/FAK tyrosine caused

the inhibition of cell proliferation and the arrest of tumor growth (White et al. 2004) In correlation with these results, increased β-1 integrin signaling may reintroduce dormant cancer cells into the cell cycle. In one study, it was revealed that cell growth was associated with the presence of fibronectin-1, and β-integrin signaling was dependent on the phosphorylation of the myosin light chain complex (Barkan et al. 2008). D2A1 and D2.0R mouse mammary carcinoma are high-grade metastatic cell lines. In a study using these cells, it was demonstrated in an in vivo model that their metastatic spread is dependent on collagen I/ β-1 integrin signaling. (Barkan et al. 2010).

Proliferation in cancer cells is provided by the regulation of the AKT pathway by β-1-Integrin/FAK signaling. β-1 Integrin-FAK signaling has been shown to regulate heterogeneous growth in vitro in human breast cancer and HCT-116 colon cancer cell lines. It is regulated by preventing the degradation of cytosolic AKT1 levels by proteasomal degradation. Studies have shown that knockdown of β-1 integrins significantly inhibits the division of metastatic D2 cells. Based on these results, β-1 Integrin signaling can be considered somehow specific for cellular dormancy. (Barkan et al. 2008; Shibue and Weinberg 2009).

Current findings reveal that the relationship of the cell with its microenvironment play an important role in elucidating cellular dormancy mechanisms. Recently, increasing tumor-niche interaction studies have shown that dormancy-promoting niches of cells express thrombospondin, fibronectin, collagen and β-1 integrin, which interact with ECM proteins in tumor cells (Ghajar et al. 2013). It has been shown that TGF- β1 and periostin, ligands of different integrin types, are secreted in niches where cellular proliferation is supported. Local secretion of osteopontin, another integrin ligand, has been shown to promote dormant behavior (Boyerinas et al. 2013).

All studies reveal how the interaction of cancer cells with the ECM plays a role in various cellular regulations. The dormant behavior that occurs at the cellular level may be directly related to the environment of cancer cells. Although more cancer dormancy-niche studies are still needed today, the data are of great importance for our understanding of cancer dormancy, the impact of factors in the microenvironment on disease progression, and the finding of new therapeutic targets.

1.3 Lung Cancer

Today, lung cancer is still one of the most common types of cancer diagnosed worldwide and one of the leading cancer-related deaths. Besides, lung cancer is one of the most critical health problems in Turkey. It is the most common type of cancer in men with a rate of 70.6 per 100,000 in Turkey and is among the top 5 cancers in women (9.8 per 100,000) (T.R. Ministry of Health, Health Statistics Yearbook, 2018).

Clinically, lung cancer is a heterogeneous disease according to its pathological features. 85% of patients diagnosed with lung cancer are classified as non-small cell lung cancer (NSCLC) and 15% as small cell lung cancer (SCLC). Staging is important to determine the treatment method for lung cancer. Stage I is the early stage for NSCLC patients, and the 5-year survival is 80%. For Stage II and Stage III, the 5-year survival rate of the disease is 13-60%. (Thai et al. 2021).

Adenocarcinomas in the NSCLC class are the most common type, followed by squamous cell carcinomas (Parker and Cox 2020). Large cell carcinoma (LCC, LCLC) is seen in less than 5% of patients diagnosed with NSCLC. Molecular characterization of these tumors is more complex. LCC is not a distinct histological subtype of NSCLC, because it has subtype features of adenocarcinoma or squamous carcinoma. It is seen as the undifferentiated form of squamous carcinoma and adenocarcinoma. Distal growth is observed in adenocarcinomas while squamous carcinomas develop and grow in the center of the lung.

Relapse of the disease is quite common, including in patients with early-stage NSCLC. It has been shown that 30-60% of early-stage patients develop recurrence in local or distant tissues. (Maeda et al. 2010; Winton et al. 2005). Although both NSCLC subtypes have similar metastatic profiles, adenocarcinomas have a higher metastasis potential than squamous carcinoma. The site of metastasis depends on the histology and genomic profile of the primary tumor. (Paik et al. 2016; Shih et al. 2020). Brain (12-47%), liver (7-22%), bone (16-39%) are the regions where NSCLC cells metastasize (Hess et al. 2006; Oikawa et al. 2012; Riihimäki et al. 2014; Shih et al. 2020). Although many studies have been done on lung cancer in the last decade, treatments are for patients in the early stages. There are ongoing challenges to medicine and treatment today.

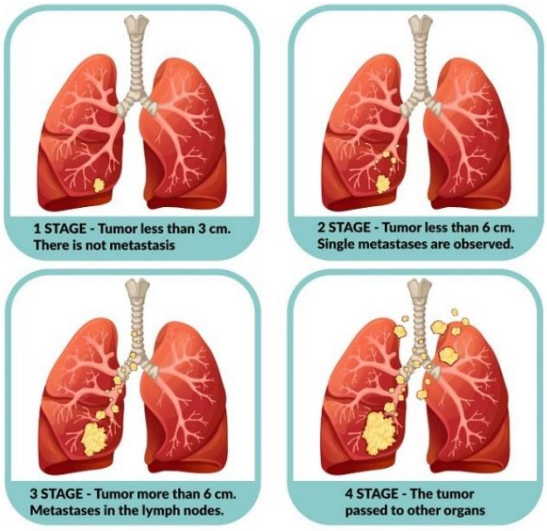

Figure 1:6 Stages of Lung Cancer

(Narayana Health, 2018).

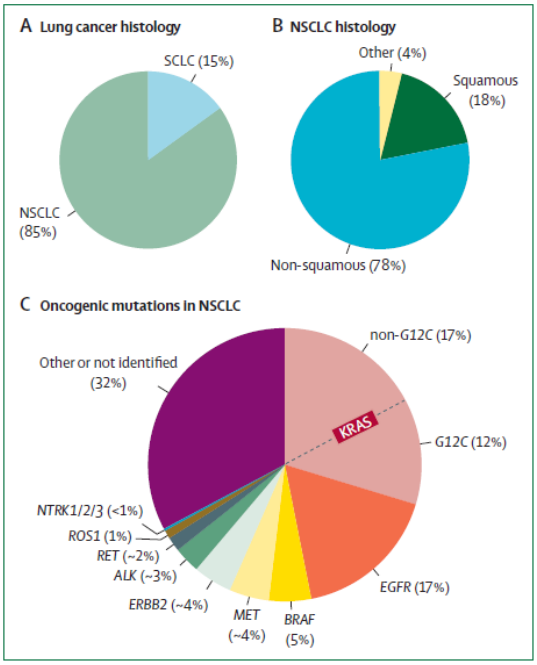

Figure 1:7 Lung cancer histology.

A. Lung cancer are classified as non-small cell lung cancer (NSCLC) and 15% as small cell lung cancer (SCLC). B. Adenocarcinomas in the NSCLC class are the most common type, followed by squamous cell carcinomas. C. The frequencies of common mutations in NSCLC (4064 patients with metastatic NSCLC) (Thai et al. 2021).

Although clinical data show that the dormancy of lung cancer cells contributes to the recurrence of lung cancer (Demicheli et al. 2012), the study on the subject is insufficient.

In addition, the mechanisms of dormancy and recurrence of lung cancer have not yet been clarified. The high recurrence rates and the high mortality of the disease, as well as insufficient knowledge about the subject, make it valuable to examine drowsiness in lung cancer.

1.3.1 Cancer Dormancy in Non-Small Lung Cancer

Clinical data indicate that lung cancer can go dormant as in many other types of cancer. *Demicelli et al.* investigated the recurrence rates of NSCLC lung cancer in a retrospective study of 1506 patients. It has been observed that distant metastases may peak, especially in the 2nd and 4th years after the surgical treatment of the primary tumor. It reveals similar results to the data of breast cancer patients. These results indicate that NSCLC lung cancer cells can go into dormancy to wake up years later (Demicheli et al. 2012).

The dormancy state is commonly observed in experimental models of lung cancer. In many studies by Judah Folkman, it has been observed that many micro metastases that are not actively dividing, as well as lung metastases that occur after subcutaneous injection of cancer cells in the mouse Lewis lung cancer experimental model (Naumov, Akslen, et al. 2006; Naumov, Folkman, and Straume 2009). It has been suggested that treatment with an angiogenesis inhibitor in mice leads to an increase in dormant micro metastases (Holmgren et al. 1995). In the study, inhibition of angiogenesis using the VEGF-A2 inhibitor bevacizumab was shown to induce prolonged dormancy of brain metastases of the PC14-PE6 human NSCLC cell line. (Kienast et al. 2010). Activation of microglia around lung cancer brain metastasis cells in brain biopsies and observed that microglia kill cancer cells in vitro, suggesting that the microglia-lung cancer relationship may contribute to dormancy (He et al. 2006).

Few studies with lung cancer models provide limited findings on the molecular mechanisms of observed dormancy. In a study with A549 and H460 human and Lacun3 mouse lung cancer cells, it has been observed that establishing spheroid tumor cell cultures puts the cells into a state of quiescence-like seen in stem cells, reduces the number of primary tumors and metastases occurring after injection into mice (Bleau et al. 2015). It was observed that the amount of p27 was higher in the cells grown as a spheroid culture at the molecular level compared to the actively dividing cells, and the phospho-

ERK levels decreased significantly (hence reduced pERK/p38 ratios). All these data indicate that lung cancer cells are dormant in spheroid cultures.

Two independent studies point to the association of lung cancer sleepiness with p53. In a study with A549 and H460 cells, they examined the dormancy-inducing effects of 5-fluorouracil (5-FU) (Dai et al. 2016). Cells that do not die after treatment with 5-FU undergo EMT-like changes and express stem cell markers. DNA damage by 5-FU led to p53 activation in dormant cells, APC/C-dependent cyclin degradation, and thus cell cycle arrest in the G0-G1 phase. In these conditions, p21 and p27 levels were also increased. It has also been shown that TGF-β/Smad2-slug signal activation in cells exposed to 5-FU is important in the transition to EMT (Dai et al. 2016). In a study with A549, H1299, H460 and H3122 lung cancer cells, they showed that EGFR inhibitors (BIBX or erlotinib) reduced cell growth and caused p53-dependent G1 cell cycle arrest, especially when used with ionizing radiation (Kienast et al. 2010). They showed that G1 arrest in lung cancer cells depends on p21 expression stimulation by p53. It was observed that removal of BIBX or erlotinib after the treatment caused cells to exit from their dormant state. No other study examining dormancy in lung cancer cells could be found in the literature.

1.4 MicroRNAs as Regulator Molecules

MicroRNAs (miRNAs) are single-stranded small RNAs that are transcribed from DNA and play a role in regulating the expression of genes in the cell. They are usually 18-22 nucleotides in length. It regulates gene expression by causing "seed" sequences to interfere with messenger RNA (mRNA)'s translation or binding to the ribosome, usually by interacting with 3'-ended (rarely 5') mRNA transcripts (Cai et al. 2009; Wahid et al. 2010). As a result of genetic analysis, it was revealed that 60% of the entire human genome consists of regions that could be potential miRNA targets. Therefore, miRNAs are thought to be of great importance in the transcription profiles of cells. (Leclercq, Diallo, and Blanchette 2017). Numerous studies conducted to date have revealed that miRNA expression has a critical role and causes remarkable changes in various diseases, especially cancer, and (Di Leva and Croce 2013). In line with these studies, examining miRNAs in diagnosis, treatment and elucidation of molecular arrangements has become even more important.

1.4.1 MiRNA Biogenesis

MiRNAs can be found on the genome in intron regions (intronic) and within the gene (intergenic). Polycistronically transcribed genes, i.e., miRNA clusters within the same gene can be regulated by common transcription factors. The expression of intragenic miRNAs is coordinated chiefly with the location of the miRNA in the gene.

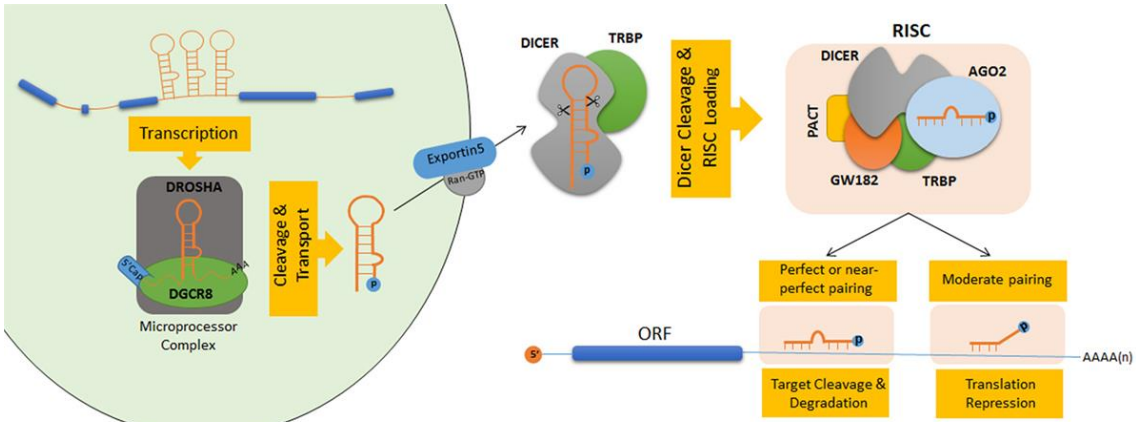

Figure 1:8 miRNA Biogenesis

(Gozuacik et al. 2017)

The first form of miRNA transcribed in the cell nucleus is called pri-miRNA. pri-miRNA transcripts have a unique hairpin structure. This structure enables miRNAs to be recognized by some specific miRNA binding proteins. After transcription, pri-miRNA is recognized by RNA-binding DGCR8 and RNAse II protein Drosha in the cell nucleus, and RNAse-dependent cutting occurs. As a result, the hairpin structure becomes pre-miRNA. The length of the pre-miRNA is usually 60-70 nucleotides. After cleavage, the pre-miRNA is recognized by Exportin-5 in the nuclear membrane and is GTP-dependently transported from the nucleus to the cytoplasm (Finnegan and Pasquinelli 2013; Lin and Gregory 2015).

After transport, the pre-miRNA is recognized by the TRBP and RNAse III Dicer proteins in the cytoplasm, and the hairpin structure is cut to form a 21-22 nucleotide long miRNA duplex. The thermodynamically most stable strand is loaded into the RNA-induced silencing complex (RISC). This complex contains DICER, TRBP, PACT, AGO2 and GW182 proteins (Gozuacik et al. 2017; Graves and Zeng 2012; Santa et al. 2012). AGO2 is the most critical component that binds the protein miRNA to RISC. MiRNA response elements (MREs) are found in the 3'UTR of mRNAs. Mature miRNA seed

sequences make perfect or non-perfect base pairing with the MRE depending on AGO2, causing the mRNA of its target to be truncated. As a result, the cut mRNA is cleaved by endonucleases. On the other hand, mRNA is translationally repressed if the miRNA makes a match moderately to the target mRNA (Mauri et al. 2017). The biogenesis of miRNAs is schematized in detail in Figure 1.8.

1.4.2 Cancer Dormancy-related MiRNAs

The effects and relationships between tumor dormancy and miRNAs are poorly understood so far. The lack of studies in the literature is a very interesting research area to investigate the roles of miRNAs in cancer dormancy and tumor recurrence.

In a study, it was reported that array screening analyses revealed overexpressed mir-190 expression in osteosarcoma and glioblastoma dormancy tumor models and detected that microscopic tumor was formed. In the dormancy model, osteosarcoma and glioblastomas remained stable for 125 days and 88 days respectively. It has been determined that dividing cells are also present in dormant microtumors. Analysis of mir-190 and dormancy-related signaling pathways revealed that it is associated with immune escape-related pathways (N. et al. 2013).

In one study, dormant glioblastoma, breast cancer, and liposarcoma tumor cells were studied in vivo. High apoptotic and proliferation rates were detected in all tumor types. Moreover, defective angiogenesis has been found. When the miRNA profiles of these tumors were analyzed, similar miRNAs were found in all tumors. According to the results, 84% (16/19) of miRNAs were found to be up regulated in dormant cells. Manipulation of expression levels of miR-580, miR-588, and miR-190 has been reported to cause tumor growth delay in fast-growing glioblastoma cells. Target gene analyzes of these miRNAs have been shown to be associated with carcinogenesis (N. et al. 2013).

A cDNA library was created to identify miRNAs that play a role in regulating the transition of dormant breast cancer cells to metastatic state. Murine miRNAs that cause lung metastasis were transfected into 4TO7 cells that were previously present in the lungs but did not cause metastasis. These cells were then injected into mice. MiR-340, miR-346 and miR-138 and miR-223 expressions were detected in each animal in which breast cancer lung metastases developed in miRNA expression analyzes performed on tumors formed after injection. In line with this study, it has been reported that these miRNAs

may play a role in transition of the metastatic state from a dormant state (Gao et al. 2014). In a study using murine breast tumor cell lines, the role of miRNAs in the transition of dormant cancer cells to the proliferative state was investigated. The miR-200a/200b/429 cluster targets mesenchymal transcription factors and is associated with the proliferation and migration of stem cells. Restoration of expression of miR-200a/200b/429 cluster in murine mammary tumors has been shown to decrease cell division and transform into epithelial cell morphology. It has been shown that the target genes of this miRNA, Snail, Twist1, Twist2 and Zeb1 are decreased. Moreover, these cells have been reported to induce dormant tumor transition in vivo (Watson et al. 2018).

In another study, it was shown that mir-200c plays a role in maintaining dormancy in osteosarcoma tumors. No sign of angiogenesis and no change in tumor volume for 140 days, and an in vivo mouse model was created using osteosarcoma cells that cause small tumors but are not tumorigenic. Expression of mir-200c was found to be higher in quiescence tumor-forming cells compared to rapidly growing cells. It has also been said to be associated with long-term survival in vivo. (Tiram et al. 2016).

In a study with gastrointestinal cancer stem cells, cancer stem cells were defined as CD13-/CD90+ proliferative and CD13+/CD90- quiescence cancer stem cells. It was found that mir-101 was downregulated in dormant cancer stem cells compared to proliferative cells. As a result of bioinformatic analyzes, it has been reported that mir-101 plays a role in the cytokine/chemokine regulatory pathway, and the immune system is associated with the maintenance of the dormant state. Moreover, this study characterized the regulation of dormant cancer stem cells in developing drug resistance via the P53 signalling pathway (Nishikawa et al. 2012).

A previous study has shown that ΔNp63α plays a role in mammary stem cell stagnation. Moreover, ΔNp63α has been reported to play a role in reversible growth arrest in transition to dormancy. In MCF7 breast cancer cells overexpressing ΔNp63α, mir-205 was found to be the most overexpressed miRNA. As a result of the application of antagomir against miR-205, a decrease in the proliferation of cells was observed. Moreover, it has been reported that miR-205 causes down-regulation in DNA binding 1 (ID1), ID3 inhibitor, and BAMBI (these are genes associated with the bone morphogenetic signalling pathway), dormancy-related genes, which are among the target genes (Moses et al. 2016).

Other dormancy-associated miRNAs are mir-221 and mir-222. Decreased expression of mir-221 and mir-222 was observed when acute lymphoblastic leukemia cells were co-cultured with bone marrow stromal cells and primary human osteoblasts. These miRNAs have previously been shown to target the cell cycle inhibitor p27. As mentioned before, P27 is a gene associated with dormancy and has been shown to play a role in the dormancy of acute lymphoblastic leukemia cells. Increased p27 levels due to downregulation of mir221 and mir22 have been shown to cause arrest in cell division and increased drug resistance in other cells cultured acute lymphoblastic leukemia cells independently from the bone marrow niche. (Furuichi et al. 2007). In another study, it was revealed that these two miRNAs cause dormancy in leukemia cells (Moses et al. 2016). Similarly, mir-221 and mir-222 levels increased in cells entering the cell cycle in glioblastomas. Transfection with the antimiR-222 inhibitor resulted in an increased number of cells in the G0 phase.

In contrast, miR-221 and miR-222 induce cells to enter the synthesis (S) phase, followed by apoptotic death. Anti-miR-222/223 transfection in mesenchymal stem cells transformed them into dormant cancer cells resulting in a reducing in the proliferation rate of cancer cells and long-term survival rates in vivo (Bliss et al. 2016). Thus, low levels of miR-221 and miR-222 in dormant cancer cells are thought to act as a mechanism to protect against an undesirable shift from the dormant state to the proliferative state before the triggering of apoptosis (Medina et al. 2008).

In a recent study, a gene that supports dormancy in prostate cancer was detected by differential gene expression analysis. Regucalsin (RGN) is a highly conserved protein that maintains intracellular calcium balance. It also interacts with many proteins and transcripts, affecting many different signalling pathways, affecting cell growth and the programmed cell death pathway. Prostate tumors can remain dormant for long periods, either locally or in distant regions, without being detected for a long time. Ectopic expression of RGN in prostate tumors induced dormancy in in vivo models, and tumor growth was observed to be re-induced because of suppression of RGN. It was determined that the levels of mir-23c detected in exosomes released by cells were increased by RGN, and mir-23c significantly suppressed angiogenesis. The role of RGN in the dormancy of

prostate cancer and the regulatory role of exosomal mir-23c in dormancy have been demonstrated. (Sharma et al. 2021).

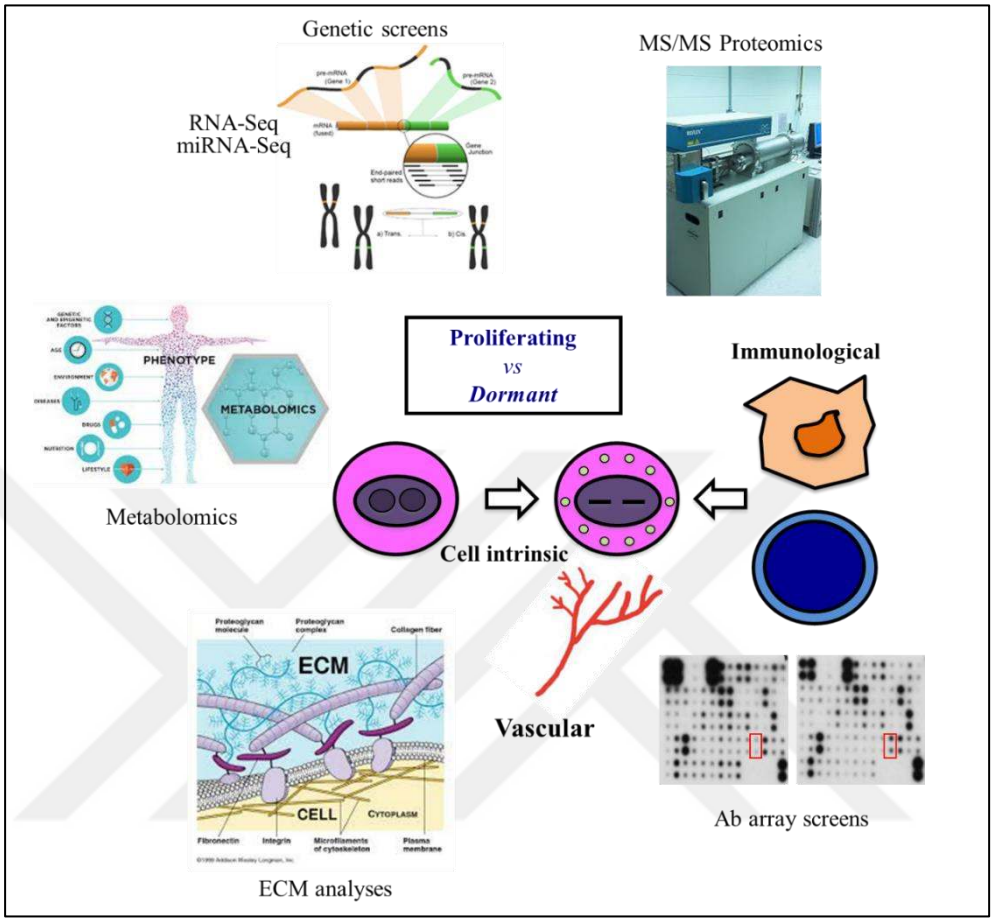

Figure 1:9 Discovery of new players in cancer dormancy using omics analyses.

As a result, the roles and mechanisms of miRNAs that regulate cancer dormancy in the transition of cells from dormancy to proliferative state are explained. The miRNAs obtained in studies conducted so far play a role in balancing dormancy-proliferative states. MiRNA profiling from dormant cancer cells is required to reveal miRNAs expressed during dormancy. In the cancer dormancy model obtained within the scope of this study, miRNA, RNA, proteomic and metabolomics profiling of dormant cells were performed from the cancer cells were in a dormant state. In this thesis, miRNA, RNASeq and Proteomics data are focused (Figure 1.9).

Chapter 2:
MATERIALS AND METHODS

2.1 Cell Culture

Human embryonic kidney cells (HEK293T), Platinum-A (Plat-A) and A549 cells were obtained from ATCC (USA). HEK293T and a potent retrovirus packaging cell line the Plat-A cells were cultured in Dulbecco's modified Eagle's medium (DMEM, Biological Industries, #BI01-050-1A), and the non-small lung cancer cell line A549 was cultured in RPMI 1640 medium (SIGMA-Aldrich #R8758). Both of the culture media were supplemented with 10% (v/v) fetal bovine serum (FBS, PAN, #P30-3302), antibiotics (Penicillin/streptomycin, Biological Industries, #BI03-031-1B) and L-Glutamine (Biological Industries, #BI03-020-1B) in a 5% CO2 humidified incubator at 37°C. HEK293T and Plat-A cells were transiently transfected with calcium phosphate transfection method according to standard protocols.

2.2 Plasmid constructs

To produce lentiviruses, the lentiCRISPR v2 vector (Addgene, Plasmid #52961), the helper vectors psPAX2 and pMD2.G (Addgene plasmid #12260 and #12259). To produce retroviruses, pMSCV-puro-MIR362 and pMSCV-puro-MIR190A (Addgene, Plasmid #75079) overexpression retroviral plasmids (from DG Lab plasmid stocks), were used.

2.3 Molecular Cloning of CRISPR/CAS9/MIR210 plasmid

To use the CRISPR/Cas9 method, guide RNAs (gRNA) targeting the palindromic sequence-containing regions (PAM sequence) of the genes were designed. The Integrated DNA Technologies IDT (https://www.idtdna.com/pages) tool was used as a gRNA design tool. gRNAs were designed to contain the BsmBI restriction enzyme binding site. The BsmBI region in the target vector, lentiCRISPRv2 (Addgene, #52961), was cut and then double-stranded forward and reverse gRNAs were ligated into this region. The selected vectors were confirmed by DNA sequencing to check whether the plasmid contain gRNA.

MIR210 Forward gRNA: 5'- CACCACCCACTGTGCGTGTGACAG - 3'
MIR210 Reverse gRNA: 5'- AAACCTGTCACACGCACAGTGGGT -3'

2.4 Transfection

HEK293T and Plat-A cells were transiently transfected with the calcium phosphate transfection method according to standard protocols. Lentivirus vector was transfected into HEK293T cells, retrovirus vector was transfected into Plat-A cells. Cell medium containing lentiviruses and retroviruses were collected after 48 and 72 hours. After centrifugation (at 500g, 5 min) and filtration (0,2-micron filter), stored at -80 C for use.

2.5 Production of A549 Stable Cell Lines

To produce stable cell lines, cells were seeded at 2x105 cells in a 6-well petri dish 24 hours before being treated with the viruses. Cells were then grown for 8 hours in nutrient media prepared with the addition of 5 μg/mL polybrene (Sigma, H9268) to a 1:1 mixture of lentivirus or retrovirus solution and RPMI 1640.

Plasmid vectors contain a resistance gene to the antibiotic Blasticidin or Puromycin. After 48 hours, appropriate antibiotics were added to the medium at an optimum concentration (10μm/ml for Blasticidin and 5μm/ml for Puromycin) selection was made after 3-4 weeks of culture.

2.6 Establishment of the Cancer Dormancy Model

In our laboratory, the Matrigel 3D cell culture system was optimized as an in vitro cancer dormancy model by testing the ability of the A549 cell line to enter the dormant state in Matrix. Matrigel was used in a two-layer 3D culture system. Liquid Matrigel was spread on a 96-well petri dish at 50 μl/well as a bottom layer (final concentration 4 μg/μl). It was waited for 30 minutes for polymerization. A549 cells were seeded with a medium containing 0.08mg/ml Matrigel to a final concentration. Cells were prepared with 150 μl of medium per 2000 cells with dormancy trigger medium (Low glucose DMEM, 2% FBS, Pen/Strep antibiotics and 2% Matrigel) and seeded on polymerized Matrigel. 3D cultures were observed for 14 days, with the medium being refreshed in 4 days. The resulting 3D cell spheroids were analyzed.

2.7 Awakening Experiments of Dormant Spheroids

Spheroids were purified from Matrigel, treated with trypsin, and cultured in the rich nutrient medium (10% FPS, high glucose (4.5 g/L) at the end of the 14th day. As a control Cells actively grown in 2D culture and never dormant were used. Cell division rates were examined by the MTT cell growth test.

2.8 Beta-galactosidase staining in 3D cultured spheroids

Matrigel was removed by treatment with PBS-EDTA: After diluting the Matrigel with cold PBS-EDTA solution, the tubes were incubated on ice for 10 minutes with mixing every 2 minutes. The samples were then incubated with cold PBS at 115 x g for 2 min. centrifuged and washed twice. Then, 3D spheroids were placed on slides and fixed with 4% PFA. Then, the cells were incubated for 12 hours at 37 °C without carbon dioxide with a staining solution prepared in citric acid-phosphate buffer (pH 6) and containing potassium ferricyanide, potassium ferrocyanide and X-gal. As a positive control, spheroids were treated with 1μM hydrogen peroxide (H2O2) for 2 hours while in Matrigel.

2.9 Total RNA Isolation and RT-PCR Analysis

Total RNA isolation was performed using TRIzol reagent (Sigma-Aldrich, #T9424) according to the manufacturer's instructions. Total RNA was treated with DNase I (Thermo, EN0521). cDNA was reverse transcribed from DNase-treated total RNA using RevertAid enzyme (ThermoScientific, EP0441) RiboLock RNase inhibitor (Thermo, EL0012) and random hexamers (Invitrogen, 48190-011), stem-loop primers for MIRNAs. Stem-loop Primers designed during the study were in Table 2.1

Table 2:1 Stem-loop primers for miRNAs.

miRNA	Stemloop Primer	Forward Primer Sequence (5'-->3')
MIR1180-3P	GTCGTATCCAGTGCAGGGTCCGAGGT ATTCGCACTGGATACGACACACACC	GTTTCCGGCTCGCGTG
MIR1180-5P	GTCGTATCCAGTGCAGGGTCCGAGGT ATTCGCACTGGATACGACTATTCCC	TTAGTTAGGACCCACCCGG
MIR1304-3P	GTCGTATCCAGTGCAGGGTCCGAGGT ATTCGCACTGGATACGACGGGGTTC	TCGCTCTCACTGTAGCCTC
MIR1304-5P	GTCGTATCCAGTGCAGGGTCCGAGGT ATTCGCACTGGATACGACCACATCT	GCCGTTTGAGGCTACAGTG
MIR130B-3P	GTCGTATCCAGTGCAGGGTCCGAGGT ATTCGCACTGGATACGACATGCCCT	GGGCCAGTGCAATGATGAA
MIR130B-5P	GTCGTATCCAGTGCAGGGTCCGAGGT ATTCGCACTGGATACGACGTAGTGC	GCCGACTCTTTCCCTGTTG
MIR138-2-3P	GTCGTATCCAGTGCAGGGTCCGAGGT ATTCGCACTGGATACGACAACCCTG	GCCAGCTGGTGTTGTGAA
MIR138-2-5P	GTCGTATCCAGTGCAGGGTCCGAGGT ATTCGCACTGGATACGACCGGCCTG	CCGGGCTATTTCACGACAC
MIR2278	GTCGTATCCAGTGCAGGGTCCGAGGT ATTCGCACTGGATACGACCCAGGCA	GATCCTGTGCGTGTGACAG
MIR301A-3P	GTCGTATCCAGTGCAGGGTCCGAGGT ATTCGCACTGGATACGACGCTTTGA	TATAGCCCCTGCCCACCG
MIR301A-5P	GTCGTATCCAGTGCAGGGTCCGAGGT ATTCGCACTGGATACGACAGTAGTG	AGCTGAGAGCAGTGTGTGT
MIR330-3P	GTCGTATCCAGTGCAGGGTCCGAGGT ATTCGCACTGGATACGACTCTCTGC	CGGCGCAGTGCAATAGT
MIR330-5P	GTCGTATCCAGTGCAGGGTCCGAGGT ATTCGCACTGGATACGACGCCTAAG	AGGCGCTCTGACTTTATTGC
Mir-190a-3p	GTCGTATCCAGTGCAGGGTCCGAGGT ATTCGCACTGGATACGACAGGAT	ACGGCAAAGCACACGG
Mir-190a-5p	GTCGTATCCAGTGCAGGGTCCGAGGT ATTCGCACTGGATACGACACCTAA	GCTCTCTGGGCCTGTGT
Mir-362-3p	GTCGTATCCAGTGCAGGGTCCGAGGT ATTCGCACTGGATACGACTGAATC	GCGCCAACACACCTATTCA
Mir-362-5p	GTCGTATCCAGTGCAGGGTCCGAGGT ATTCGCACTGGATACGACACTCAC	CGGCAATCCTTGGAACCT

2.10 Quantitative Reverse Transcriptase Polymerase Chain Reaction (q-RT-PCR) for mRNA and miRNA quantification

For real-time RT-PCR, SYBR Green Quantitative RT-PCR kit (Roche, 04-913-914-001) and Roche Light Cycler 480 machine were used. To activate the SYBR green, an initial cycle of 95°C, 5 min performed followed by PCR reactions: 45 cycles of 95°C for 10 sec and 60°C for 1 min. Then a thermal denaturation protocol was used to generate the dissociation curves for the verification of amplification specificity (a single cycle of 95°C for 5 sec, 55°C for 60 sec and 80 cycles of 55°C for 10 sec).

Changes in mRNA levels were quantified using the 2-ΔΔCT method using GAPDH (Gyceraldehyde-3- phosphate dehydrogenase) mRNA as control. Changes in miRNA levels were quantified using the 2-ΔΔCT method using U6 (U6 spliceosomal RNA) as control. Reactions were performed in duplicates and the number of independent experiments (n) was marked.

Primers used during the study were in Table 2.2 and Table 2.3.

Table 2:2 PCR primer sequences for genes.

Target Gene	Primer	Sequences
DDX46	Forward	GCCCCAAACCAATTAAATCCTG
	Reverse	CAATGCCAATCAAATCTCGTC
CAPZA1	Forward	AATGAAGCCCAAACTGCCAA
	Reverse	TTCCAGTCGATTTTGGTGCG
CBX3	Forward	GGCAGAGCCTGAAGAATTTGT
	Reverse	ACGCTTCAATCAATTCTGGACA
CORO1C	Forward	TCCTCCCTCTGCACAAGACT
	Reverse	GGATCTGCCATACCATGACC
BZW1	Forward	TACCGTCGATATGCAGAAACAC
	Reverse	CCATTAGCCAGAAGAACACCAG
CACYBP	Forward	GCTGCTGTGGTTGCTCCCAT
	Reverse	TGCACCTGCACATTCTCAGTGG
CAND1	Forward	ATGCTTCAGAGTCAGGTTCCC
	Reverse	ACACTGTCGGGTCTTCACAC
ANXA1	Forward	GCAGGCCTGGTTTATTGAAA
	Reverse	GCTGTGCATTGTTTCGCTTA

ANP32B	Forward	GGGGAAGAGGGGAACATGGA
	Reverse	ACAAGTTCTCGAACAGCTGCC
ATP2A2	Forward	CGAACCCTTGCCACTCATCT
	Reverse	CCAGTATTGCAGGTTCCAGGT
ITGAV	Forward	AAGCTGAGCTCATCGTTTCC
	Reverse	GCACAGGAAAGTCTTGCTAAGG
MCM5	Forward	CCAAGTGTCCACGTTGGATG
	Reverse	TGCTCCGGGTATTTCTGCT
MYH10	Forward	GCAGGAGAACACCTAAAGTCT
	Reverse	TGTCCCGGAATAGGAATATAGCC
DDX6	Forward	AGTGATGGCAACCACAGGAG
	Reverse	CCAGGATTCTCCCAGGGGTA
DEK	Forward	AAGCCTTCTGGCAAACCATTG
	Reverse	TTCGCTTAGCCTTCCTTGCC
G3BP1	Forward	AAGTCCTTAGCAACAGGCCC
	Reverse	CTGGCAGCTCGAGTCTTCTT
PAICS	Forward	AGCTGAGTATGAAGGGGATGG
	Reverse	ACATCACTGGTCCCAAACCA
PRKDC	Forward	CCACTGGTCGTTTTCGGAGA
	Reverse	CCATGCACTCATGCCGATTG
SERBP1	Forward	CCACCTCGTGAACGAAGATT
	Reverse	ACCACCACGACCTCGAATAG
SPTBN1	Forward	CCCGCAGATTTGATCGCAAG
	Reverse	ATGCGGCAATGTCTGTCTCA

Table 2:3 PCR primer sequences for miRNAs.

miRNAs	**Forward Primer Sequences (5'-->3')**
MIR362-3P	GCGCCAACACACCTATTCA
MIR362-5P	CGGCAATCCTTGGAACCT
MIR190A-3P	CCGCGGCCCTATATATCAAAC
MIR190A-5P	CGGCCGGTGATATGTTTGATA
MIR181-3P	TCAGACCACTGACCGTTGA
MIR1180-5P	TTAGTTAGGACCCACCCGG
MIR1180-3P	GTTTCCGGCTCGCGTG
MIR1304-5P	GCCGTTTGAGGCTACAGTG
MIR1304-3P	TCGCTCTCACTGTAGCCTC
MIR130B-5P	GCCGACTCTTTCCCTGTTG
MIR130B-3P	GGGCCAGTGCAATGATGAA

MIR138-2-5P	GCCAGCTGGTGTTGTGAA
MIR-138-3P	CCGGGCTATTTCACGACAC
MIR-2278	AGCTGAGAGCAGTGTGTGT
MIR301A-5P	AGGCGCTCTGACTTTATTGC
MIR1290	CGCCCTGGATTTTTGGATCA
MIR210-5P	TATAGCCCCTGCCCACCG
MIR210-3P	GATCCTGTGCGTGTGACAG
MIR1224-5P	ACATGTGAGGACTCGGGAG
MIR1224-3P	TGATCCCCACCTCCTCTCT
MIR181-5P	GGCGAACATTCAACGCTGT
MIR301A-3P	CGGCGCAGTGCAATAGT
MIR330-5P	GCTCTCTGGGCCTGTGT
MIR330-3P	ACGGCAAAGCACACGG
MIR374-5P	GGGCGCTTATAATACAACCTGA
MIR374-3P	CGGGCGCTTATCAGATTGTAT
Universal Reverse	GTGCAGGGTCCGAGGT

2.11 Omics Analyses

2.11.1 RNA-sequencing (RNAseq)

Samples prepared for RNAseq analyzes were obtained by Trizol method and RNA quality was confirmed. The samples were dissolved in water with DEPC. It was determined by the FastQC method that the samples were of suitable quality for processing by the company. Adapter sequences and poor-quality reads detected during quality assessment were filtered using the Trimmomatic tool (Bolger et al., 2014). A total of 4 single-ended mRNAs were sequenced, two biological repeats, for active growth and dormancy models (2 x 2D proliferating state, 2 x 3D dormancy state). Sequence analysis was performed on the Illumina NextSeq 500 system using the 40 million reads, 1x75bp Single End sequencing strategy.

The gene expression levels in each sample were assessed by reads aligned to the human GRCh38 reference genome and following the methods described in Nature Protocols (Pertea M. et al., 2016). The gene expression level was normalized by the number of fragments per kilobase per million mapped reads (FPKMs). The gene expression level in the proliferating samples and the dormant samples were compared using DESeq2 package in R language, which produced the adjusted p-value for the comparison.

2.11.2 MicroRNA-Sequencing (miR-Seq)

Three of the 2D and 3D samples were sent to the company. RNA quality was checked with the "Qubit RNA assay". Then, miRNA sequencing was performed. Sequence analysis procedures were performed by the company using the "SMARTer smRNA-Seq Kit", a sequence library belonging to Illumina. Sequence analysis was performed on the Illumina NextSeq 500 system using the 1x75bp Single End sequencing strategy. The results were obtained from the company in the form of a FASTQ file and floor change analyzes were performed.

2.11.3 Proteomics Analyzes

3D cultures were prepared according to the protocol previously mentioned above. Cells containing 2% FBS and 0.04% Matrigel on 4 mg/ml Growth factor-reduced matrigel were cultured using SILAC-DMEM cell media. 5X SILAC-DMEM was obtained as powder and was prepared by adding 420 mg/L L-arginine, 730 mg/L L-lysine, and 625 mg/L proline. 2D cells were cultured in SILAC-DMEM containing 2% FBS and 0.04% Matrigel. “Heavy” L-arginine-13C6-15N4 (Arg10) and L-lysine-13C6-15N2 (Lys8) in 3D culture or “medium-heavy” L-arginine-13C6 (Arg6) and L-lysine-2H4 in 2D culture SILAC labelling was done using (Lys4) amino acids. Cells were treated with 6X SDS-PAGE loading buffer and boiled and sent to Switzerland for analysis. Lysates were loaded onto gels and analyzed by MS by in-gel trypsin cleavage. MS analysis was analyzed with the LTQ Orbitrap XL. The raw data were mapped to the UniProt Homo sapiens database using the MaxQuant interface version 1.4.1.222 (Tölle et al., 2018).

2.12 MTT Cell Growth Assay

NSCLC A549 cells were cultured in 96-well plates at 5x104 cells per well. Experiments were followed for 24, 48, 72, and 96 hours under 2D growth conditions. At the end of the experiment, 10 µl of 5 mg/ml MTT (3-(4,5-Dimethylthiazol-2-yl)-2,5-Diphenyltetrazolium salt solution was added to each well. After 4 hours of incubation, formazan crystals were formed. The old medium was removed, and crystals were dissolved in 100 µl of DMSO. Colour change after 10 min incubation

was measured in an ELISA plate reader at dual 570-655 nm wavelengths and the values were analyzed and presented graphically.

2.13 Scratch Assay

Migration capacities of cells were examined by wound-healing assay. Briefly, cells were cultured in 12-well plates (2×10^4 cells per well) for 24 h. These cultures were then scratched using a sterile plastic micropipette tip to create an artificial wound. Photographs were taken 6, 12, 24 later using a Nikon Eclipse Ts2 inverted microscope at 4X.

2.14 Immunofluorescence Analyses

The spheroids were treated with PBS-EDTA for analysis under a confocal microscope to remove Matrigel: After the Matrigel was diluted with cold PBS-EDTA solution, the tubes were incubated on ice for 10 minutes with gently vortexing every 2 minutes. The samples were then incubated with cold PBS at 100 x g for 2 min. centrifuged. It has been washed 2 times. Then, 3D spheroids were placed on slides and fixed with 4% PFA. Spheroids on slides were permeabilized with 0.1% saponin before immunostaining. After blocking with 3% serum albumin in PBS, the samples were incubated for 60 minutes with the primary antibody diluted 1:100 in the same solution. After washing 3 x 5 minutes with PBS, it was incubated with secondary antibody (1:1000 dilution) for 60 minutes. After washing with PBS for 3 x 5 min, the samples were covered with 50% glycerin in PBS and a coverslip and examined under a confocal fluorescent microscope.

2.15 Informatic Target Analyses

Three different data tools were used for the prediction of miRNA targets. These are miRDB, TargetScanHuman and DIANATools-TarBase v7.0.

miRDB is an online database for target predictions of miRNAs using the bioinformatically developed MirTarget tool. MirTarget was developed as a result of analyzes of thousands of miRNA-target interactions obtained as a result of high-throughput sequencing experiments. miRDB predicts the binding between miRNA

and target gene using a machine learning method that identifies standard features downstream of the miRNA target (Chen and Wang 2020).

TargetScan predicts the biological targets of miRNAs by searching for the presence of conserved 8mer, 7mer and 6mer regions that match the seed region of each miRNA (Lewis, Burge, and Bartel 2005). Predictions with only poorly conserved sites and predictions with unconserved miRNAs are also provided as options. Also, sites of disparities in the seed region compensated by conserved 3' coupling have been identified (Friedman et al. 2009). TargetScanHuman considers the matching of 3'UTRs and their orthologs as defined by UCSC whole genome alignments.

DIANA Tools interpret the roles of non-coding RNAs involved in various disease and cellular pathways. It is provided with software that interprets the data in a systematic framework by revealing deep sequencing data, expression analyses, and annotations of its targets and presents this information to the user. TarBase v7.0 online tool included in DIANA Tools was used for the prediction of miRNA targets. DIANA Tools- TarBase v7.0 is a database that catalogues that have experimentally proven miRNA-gene interactions. (Vlachos et al. 2015).

2.16 Statistical Analyses

Statistical analyses were performed using Student's two-tailed t-test. Data represented as means of ±S.D. of "n" independent experiments. Values of $p<0.05$ are considered significant.

Chapter 3:
RESULTS

3.1 Defining of the In vitro 3D Matrigel Cancer Dormancy Model

A 3D Matrigel cancer dormancy model was optimized in our laboratory by Dr. Yunus Akkoç and Dr. Nesibe Peker. Spheroids have been characterized by various analyzes.

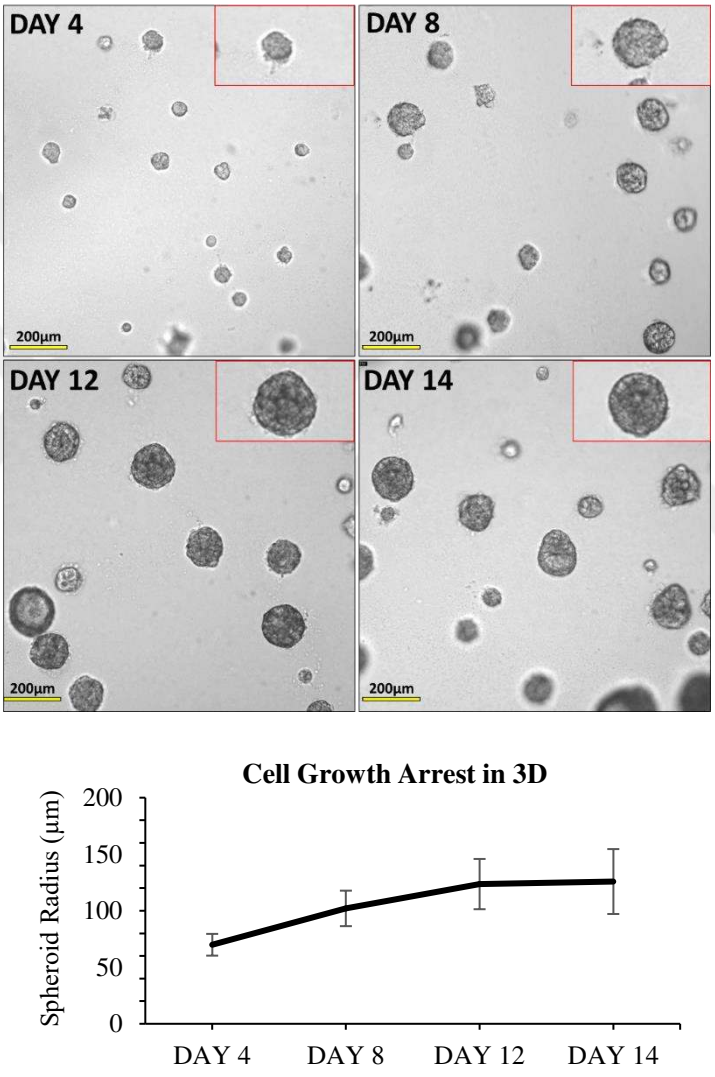

Figure 3:1 3D spheroid formation of A549 cells in Matrigel.

Representative results are shown. 10x magnification. ImageJ program was used to measure the diameters of spheroids. 150 spheroid diameters were measured for each day. 3 independent experiments (n=3) were conducted.

Phenotypes of A549 cells were observed in the 3D Matrigel cancer dormancy model for 14 days, with the medium being refreshed in 4 days. It was observed that the cells formed 3D spheroids (Figure 3.1a). These 3D spheroids were analyzed. Images of the spheroids were taken under the microscope every four days for 14 days. The diameters of the spheroids were measured. It was observed that spheroid growth slowed down between 12-14 days (Figure 3.1b).

Expression and localization of molecular markers were examined after immunostaining of spheroids to confirm dormancy. The level of cell cycle marker p27 was examined in 3D spheroids. The expression of p27 is in the nucleus in normal cells, indicating that the cell cycle is inhibited in the G1 phase. Interestingly, the p27 marker was also observed in the cytoplasm of some cells. There are studies in the literature that p27 expression can be seen in the cytoplasm of some cell types.

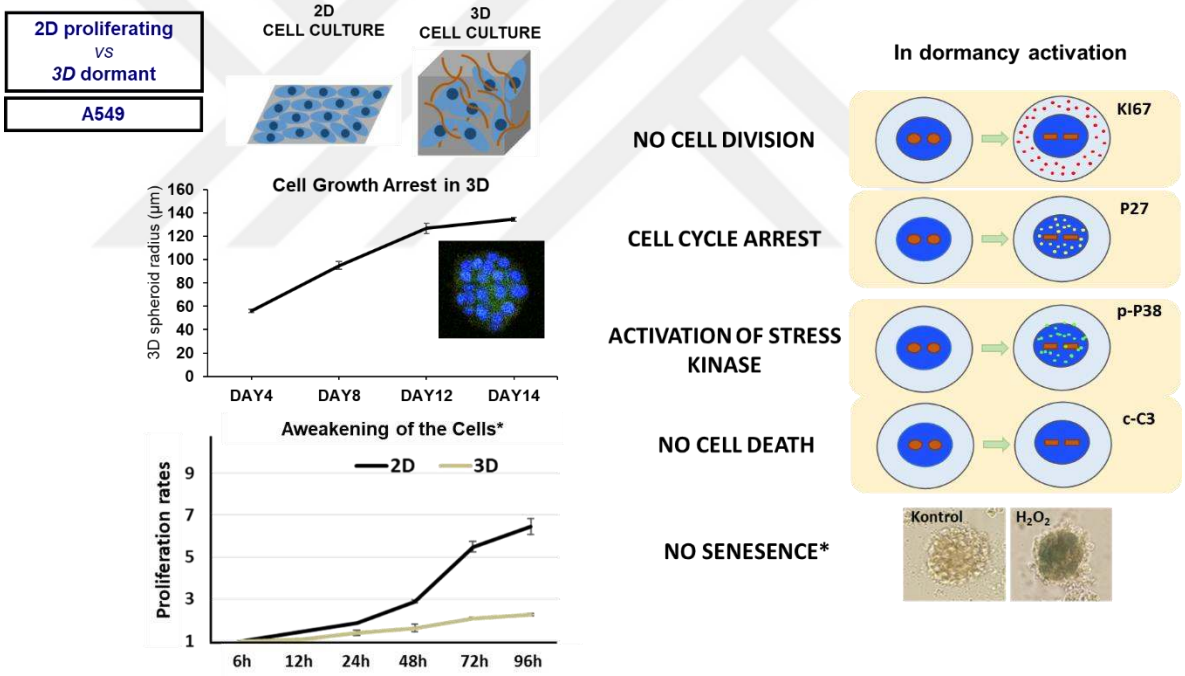

Figure 3:2 The in vitro 3D Matrigel Cancer Dormancy Model.

3 independent experiments (n=3) were conducted by Dr. Yunus Akkoc and Dr. Nesibe Peker. Representative results are shown. DAPI: DNA (core) marker (Blue); p27: Alexa fluor 568 red secondary antibody, p21: Alexa fluor 568 red secondary antibody, Active caspase-3 (c-C3): Alexa fluor 488 green secondary antibody, Ki-67: Alexa fluor 568 red secondary antibody. To test the possibility of senescence of some cells, beta-galactosidase staining was performed. As a positive control, spheroids were treated with 1µM hydrogen peroxide (H_2O_2) for 2 hours while in Matrigel.

It is expected that dormant cells will not divide actively. Ki-67 is a protein expressed in dividing cells. Ki-67 is widely used in the literature to show active mitotic cell levels in tumors. Active Ki-67 is found in the nuclei of cells. After staining, most (80-90%) of the spheroids are negative for Ki-67 protein in the nucleus. This result indicates that most cells forming the spheroids are not actively dividing. Positive phospho-p38 signal in the nucleus indicates a dormant state. It was determined that most of the cells forming the spheroids were Ki-67 negative and many cells had phospho-p38 protein signal in their nuclei (Figure 3.2).

The dormant cells do not divide, but they are not dead. Activated caspase-3 staining shows apoptotic cells. Caspases, which are stimulated after the apoptotic death signal, cleave, and activate caspases, including active caspase 3. This activity initiates programmed cell death that targets other vital proteins and even DNA. No active caspase-3 signaling was observed in cells in the spheroids. As a result, although the cells in the spheroids did not divide, they were not apoptotic and were alive (Figure 3.2).

There are data showing that autophagic activity increases in dormant cells. LC3 is a marker of autophagy and the increased form of LC3-II in the cytoplasm indicates autophagic activity. The level of autophagy in the spheroids was analyzed with an antibody recognizing the LC3-II form. It was determined that LC3-II levels were high in cells and the protein showed a dense but granular distribution, indicating autophagic vesicle accumulation. It has been also observed that when the spheroids were cultured from the dormancy stimulating medium (low glucose DMEM, 2% FBS) to the rich medium (10% FBS), it was determined that the cells started to divide again, that is, the spheroids were reversible (Figure 3.2). Lastly, Beta-galactosidase staining was performed to test the possibility of senescence of some cells. Under these conditions, no notable staining was observed in the A549 spheroids (4-6% beta galactosidase positive) (Figure 3.2).

At the end of the 14th day, spheroids were purified from Matrigel, treated with trypsin, and cultured in the rich nutrient medium. It was observed that dormant A549 cells did not grow during the first 24 hours after 2D culture in rich media. However, it was observed that cells started to grow actively after 24 hours. Cells actively grown in 2D culture and never dormant were used as controls. It has been observed that the dormant cells awaken and divide actively when cultured in a suitable environment for growth. As

a result, the awakening of dormant micro metastases that cause macro metastases in the clinic is modelled in this system.

In our system, dormancy, growth arrest after 12-14 days of 3D culture, formation of regular and tight spheroids, molecularly, p27 accumulation in the nucleus, Ki-67 negativity, absence of apoptosis (active caspase-3 negativity), autophagy activation (LC3-II accumulation) and phospho-P38 accumulation. Cells were not in senescence. Spheroids are reversible. They start to divide again when the condition is suitable. In conclusion, it has been shown that A549 cells are dormant in the Matrigel 3D culture system under the experimental conditions.

3.2 Identification of the in vitro 3D Matrigel Cancer Dormancy Model by qRT-PCR

In the literature, markers associated with dormancy have been used in immunofluorescence staining to characterize cells (KI-67, p27, p38, LC3, c-caspase-3). However, certain genes were confirmed in accordance with the RNA-Seq and qPCR results to avoid immunofluorescence each time (high-cost) and to confirm dormant cells more easily. Measurements of spheroid morphology and growths and qPCR were checked each time for these genes and correlated with each other (Figure3:3).

Table 3:1 RNA-Seq results of Selected Dormancy Markers

Gene	Gene Name	Fold Change 3D to 2D	P-val
PCNA	Proliferating cell nuclear antigen	0,388878215	$3{,}30\text{x}10^{-10}$
MKI67	Marker of proliferation Ki-67	0,029586731	$1{,}94\text{x}10^{-73}$
MCM2	Minichromosome maintenance complex component 2	0,230443817	$6{,}53\text{x}10^{-18}$
MCM6	Minichromosome maintenance complex component 6	0,16383595	$7{,}52\text{x}10^{-31}$
CDK1	Cyclin dependent kinase 1	0,053342217	$2{,}63\text{x}10^{-52}$
FN1	Fibronectin 1	4,033477843	$6{,}21\text{x}10^{-16}$

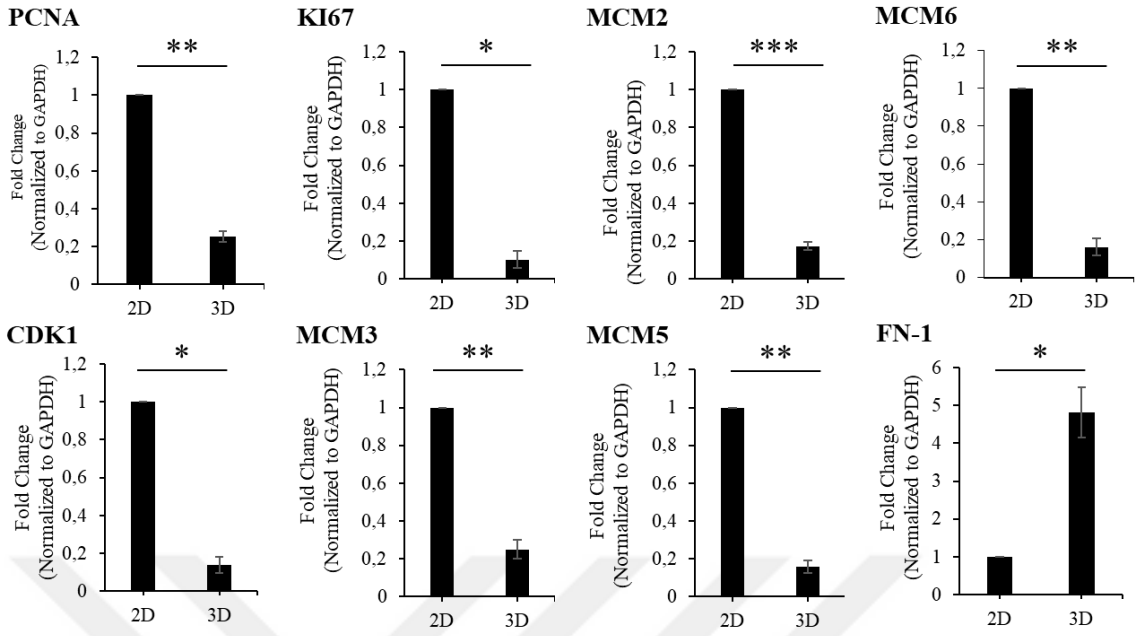

Figure 3:3 qPCR Analysis for dormancy markers.

Gene expressions were compared in A549 cells grown on 3D Matrigel for 14 days and in A549 cells grown in 2D cell culture. Graphs were created by averaging 4 independent experiments (n=4). ns, p-value > 0.05; *, p-value < 0.05; **, p-value < 0.01; ***, p-value < 0.001. FN1: Fibronectin-1, CDK1: Cyclin Dependent Kinase-1, MCM2: Mini-Chromosome Maintance-2 protein.

3.3 Omics Analyzes of 3D Dormant versus 2D Proliferating A549 Cells

3.3.1 RNA Sequencing (RNA-Seq) Analysis

Quality control results performed prior to miRNA sequencing are shown in Table 3.1

Table 3:2 Adapter sequences and quality values detected during the quality assessment before the RNA-Seq method.

Sample Name	Number of Reads	R1 Q20%	R1 Q30%	R1 GC%
2D-WT-1	62,276,431	99	91	48
2D-WT-2	54,394,643	99	92	48
3D-WT-1	60,138,648	99	92	49
3D-WT-2	50,002,764	99	92	49

Genes with a significance (p-value < 0.05) and showing at least a 2-fold upregulation or downregulation compared to the control condition were evaluated as "dormancy-related genes" (Up-regulated: 3483; Down-regulated: 3784, a total of 7267 genes) (Figure 3.3)

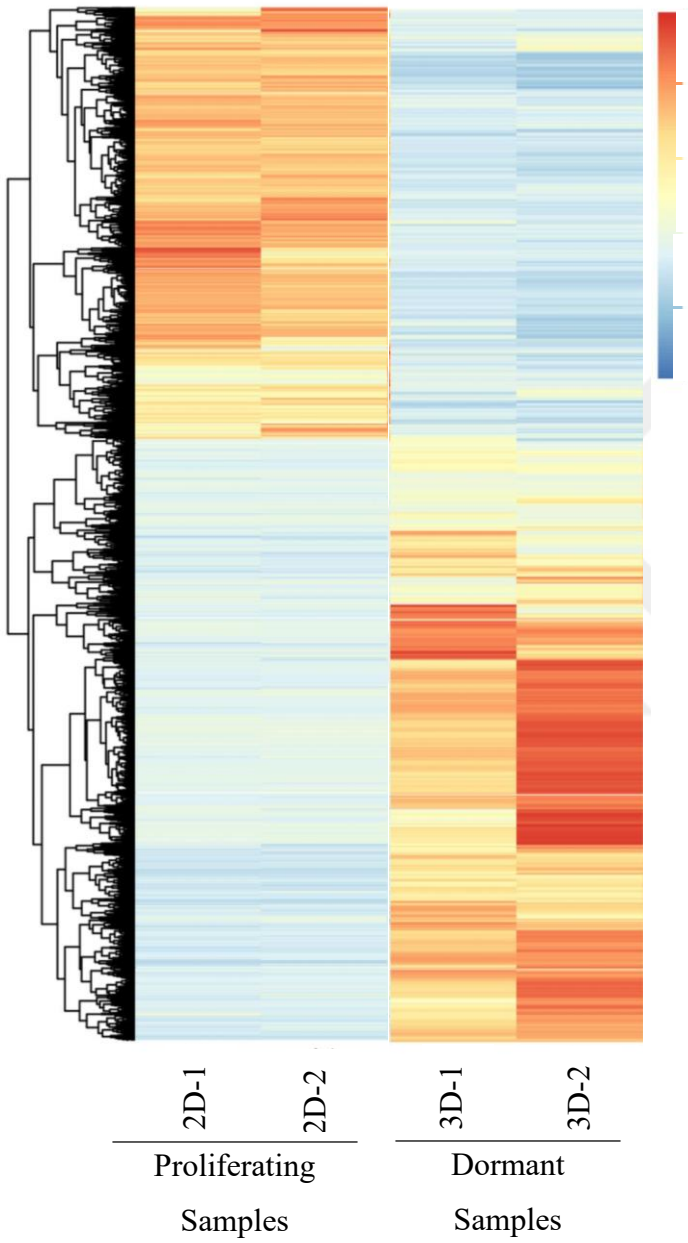

Figure 3:4 Heatmap of RNA-Seq Analysis.

All significantly differentially expressed genes (p-value < 0.05 and the fold change is 2-fold) are shown. The gene expression levels in each sample were assessed by reads aligned to the human GRCh38 reference genome and following the methods described in Nature Protocols (Pertea M. et al., 2016). The gene expression level in the proliferating samples (2D WT1 and 2D WT2) and the dormant samples (3D WT1 and 3D WT2) were compared using the program DESeq2, which produced the adjusted p-value for the comparison.

3.3.2 Proteomics Analysis

The statistical analysis revealed that the expression of a total of 1245 proteins significantly changed in the dormant state. The fold change threshold was determined as 1,5-fold-change and above for up-regulated miRNAs and 0.66 and below for down-regulated miRNAs. As result, the expression of 172 proteins increased and the expression of 287 proteins decreased in the dormant state compared to the proliferating state.

3.3.3 MicroRNA Sequencing (miR-Seq) Analysis

Quality control results performed prior to miR-Seq are shown in Table 3.1.

Table 3:3 Adapter sequences and quality values detected during the quality assessment before the miRNA-Seq method.

Sample Name	Number of Reads	R1 Q20%	R1 Q30%	R1 GC%
2D-WT-1	11,703,237	99	29	44
2D-WT-2	21,146,398	99	29	43
2D-WT-3	14,166,148	99	30	43
3D-WT-1	10,653,391	99	36	45
3D-WT-2	8,449,328	99	36	45
3D-WT-3	15,684,417	99	36	44

Significantly up- and down-regulated miRNAs in 3D dormant cells compared to 2D proliferating cells were given in Table 3.2 (p-values<0,05). It was decided to focus on miRNAs that increased 2-fold.

Table 3:4 : Fold Changes and p-values of miRNAs in 3D dormant cells comparing to 2D proliferating cells.

Gene	Approved Names	Fold Change	p-value
hsa-mir-1290	microRNA 1290	3,516664663	0,00507056
hsa-mir-210	microRNA 210	2,78177667	$1{,}23 \times 10^{-08}$
hsa-mir-1224	microRNA 1224	2,686426357	0,033045265
hsa-mir-181a-2	microRNA 181a	1,993626094	0,032708946

hsa-mir-125a	microRNA 125a	1,737817874	$4{,}14x10^{-06}$
hsa-mir-10a	microRNA 10a	1,691198728	$3{,}95x10^{-05}$
hsa-let-7a-2	microRNA let-7a-2	1,509122897	$9{,}34x10^{-05}$
hsa-let-7a-3	microRNA let-7a-3	1,501332213	$9{,}44x10^{-05}$
hsa-let-7a-1	microRNA let-7a-1	1,479623685	0,000100712
hsa-let-7e	microRNA let-7e	1,418523179	0,000362274
hsa-mir-92b	microRNA 92b	1,415652947	0,021270103
hsa-mir-196a-2	microRNA 196a-2	1,374980117	0,015161222
hsa-mir-361	microRNA 361	1,367491314	0,038432829
hsa-mir-125b-1	microRNA 125b-1	1,362980475	0,028796157
hsa-let-7b	microRNA let-7b	1,357369569	0,002618505
hsa-let-7f-1	microRNA let-7f-1	1,345308003	0,000949357
hsa-mir-196a-1	microRNA 196a-1	1,335238379	0,013260055
hsa-let-7c	microRNA let-7c	1,3196774	0,007268019
hsa-let-7f-2	microRNA let-7f-2	1,319360795	0,002333802
hsa-mir-183	microRNA 183	1,268269638	0,031853566
hsa-mir-30a	microRNA 30a	1,240216682	0,033674689
hsa-mir-23b	microRNA 23b	0,842826515	0,036182136
hsa-mir-191	microRNA 191	0,819301352	0,02985056
hsa-mir-12136	microRNA 12136	0,7506867	0,041488375
hsa-mir-25	microRNA 25	0,746195568	0,000620422
hsa-mir-29a	microRNA 29a	0,744075815	0,041258291
hsa-mir-23a	microRNA 23a	0,738800393	0,000675086
hsa-mir-31	microRNA 31	0,733498453	0,002868899
hsa-mir-24-2	microRNA 24-2	0,727388317	0,001069452
hsa-let-7d	microRNA let-7d	0,72634694	0,000819901
hsa-mir-221	microRNA 221	0,714672015	0,007522648
hsa-mir-425	microRNA 425	0,693068164	0,015860645
hsa-mir-151a	microRNA 151a	0,689846227	0,000384138
hsa-mir-16-2	microRNA 16-2	0,687808701	0,018001691
hsa-mir-34a	microRNA 34a	0,682033518	0,033309969
hsa-mir-140	microRNA 140	0,681457334	0,017074483

hsa-mir-324	microRNA 324	0,677132292	0,004079943
hsa-mir-15b	microRNA 15b	0,672048893	0,001148526
hsa-mir-192	microRNA 192	0,665141939	0,000252161
hsa-mir-126	microRNA 126	0,662642913	0,001518436
hsa-let-7i	microRNA let-7i	0,660117682	0,000215507
hsa-mir-16-1	microRNA 16-1	0,646653808	0,008681441
hsa-mir-32	microRNA 32	0,646378602	0,007162611
hsa-mir-335	microRNA 335	0,646160008	0,026215668
hsa-mir-146b	microRNA 146b	0,638450886	0,016833533
hsa-mir-505	microRNA 505	0,637927997	0,008426141
hsa-mir-93	microRNA 93	0,636255147	0,000105525
hsa-mir-744	microRNA 744	0,626382969	0,007319768
hsa-mir-106b	microRNA 106b	0,623655777	0,000608275
hsa-mir-877	microRNA 877	0,618164835	0,011647266
hsa-mir-421	microRNA 421	0,609366139	0,010717873
hsa-mir-138-1	microRNA 138-1	0,60282476	0,035806459
hsa-mir-625	microRNA 625	0,599669547	0,001099648
hsa-mir-1908	microRNA 1908	0,574310931	0,00081796
hsa-mir-454	microRNA 454	0,559157391	$5{,}36\text{x}10^{-05}$
hsa-mir-148b	microRNA 148b	0,53381486	0,044052999
hsa-mir-378a	microRNA 378a	0,508957387	0,001431199
hsa-mir-1275	microRNA 1275	0,506960236	0,02505606
hsa-mir-130b	microRNA 130b	0,496798365	$5{,}55\text{x}10^{-06}$
hsa-mir-185	microRNA 185	0,489664623	$1{,}38\text{x}10^{-06}$
hsa-mir-6724-4	microRNA 6724-4	0,463743179	0,000555426
hsa-mir-6724-1	microRNA 6724-1	0,447858952	$2{,}93\text{x}10^{-05}$
hsa-mir-330	microRNA 330	0,447712456	0,019238135
hsa-mir-138-2	microRNA 138-2	0,447475879	0,032170617
hsa-mir-629	microRNA 629	0,446025381	0,001751922
hsa-mir-33a	microRNA 33a	0,427771141	0,02204706
hsa-mir-1304	microRNA 1304	0,419163554	0,043825992
hsa-mir-7-1	microRNA 7-1	0,418646298	$1{,}14\text{x}10^{-08}$

hsa-mir-19b-2	microRNA 19b-2	0,416975869	$1,44x10^{-08}$
hsa-mir-6724-2	microRNA 6724-2	0,416229367	$7,34x10^{-06}$
hsa-mir-6724-3	microRNA 6724-3	0,414710915	$4,89x10^{-06}$
hsa-mir-452	microRNA 452	0,396803072	$6,12x10^{-07}$
hsa-mir-20a	microRNA 20a	0,391703023	0,006132053
hsa-mir-19b-1	microRNA 19b-1	0,384479565	$4,45x10^{-10}$
hsa-mir-374a	microRNA 374a	0,382258029	0,022515191
hsa-mir-1180	microRNA 1180	0,369025407	0,016869773
hsa-mir-101-1	microRNA 101-1	0,351800933	0,000382605
hsa-mir-376c	microRNA 376c	0,350978384	0,031739154
hsa-mir-590	microRNA 590	0,348871237	0,000765966
hsa-mir-130a	microRNA 130a	0,347591347	$5,54x10^{-18}$
hsa-mir-17	microRNA 17	0,338707972	$1,42x10^{-15}$
hsa-mir-101-2	microRNA 101-2	0,318740097	$2,59x10^{-05}$
hsa-mir-7-3	microRNA 7-3	0,305962106	$2,25\ x10^{-05}$
hsa-mir-671	microRNA 671	0,298699912	0,005677395
hsa-mir-188	microRNA 188	0,276063837	0,000398761
hsa-mir-542	microRNA 542	0,276018568	0,008087266
hsa-mir-2278	microRNA 2278	0,274272	0,049192833
hsa-mir-19a	microRNA 19a	0,236804444	$3,61x\ 10^{-10}$
hsa-mir-942	microRNA 942	0,227379587	0,038174197
hsa-mir-424	microRNA 424	0,214709553	$3,75x10^{-35}$
hsa-mir-106a	microRNA 106a	0,209497042	0,002298256
hsa-mir-585	microRNA 585	0,18499873	0,000700791
hsa-mir-33b	microRNA 33b	0,177778252	0,000557457
hsa-mir-362	microRNA 362	0,177206418	0,001110805
hsa-mir-190a	microRNA 190a	0,167836639	$5,72x\ 10^{-07}$
hsa-mir-301a	microRNA 301a	0,157213948	$1,20x\ 10^{-07}$

The statistical analysis revealed that the expression of a total of 96 miRNAs significantly changed in the dormant state. The fold change threshold was determined as 2-fold-change and above for up-regulated miRNAs and 0.5 and below for down-regulated

miRNAs. As results, the expression of 4 miRNAs increased and the expression of 40 miRNAs decreased in the dormant state compared to the proliferating state.

3.4 First target analyzes of up-regulated miRNAs with the online tool "TargetScan"

MiRNA target analyzes were performed with the TargetScan online tool by selecting 4 miRNAs whose expression increased at least 2 times. The target genes from the online database were crossed with genes from RNA-Seq and proteomics results. Theoretically, miRNAs are known to affect and generally decrease the expression of their target genes. Therefore, for upregulated miRNAs, target gene mRNAs should be among genes with decreased expression (0.5-fold or less) in the RNA-Seq and proteomic analyzes. The putative targets of up-regulated miRNAs whose expression is decreased in RNA-Seq and proteomic analyzes are shown in Table 3.3.

Table 3:5 Up-regulated four miRNAs and their putative targets found to be down-regulated in RNA sequencing and Proteomics analysis.

Target Gene	**miRNA**	**Gene Name**	**mRNA fold change**	**Proteomics fold change**
AHNAK	hsa-mir-1224	AHNAK nucleoprotein	0,291437952	0,274829497
	hsa-mir-181a-2			
ANP32B	hsa-mir-1290	acidic (leucine-rich) nuclear phosphoprotein 32 family, member B	0,451465176	0,196735252
ANXA1	hsa-mir-181a-2	annexin A1	0,364493197	0,346178788
ATP2A2	hsa-mir-1224	ATPase, Ca++ transporting, cardiac muscle, slow twitch 2	0,453652308	0,129441071
	hsa-mir-181a-2			
BZW1	hsa-mir-1224	basic leucine zipper and W2 domains 1	0,435375716	0,436904359
	hsa-mir-1290			
	hsa-mir-181a-2			
CACYBP	hsa-mir-1290	calcyclin binding protein	0,345866686	0,139147227
	hsa-mir-1224			
CAND1	hsa-mir-1224		0,440862902	0,180182086

	hsa-mir-1290 hsa-mir-181a-2	cullin-associated and neddylation-dissociated 1		
CAPZA1	hsa-mir-181a-2 hsa-mir-210 hsa-mir-1224 hsa-mir-1290	capping protein (actin filament) muscle Z-line, alpha 1	0,326756446	0,378375405
CAV1	hsa-mir-1224 hsa-mir-181a-2	caveolae protein, 22kDa	0,092132235	0,367839739
CAV2	hsa-mir-1290	caveolin 2	0,346436472	0,249506143
CBX3	hsa-mir-1290 hsa-mir-1224 hsa-mir-181a-2	chromobox homolog 3	0,228463613	0,429077332
CELF1	hsa-mir-1224 hsa-mir-1290 hsa-mir-181a-2 hsa-mir-210	CUGBP, Elav-like family member 1	0,43454722	0,482095714
CMPK1	hsa-mir-181a-2	cytidine monophosphate (UMP-CMP) kinase 1, cytosolic	0,494477613	0,242112691
CORO1C	hsa-mir-1290 hsa-mir-181a-2	coronin, actin binding protein, 1C	0,449668248	0,178176769
CTPS1	hsa-mir-1224 hsa-mir-181a-2	CTP synthase 1	0,27445847	0,374189379
DDX21	hsa-mir-1290 hsa-mir-181a-2	DEAD (Asp-Glu-Ala-Asp) box helicase 21	0,23727649	0,066195086
DDX46	hsa-mir-1290 hsa-mir-1224 hsa-mir-181a-2	DEAD (Asp-Glu-Ala-Asp) box polypeptide 46	0,289593496	0,091378169
DDX6	hsa-mir-1290 hsa-mir-1224	DEAD (Asp-Glu-Ala-Asp) box helicase 6	0,371507339	0,324110605
DEK	hsa-mir-1224 hsa-mir-1290 hsa-mir-181a-2	DEK oncogene	0,145711107	0,35552203
EIF3J	hsa-mir-1224		0,298389933	0,449524938

	hsa-mir-1290	eukaryotic translation initiation factor 3, subunit J		
EIF4A1	hsa-mir-1224	eukaryotic translation initiation factor 4A1	0,30215723	0,25515452
EIF5	hsa-mir-1290	eukaryotic translation initiation factor 5	0,429342799	0,122332936
FAM49B	hsa-mir-210	family with sequence similarity 49, member B	0,497640103	0,317025702
FARSB	hsa-mir-181a-2	phenylalanyl-tRNA synthetase, beta subunit	0,395005506	0,253285379
	hsa-mir-210			
	hsa-mir-1224			
G3BP1	hsa-mir-1224	GTPase activating protein (SH3 domain) binding protein 1	0,398607332	0,279848357
	hsa-mir-1290			
	hsa-mir-210			
	hsa-mir-181a-2			
GGH	hsa-mir-1290	subunit 1, 155kDa gamma-glutamyl hydrolase (conjugase, folylpolygammaglutamyl hydrolase)	0,399561872	0,228715779
HNRNPA2B1	hsa-mir-1224	heterogeneous nuclear ribonucleoprotein A2/B1	0,294802731	0,242960492
	hsa-mir-181a-2			
HNRNPA3	hsa-mir-1224	heterogeneous nuclear ribonucleoprotein A3	0,254979316	0,279720743
HNRNPR	hsa-mir-1224	heterogeneous nuclear ribonucleoprotein R	0,297888088	0,120218805
	hsa-mir-181a-2			
HPRT1	hsa-mir-1290	hypoxanthine phosphoribosyltransferase 1	0,346596539	0,251307301
	hsa-mir-181a-2			
HSPA4	hsa-mir-1224	heat shock 70kDa protein 4	0,494564289	0,00984129
IPO5	hsa-mir-1290	importin 5	0,386939809	0,464171778
	hsa-mir-181a-2			
	hsa-mir-1224			

	hsa-mir-181a-2			
IPO7	hsa-mir-1224	importin 7	0,345607782	0,059280925
ITGAV	hsa-mir-1290	integrin, alpha V	0,217857281	0,257575844
	hsa-mir-210			
	hsa-mir-1224			
	hsa-mir-181a-2			
KPNA2	hsa-mir-1224	karyopherin alpha 2 (RAG cohort 1, importin alpha 1)	0,22291486	0,081854342
	hsa-mir-1290			
	hsa-mir-210			
KPNB1	hsa-mir-1290	karyopherin (importin) beta 1	0,358286527	0,294960838
LARS	hsa-mir-1224	leucyl-tRNA synthetase	0,494610031	0,100755279
LRPPRC	hsa-mir-1224	leucine-rich pentatricopeptide repeat containing	0,432539399	0,143525372
	hsa-mir-181a-2			
LUC7L2	hsa-mir-181a-2	LUC7-like 2 (S. cerevisiae)	0,482652779	0,423681434
LUC7L3	hsa-mir-1224	LUC7-like 3 (S. cerevisiae)	0,387524319	0,285429048
	hsa-mir-181a-2			
	hsa-mir-181a-2			
MAGOHB	hsa-mir-181a-2	mago-nashi homolog B (Drosophila)	0,46325487	0,489104294
MAP1B	hsa-mir-1224	microtubule-associated protein 1B	0,343760609	0,042583616
	hsa-mir-181a-2			
	hsa-mir-1224			
	hsa-mir-1290			
MCM5	hsa-mir-1290	minichromosome maintenance complex component 5	0,26007119	0,052791962
	hsa-mir-1224			
NCL	hsa-mir-181a-2	nucleolin	0,335270208	0,22411393
	hsa-mir-1290			
NPM1	hsa-mir-1224	nucleophosmin (nucleolar phosphoprotein B23, numatrin)	0,376182373	0,474209576
	hsa-mir-1290			
NUP160	hsa-mir-181a-2	nucleoporin 160kDa	0,333604119	0,497949933

	hsa-mir-1290			
NUP205	hsa-mir-181a-2	nucleoporin 205kDa	0,302810867	0,105351392
PAICS	hsa-mir-1224	phosphoribosylaminoimidazole carboxylase, phosphoribosylaminoimidazole succinocarboxamide synthetase	0,328304257	0,241738475
	hsa-mir-1290			
	hsa-mir-210			
	hsa-mir-181a-2			
PLS3	hsa-mir-1224	plastin 3	0,42666388	0,164314159
PNN	hsa-mir-1224	pinin, desmosome associated protein	0,226145722	0,498167447
	hsa-mir-181a-2			
PRKDC	hsa-mir-181a-2	DNA-activated, catalytic polypeptide	0,23727649	0,066195086
SERBP1	hsa-mir-1224	SERPINE1 mRNA binding protein 1	0,382732682	0,49889179
	hsa-mir-181a-2			
SET	hsa-mir-1224	SET nuclear oncogene	0,337288768	0,288087386
	hsa-mir-1290			
	hsa-mir-181a-2			
SF3B1	hsa-mir-1290	splicing factor 3b, subunit 1, 155kDa	0,41545627	0,421488401
	hsa-mir-1290			
SMC1A	hsa-mir-1224	structural maintenance of chromosomes 1A	0,32173374	0,167802024
	hsa-mir-1290			
	hsa-mir-181a-2			
SPTBN1	hsa-mir-1224	spectrin, beta, non-erythrocytic 1	0,481490796	0,108250541
SRSF11	hsa-mir-1224	serine/arginine-rich splicing factor 11	0,365025991	0,270138518
	hsa-mir-1290			
	hsa-mir-181a-2			
SYNCRIP	hsa-mir-181a-2	synaptotagmin binding, cytoplasmic RNA interacting protein	0,311978589	0,120206302
TFRC	hsa-mir-1290	transferrin receptor	0,458298942	0,375892227
TXNRD1	hsa-mir-1290	thioredoxin reductase 1	0,474386585	0,132754794
UGGT1	hsa-mir-1224		0,462887448	0,213207268
	hsa-mir-1290			

	hsa-mir-181a-2	UDP-glucose glycoprotein glucosyltransferase 1		

Some genes are targeted by more than one miRNA. These putative target genes are previously associated with cell growth, cell cycle, cancer metastasis and invasion etc. were determined. These genes and their functions related to cancer according to the literature are listed in Table 3.4

Table 3:6 Putative Targets and Their Functions

Genes	miRNAs	Function	Reference
ANP32B	hsa-mir-1290	Cell Growth	Yang et al., 2016; Reilly et al, 2011
ANXA1	hsa-mir-181a-2	Cancer migration and invasion Cell Cycle and Cell Growth	Liu et al., 2015; Hasan et al, 2020; Li et al.; 2020, Khau et al, 2011
ATP2A2	hsa-mir-1224, hsa-mir-181a-2	Cell Cycle, Cell Growth and Cancer Migration	Yang et al., 2015; Lassmann et al., 2007; Crépin et al, 2007; Fan et al., 2014
BZW1	hsa-mir-1290, hsa-mir-1224, hsa-mir-181a-2	Cancer Migration and Invasion, Cell Cycle and Cell Growth	Chiou et al., 2019; Li et al., 2009; Liu et al., 2018; Xu et al., 2020
CACYBP	hsa-mir-1290, hsa-mir-1224	Cell cycle and Cell Growth	Zhai et al, 2017; Niu et al, 2016; Shi et al, 2014; Zhao et al, 2020; Chen et al, 2011
CAND1	hsa-mir-1290, hsa-mir-1224, hsa-mir-181a-2	Cell Cycle and Cancer Migration	Eigentler et al., 2020; Che et al., 2018; Kang et al., 2017; Qian ve ark., 2016
CAPZA1	hsa-mir-1290, hsa-mir-181a-2	Cancer Migration and Invasion	Huang et al., 2017
CBX3	hsa-mir-1224, hsa-mir-181a-2	Cell Growth and Cell Cycle	Zhang et al., 2018
CELF1	hsa-mir-1290, hsa-mir-1224, hsa-mir-210, hsa-mir-181a-2	Cell Growth and Cancer Migration	Wang et al., 2020; Xia et al. 2015

CORO1C	hsa-mir-1290, hsa-mir-181a-2	Cell Growth, Cancer Migration and Invasion	Mataki et al., 2015; Lim et al., 2017
DDX21	hsa-mir-181a-2	Cell Growth, Cell Cycle, Cancer Invasion and Drug-Resistance	Ambrosini et al., 2012; Cao et al., 2018
DDX46	hsa-mir-1224, hsa-mir-181a-2	Cell Growth, Autophagy and Cancer Invasion	Lin et al., 2020; Li et al., 2016; Jiang et al., 2017
DDX6	hsa-mir-1290, hsa-mir-1224	Cell Growth and Radiotherapy-Resistance	Taniguchi et al., 2018; Wang et al., 2015; Cho et al., 2016; Lin et al., 2008
DEK	hsa-mir-1224, hsa-mir-181a-2	Cell Growth, Cancer Invasion and Cell Cycle	Yang et al., 2020; Feng et al., 2017; Zhou et al., 2018
FAM49B	hsa-mir-210	Cell Growth	Zhang et al., 2020
G3BP1	hsa-mir-1290, hsa-mir-1224, hsa-mir-210, hsa- mir-181a-2	Cell Growth, Cancer Migration and Invasion	Zhang et al., 2019; Wang et al., 2018; Li et al., 2020
ITGAV	hsa-mir-1290, hsa-mir-1224, hsa-miR-125a	Cell Growth, Cancer Migration and Invasion	Ding et al., 2017; Luo et al., 2016; Morandi et al.,2016; Pei et al., 2019
MCM5	hsa-mir-1224	Cell Growth and Cell Cycle	Gong et al., 2019, Ryu et al., 2005, Mio et al.,, 2016
PAICS	hsa-mir-1290, hsa-mir-210, hsa- mir-1224	Cell Growth, Cell Cycle, Cancer Migration and Invasion	Meng et al., 2018; Agarwal et al., 2020; Chakravarthi et al., 2018
PNN	hsa-mir-1290	Cell Growth and Cancer Migration	Yang et al., 2016; Wei et al., 2016
PRKDC	hsa-mir-1290	Cell Growth, Cell Cycle, Cancer Migration	Sun et al., 2016; Zhang et al., 2019; Zhang et al., 2019; Zhang et al., 2017
SERBP1	hsa-mir-1290, hsa-mir-1224	Cell Growth and Cancer Migration	Zhao et al., 2018
SET	hsa-mir-1224	Cell Growth and Radiotherapy-Resistance	Almeida et al., 2014; Leopoldino et. al, 2012
SPTBN1	hsa-mir-1224	Cell Growth and Cancer Migration	Chen et al.,2020; Zhi et al., 2015

3.5 Confirmation of Omics Analyzes by q-RT-PCR

MiRNAs and putative target genes targeted by them, and miRNAs were analyzed bioinformatically. It was compared with RNA sequencing and proteomic analyzes to identify dormancy-related candidate genes. Subsequently, expression levels of candidate dormancy associate miRNAs and their targets were confirmed by q-RT-PCR in 3D dormant cells compared to 2D proliferating cells.

According to miR-Seq analysis, up-regulated miRNAs: MIR1290 and MIR210-5P was found to be significantly increased in 3D dormant state while no significant changes were observed in the expressions of MIR181A-5P and MIR181A-3P, MIR1224-5P and MIR1225-3P and, MIR210-3P. (Figure 3.4)

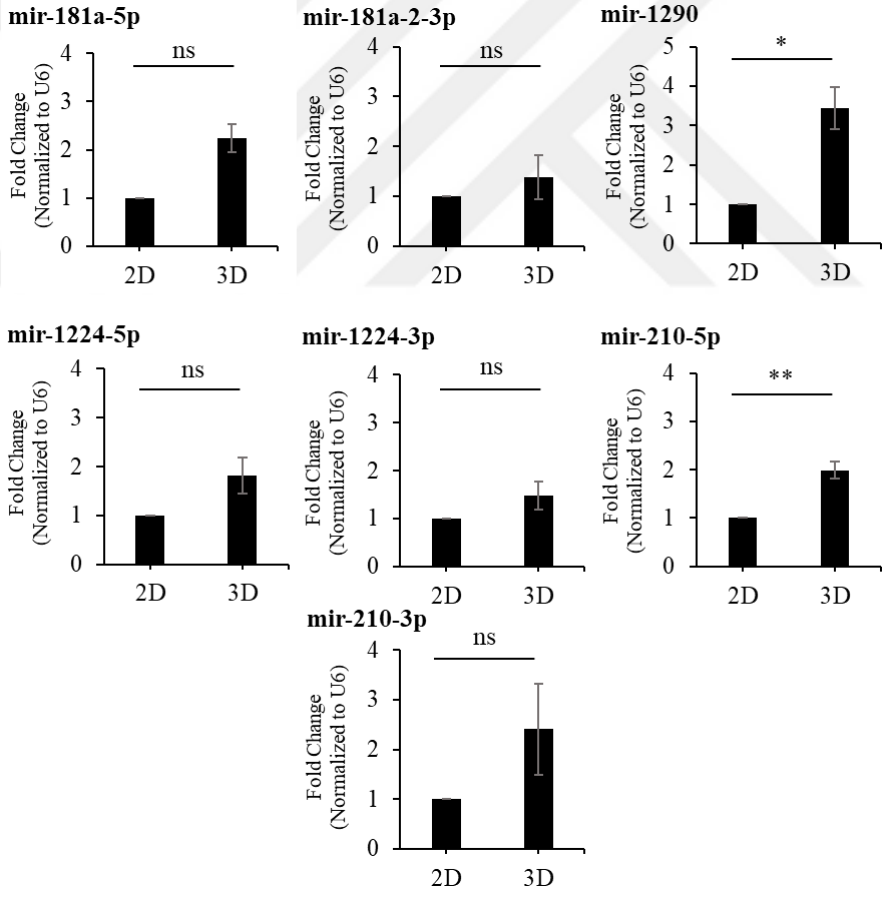

Figure 3:5 Confirmation by qPCR of the most up-regulated miRNAs in miR-Seq.

Gene expressions were compared in A549 cells grown on 3D Matrigel for 14 days and in A549 cells grown in 2D cell culture. Graphs were created by averaging 4 independent experiments (n=4). *, p-value >0.05; **, p-value > 0.01.

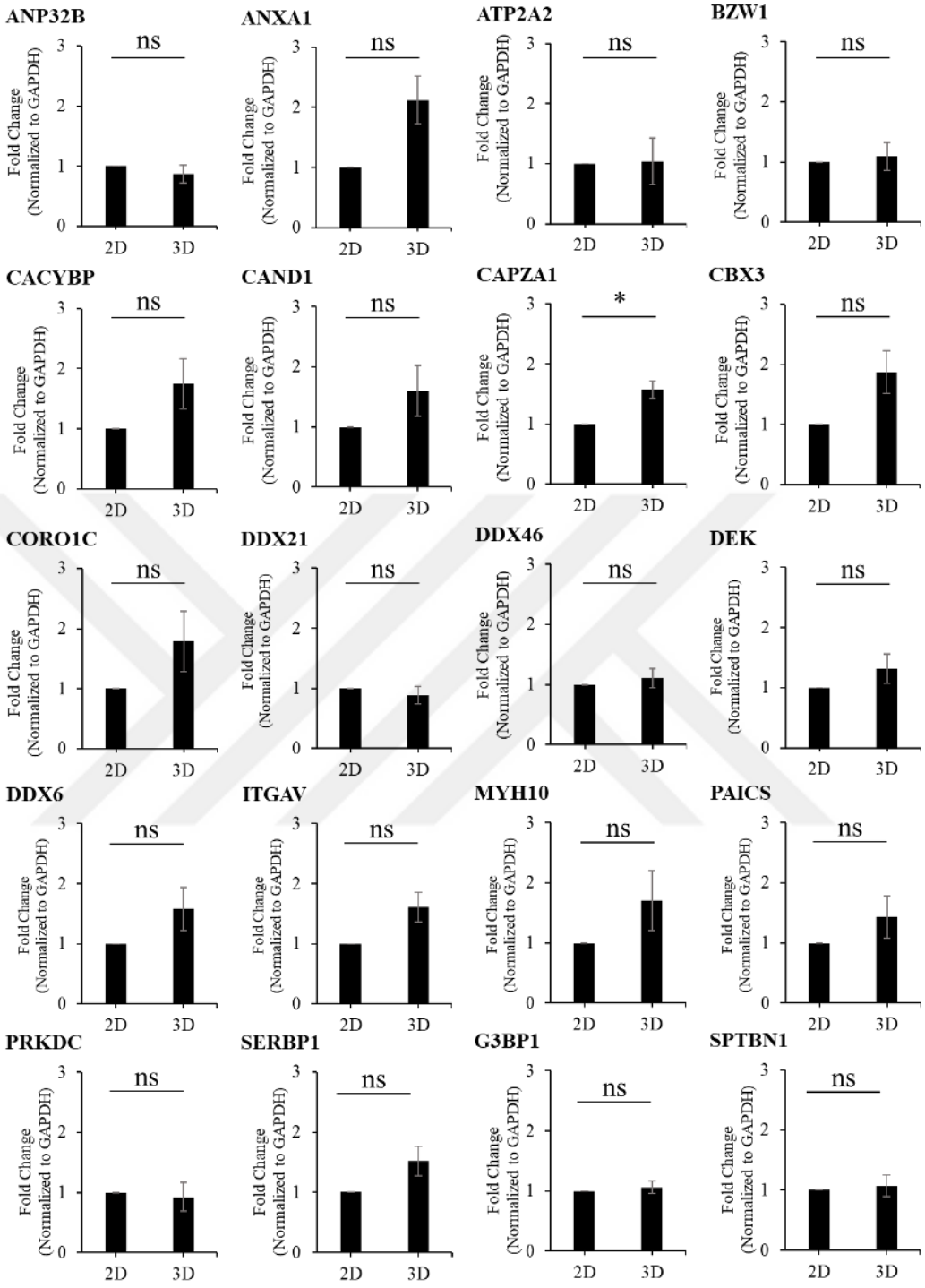

Figure 3:6 Confirmation of selected putative targets that targeted by up-regulated miRNAs.

Gene expressions were compared in A549 cells grown on 3D Matrigel for 14 days and in A549 cells grown in 2D cell culture. Graphs were created by averaging 4 independent experiments (n=4). ns, p-value > 0.05; *, p-value < 0.05.

In addition to confirming the up-regulated miRNAs in the 3D dormant state, these down-regulated miRNAs were also confirmed in the 3D Matrigel Dormancy model compared to 2D proliferate model.

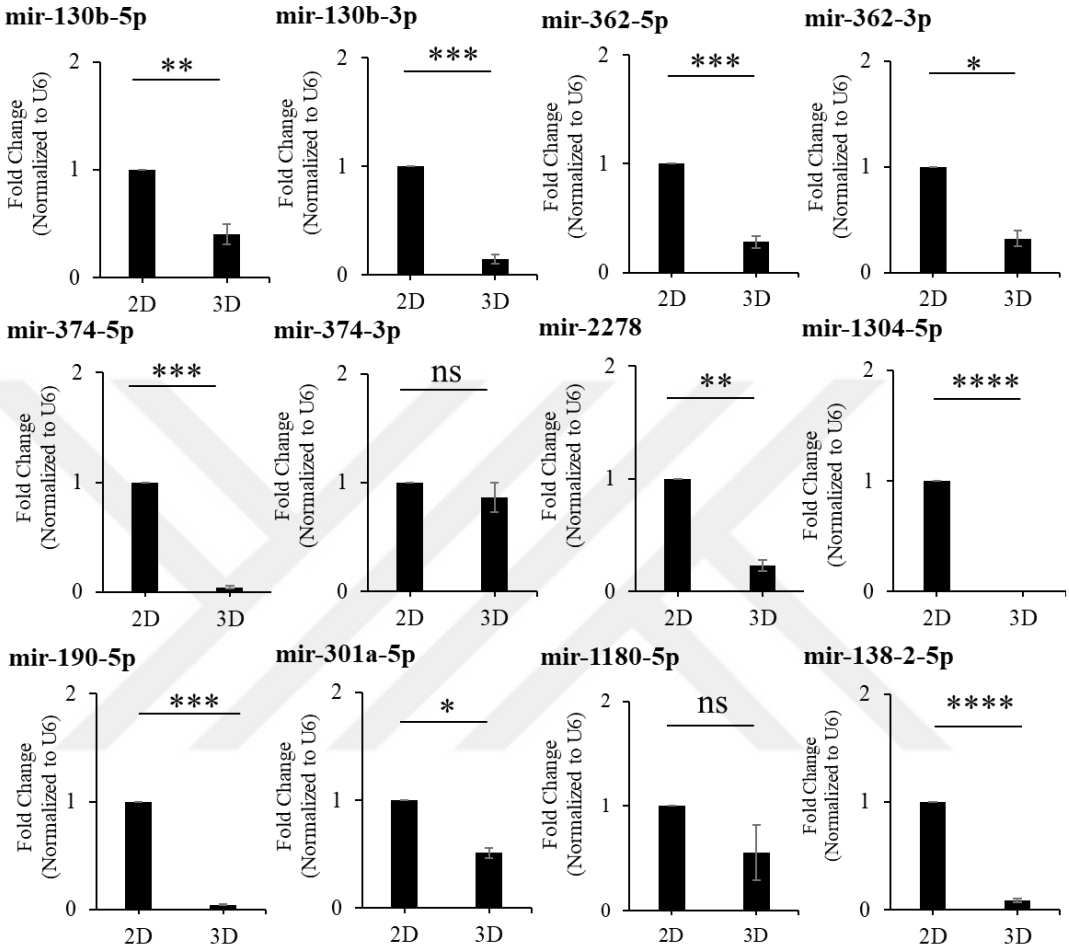

Figure 3:7 Confirmation by qPCR of the some down-regulated miRNAs in miR-Seq.

Gene expressions were compared in A549 cells grown on 3D Matrigel for 14 days and in A549 cells grown in 2D cell culture. Graphs were created by averaging 4 independent experiments (n=4). ns, p-value > 0.05; *, p-value < 0.05; **, p-value < 0.01; ***, p-value < 0.001; ****, p-value < 0.0001.

Down-regulated miRNAs: MIR130B-5P, MIR130B-3P, MIR362-5P, MIR362-3P, MIR374-5P, MIR2278, MIR1304-5P, MIR1304-5P, MIR190-5P, MIR301A-5P MIR138-2-5P was found to be significantly reduced while no significant changes were observed in the expressions of MIR374-3P and MIR1180-5P in 3D dormancy state.

3.6 Analysis of A549 MIR362 Overexpression Cells in Dormancy Model Compared to A549 WT Cells

It has been shown by many different methods that Mir362 is reduced in dormancy. To examine how mir362 affects the dormant behavior of cells, stable A549 cell lines overexpressing mir362 were successfully generated (Figure 3.8). Monoclones were obtained from the resulting polyclonal cell populations, and 10 clones were selected for testing among them. Selected monoclones derived from 2 different polyclones that significantly overexpress mir362 were selected based on qPCR results for further experiments (Mono-2: Overexpression Clone-1, OE-1 and mono-5: Overexpression Clone -2, OE-2).

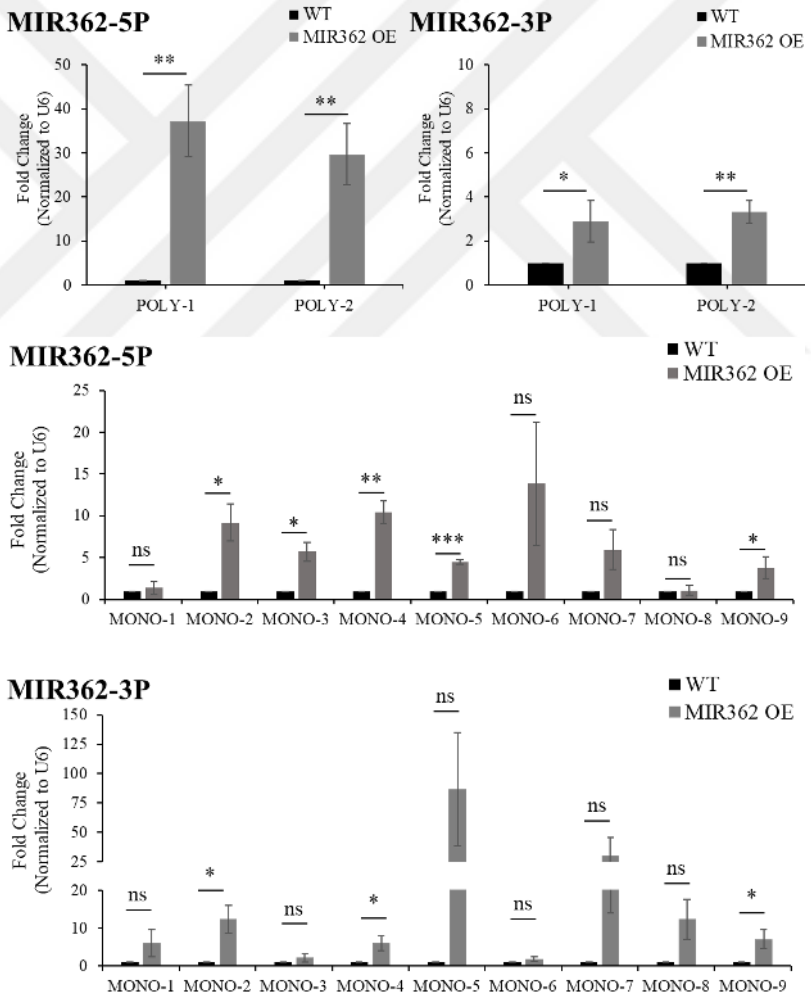

Figure 3:8 Confirmation by qPCR of overexpression of MIR362 genes after transduction of A549 cells.

A. Polyclonal, B. and C. Monoclonal. Graphs were created by taking the average of 3 independent experiments (n=3). ns, p-value > 0.05; *, p-value < 0.05; **, p-value < 0.01; ***, p-value < 0.001. Poly: Polyclonal Mono: Monoclonal.

MTT assay was performed for the effect of overexpression of MIR362 on the growth of cells. No significant changes were observed in the growth of MIR362 overexpressing cells (MIR 362 OEs) compared to WT cells (Figure 3:9 A). The effect of MIR362 on the dormancy model was investigated. The radius of the spheroids formed by the clones and WT cells observed for 14 days were measured. According to the results, it was observed that while WT cells formed tight and regular spheroids, MIR362 OE clones did not form similar structures. The structures formed by the MIR362 OE clones were scattered, disrupted and irregular (Figure 3:9 D and Figure 3:9 E). However, there is no significant difference in the radius of the structures (Figure 3:9 C).

Moreover, PCNA, CDK1, and KI67 expression levels of MIR362 OE clones were checked by qPCR and compared with WT cells. PCNA, CDK1 and KI67 expression levels were significantly reduced in WT and MIR362 overexpressing clones under dormant conditions. The reasons why the non-spheroid structures of MIR362 OE clones increase compared to WT and are irregularly distributed under dormancy conditions may be since MIR362 may target genes that play a role in the adhesion of cells and formation of tight and regular structures.

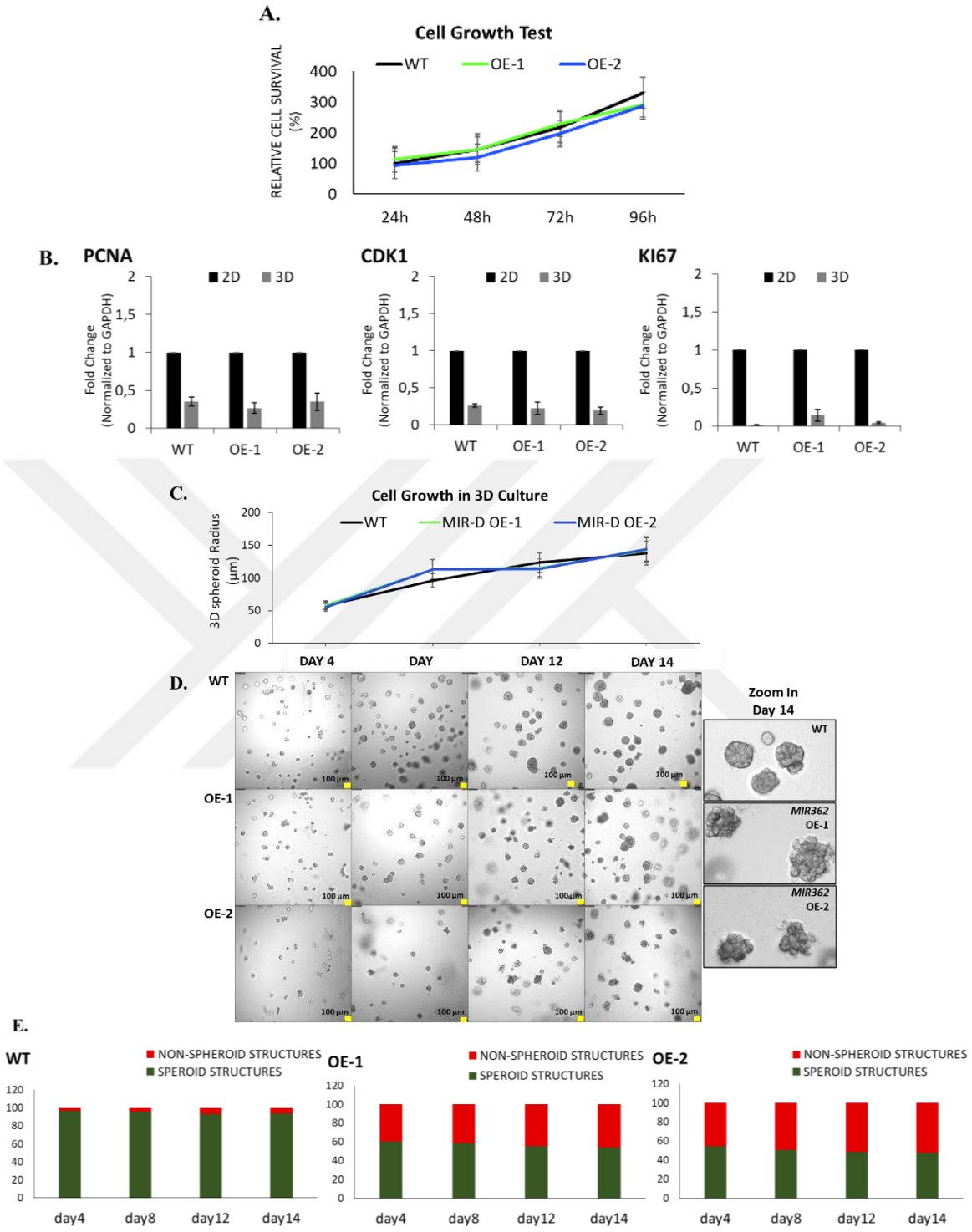

Figure 3:9. Investigation of dormancy behavior of A549 MIR362 overexpressed cells.

A. MTT Growth Test, B. qPCR results of selected dormancy markers, C. Radius of 3D spheroids, Cell Growth in dormancy model. D. Representative images captured by light microscope E. Ratio of spheroid and non-spheroids in 3D culture. 3 independent experiments (n=3) were conducted. **, p-value < 0.01; ***, p-value < 0.001.

OE: Overexpression clone, WT: Wildtype

3.7 Analysis of A549 MIR210 Knockout Cells in Dormancy Model Compared to A549 WT Cells

It has been shown by many different methods that Mir210 increases in dormancy. To examine how mir210 affects the dormant behavior of cells, stable A549 cell lines with deletion of the MIR210 gene were successfully generated by CRISPR/CAS9 method (Figure 3.9). Monoclones were obtained derived from the polyclonal cell populations, and 10 clones were selected for testing. It was selected based on the results of monoclone qPCR, where it significantly reduced mir210 (Mono-2: Knockout clone-1, KO-1). Further experiments for examination of the effect of the MIR210 in dormancy were performed with only one monoclone, as no significant reduction was seen in all the remaining monoclones except Mono-2 (Figure 3:10).

MTT test was performed for its effect on the growth of MIR210 KO cells. No significant changes were observed in MIR210 KO cells compared to WT cells (Figure 3:10 A). The effect of MIR210 on the dormancy model was investigated. The radius of the spheroids formed by the clones and WT cells observed for 14 days was measured. According to the results, it was observed that while WT cells formed tight and regular spheroid structures, they did not form similar structures in MIR210 KO clone. The structures formed by the MIR210 KO clone were observed to have smaller spheroid-like structures and increased dead-like populations (Figure 3:10 C, Figure 3:10 D and Figure 3:10 E).

Moreover, PCNA, CDK1, and KI67 expression levels of MIR210 KO clones were checked by qPCR and compared with WT cells. PCNA and KI67 expression levels were significantly reduced in WT and MIR210 KO clones under dormancy conditions. In contrast, there was no significant change in expression level in CDK1 MIR210 KO clones.

Under dormancy conditions, the non-spheroid structures of the MIR210 KO clone were increased compared to WT (Figure 3:10 E). However, unlike MIR362 OE clones, it was observed that MIR210 KO clones could not grow under dormancy conditions and even increased die-like structures. It can be said that MIR210 is a necessary miRNA for dormant cells to maintain themselves under certain conditions.

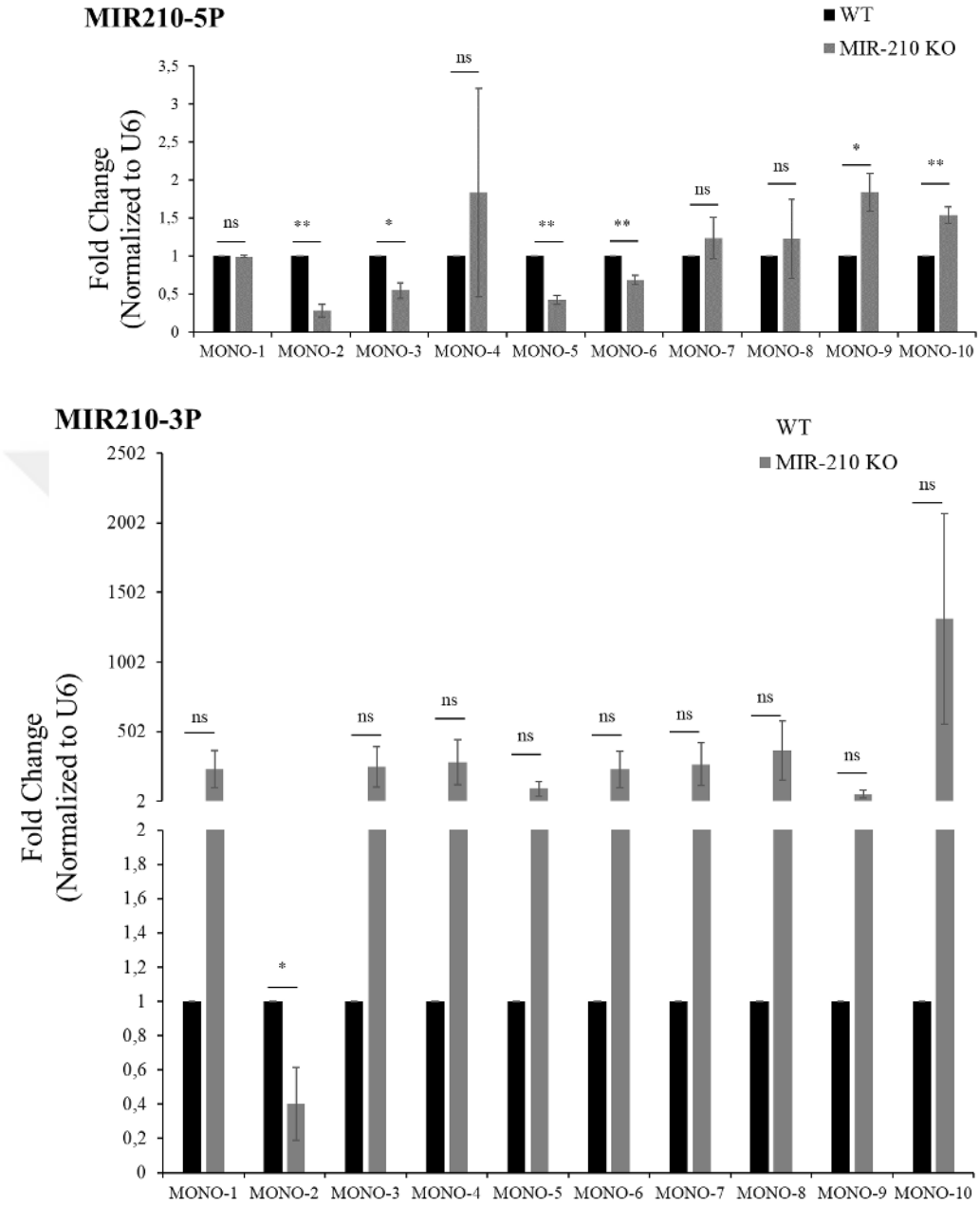

Figure 3:10 Confirmation by qPCR of knockout of *MIR210* genes after transduction of A549 cells.

Graphs were created by taking the average of 3 independent experiments (n=3). ns, p-value > 0.05; *, p-value < 0.05; **, p-value < 0.01

KO: Knock out, Mono: Monoclonal

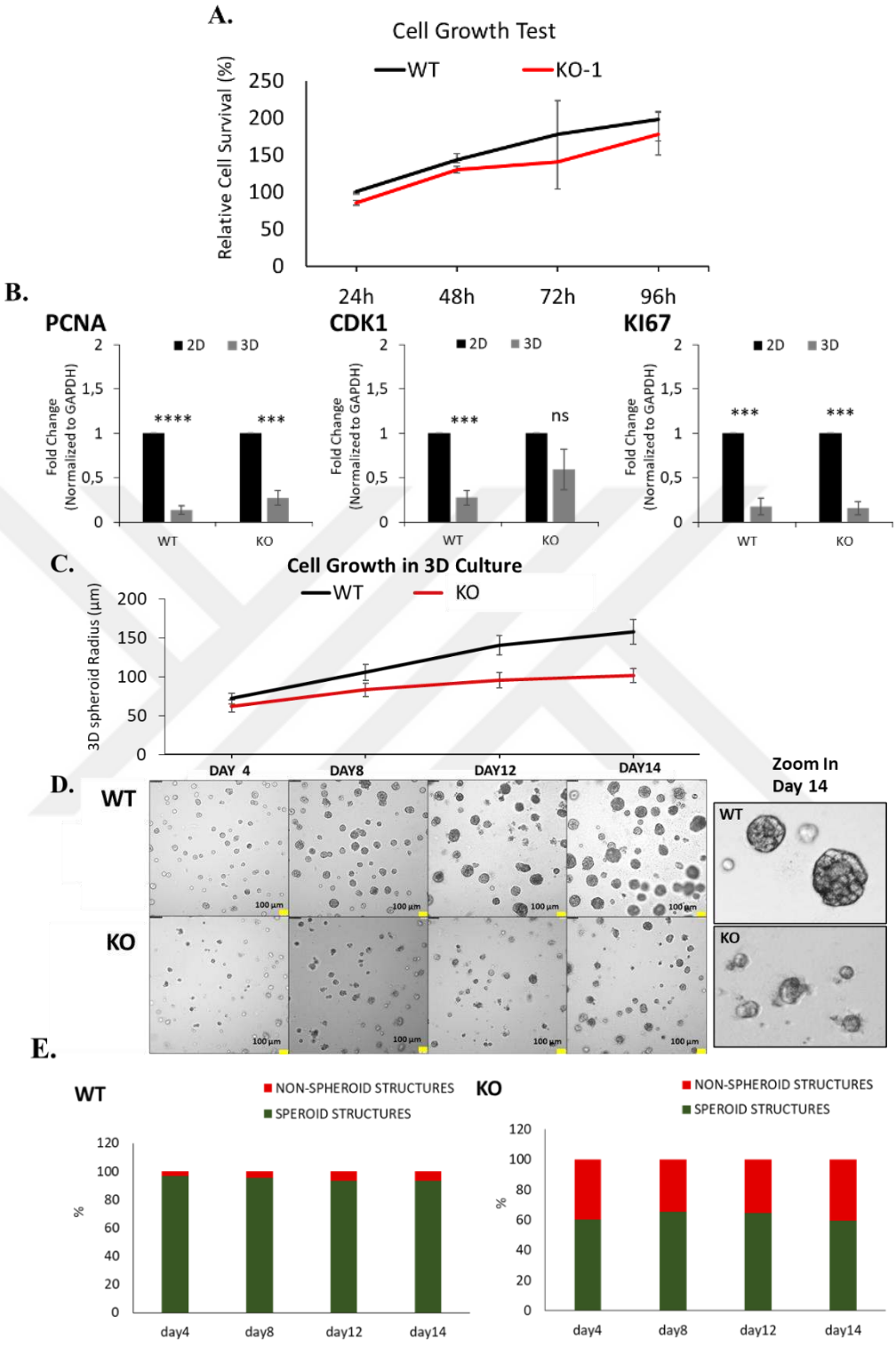

Figure 3:11. Investigation of dormancy behavior of A549 MIR210 knockout cells. A: MTT Growth Test, B: qPCR results of selected dormancy markers, C: Radius of 3D spheroids, Cell Growth in dormancy model. D: Representative images captured by light microscope E: Ratio of spheroid and non-spheroids in 3D culture. 3 independent experiments (n=3) were conducted. p-value < 0.01; ***, p-value < 0.001. KO: Knockout clone, WT: Wildtype.

3.8 Examination of migration abilities of MIR210 Knock Out, MIR362 Overexpressed A549 Cells Compared to WT

A scratch assay was performed to test the change in migration abilities of cells after genetic manipulation. Scratch (wound) formed in certain areas of the adhered cells, and the closure rates of these wounds were examined for 48 hours. Only one of the mir-362 overexpressing clones (OE-2) was found to have a significantly lower rate of scratch closure at 12 hours and 48 hours than WT (Figure 3:11). In addition, the migration ability of MIR210 knockout cells is severely affected. It was observed that closure occurred at a very low rate compared to WT cells at 12, 24, 48 hours (Figure 3:12).

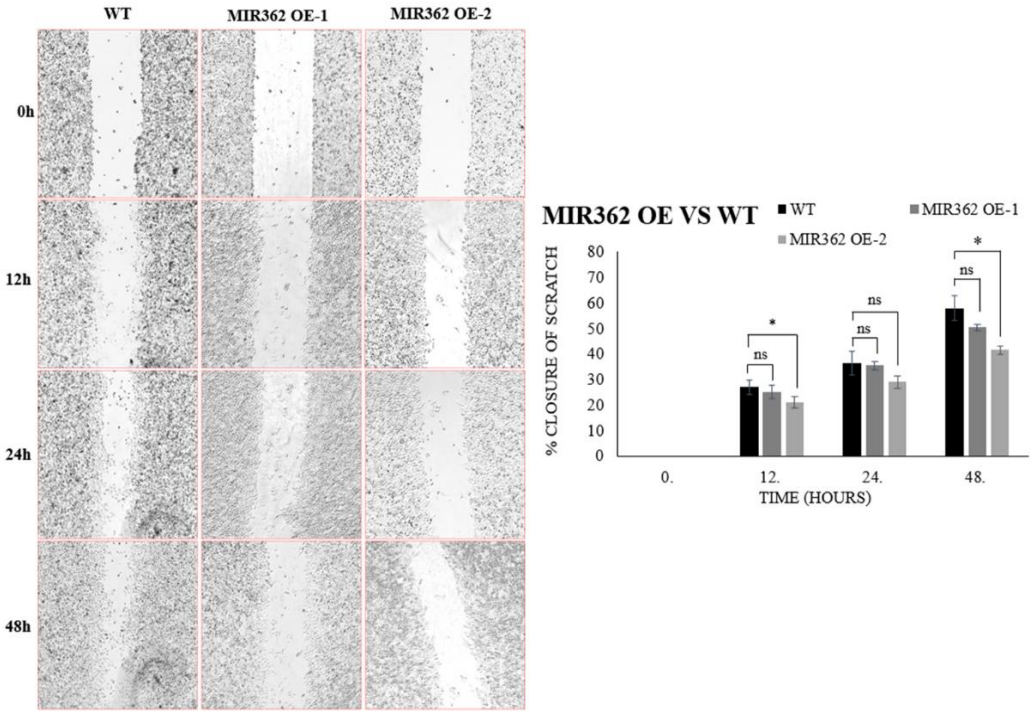

Figure 3:12 Examination of migration abilities of MIR362 overexpressed A549 cells compared to WT.

ns, p-value > 0.05; *, p-value < 0.05

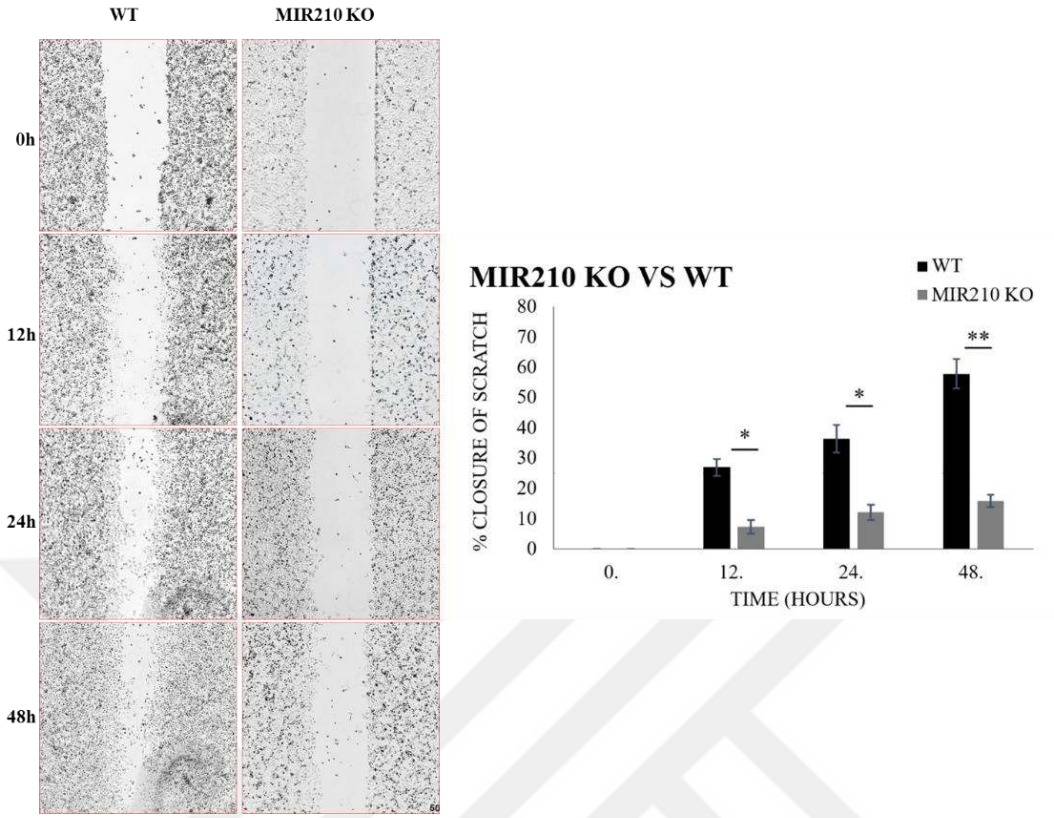

Figure 3:13 Examination of migration abilities of MIR210 knockout A549 cells compared to WT.
ns, p-value > 0.05; *, p-value < 0.05

3.9 Bioinformatics Analysis of Selected miRNAs

The USCS Genome Browser (https://genome.ucsc.edu/) was used for the location analysis of mir-362 and mir-210 on the genome (Miga et al. 2014). Mir-362 is in Intron 3 of the CLCN5 gene (Figure 3:13). Mir-210 is in the intron region of the MIR210 Host Gene (Figure 3:14). Both genes are included in the RNASeq results. Changes in expression levels are found in Table 3:7.

Table 3:7 RNA Seq results of the genes where the miRNAs located.

MiRNA	Found on	Gene Name	RNASeq Fold Change	RNASeq p-val
MIR210	*MIR210HG*	MIR210 host gene	4,911474388	$2{,}71 \times 10^{-08}$
MIR362	*CLCN5*	Chloride voltage-gated channel 5	0,480638821	0,008954869

The effects of the genes in which they are found can also e considered for examination of the observed effect of miRNAs in the dormancy model. According to the RNASeq results, it was observed that the MIR210HG, which contains mir-210, increased

significantly. Likewise, it was observed that the CLCN5 gene, where located the mir-362, which is one of the decreasing miRNAs, decreased significantly compared to RNASeq. These genes may have an effect on cancer dormancy.

Three different online data tools were used for target analysis of MIR210 and MIR362: DIANA Tool, miRDB and TargetScan. A target list was prepared for each pair of miRNAs. It was then compared with RNASeq. The genes that decreased 2-fold in RNASeq for miRNA mir210 with increasing filtering criteria, and genes that increased 2-fold in RNASeq for decreased miRNA mir362 were considered. Putative target genes mir-362-5p, mir-362-3p, mir-210-5p and mir-210-3p common to at least two tools Table 3:8, Table 3:9, Table 3:10 and Table 3:11, respectively.

According to the results, the putative target gene of mir-362-5p common to all three tools: SUCNR1, increased 2.725463042 times in RNASeq in dormancy compared to the proliferative state (Table 3:8). The putative target genes of mir-362-3p common to the three tools: DUSP10, ERI3, HHIP, PCDHAC1, significantly increased 2,632720003, 2,20098667, 3,424168775, 5,797900504, 3,098003779 and 2,982501377 times respectively, in dormancy than in the proliferative state (Table 3:9).

The putative target genes common to three possible targeting tools of mir-210-5p: AKT3, BICD2, MED13L, RAB3B, RIMS4, significantly decreased 0,426745105, 0,480928366, 0,247557326, 0,371049126, 0,002979899 times, respectively (Table 3:10).

The putative target gene common to three possible targeting tools of mir-210-3p: E2F3 significantly decreased 0,216469591 times, respectively (Table 3:11).

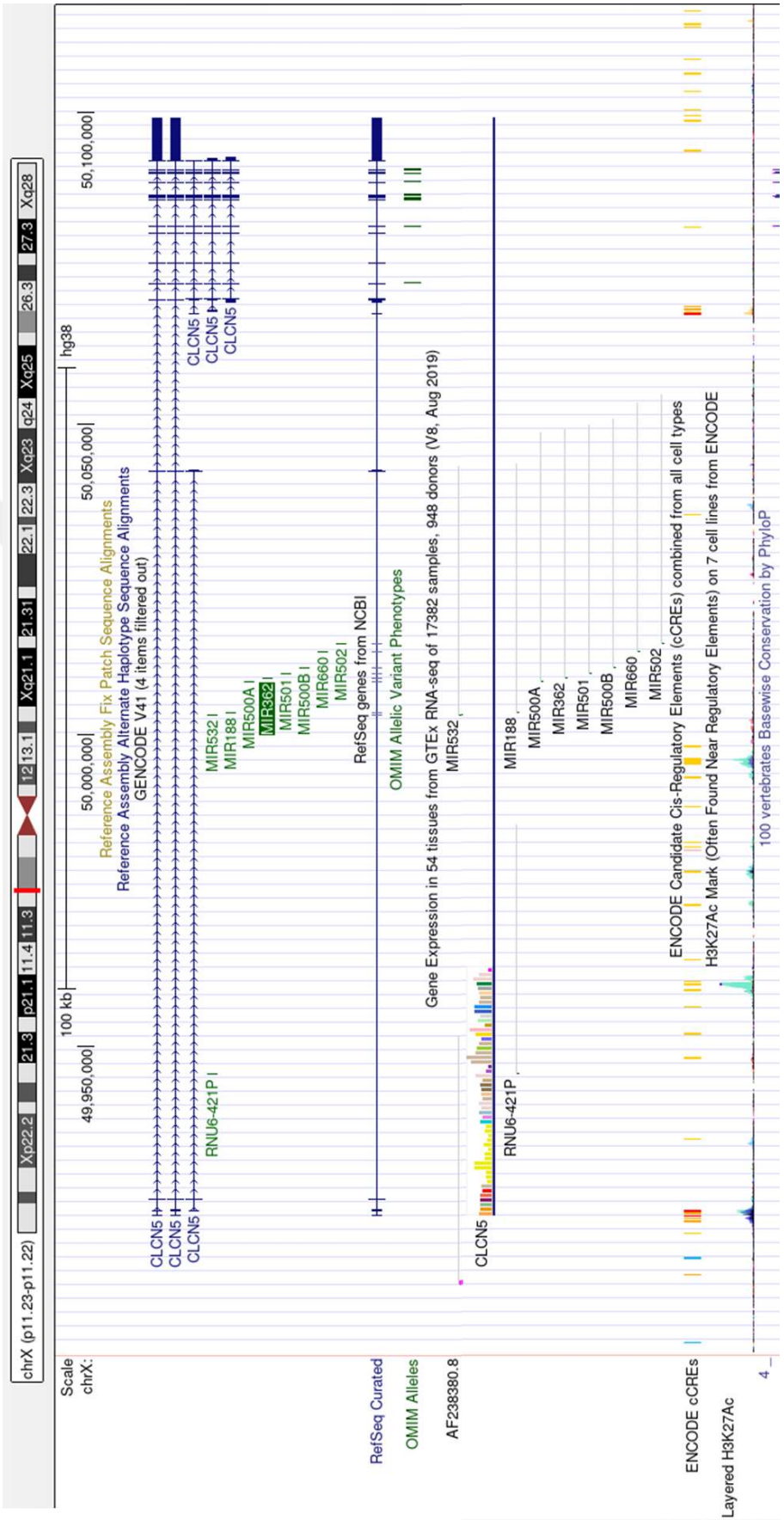

Figure 3:14 Genome location analysis of *MIR362*.

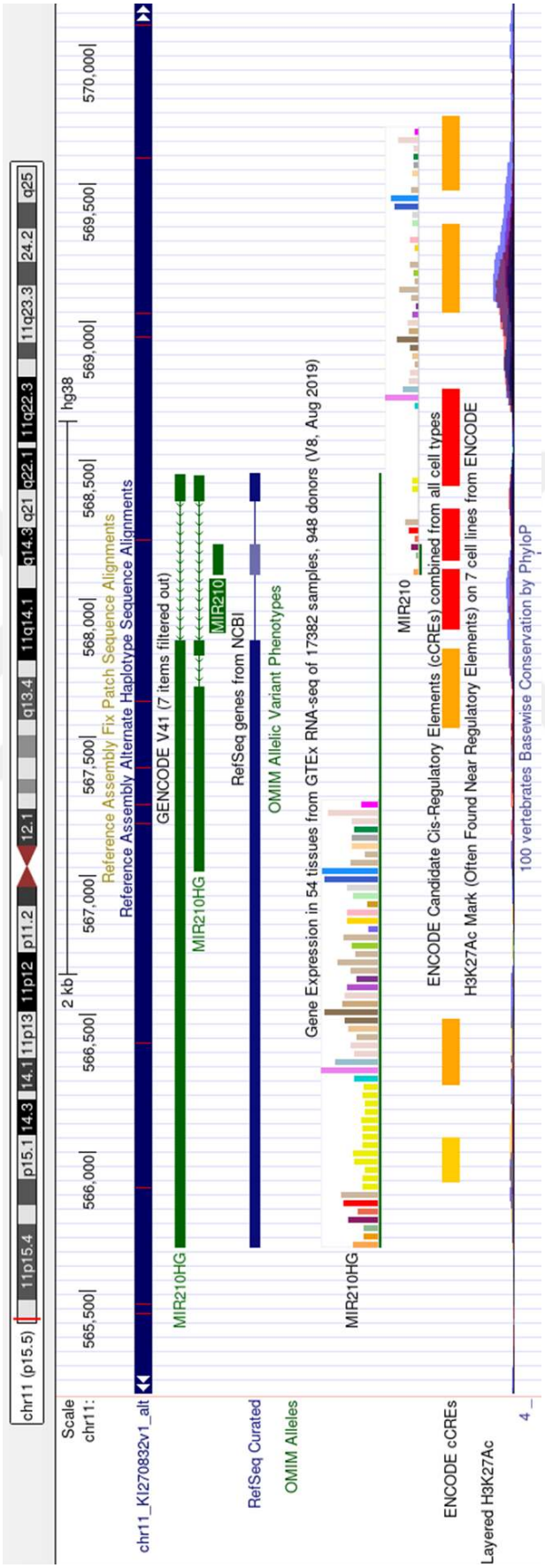

Figure 3:15 Genome location analysis of *MIR210*.

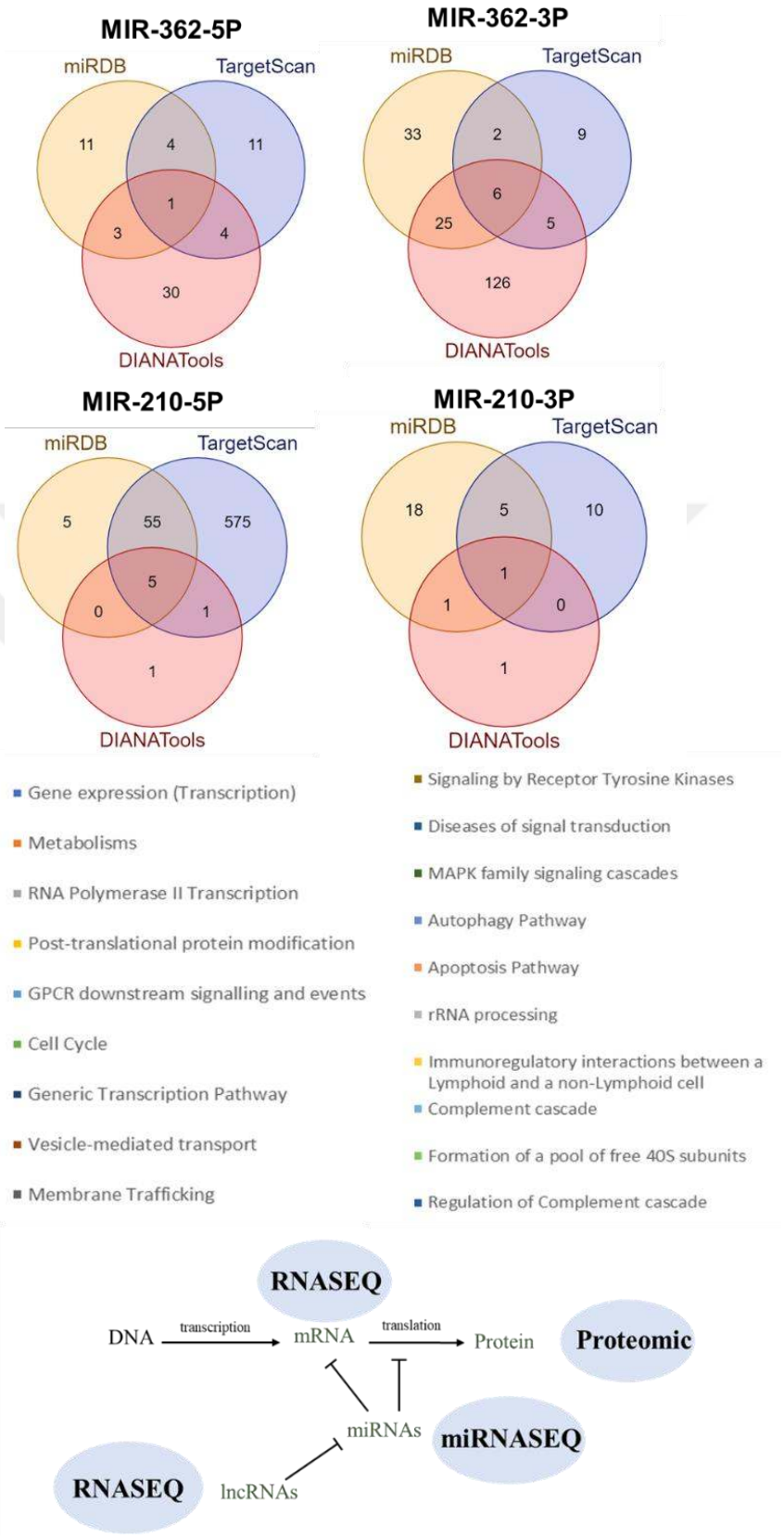

Figure 3:16 Schematic representation of putative Target Analysis for *MIR362* and *MIR210*.

Table 3:8 Putative Targets of mir362-5p.

Gene	Found In	Gene Name	RNASeq Fold Change	RNASeq p-val
SUCNR1	miRDB, TargetScan, DIANATools	succinate receptor 1	2,725463042	0,046053182
ALX1	miRDB, TargetScan	ALX homeobox 1	2,179735766	0,000215356
CEACAM5	miRDB, DIANATools	CEA cell adhesion molecule 5	7,076238294	0,029982626
CYP1B1	miRDB, TargetScan	cytochrome P450 family 1 subfamily B member 1	3,608335849	$1,93x10^{-12}$
DDX58	miRDB, DIANATools	DExD/H-box helicase 58	3,777182112	$6,17x13^{-12}$
PAQR8	TargetScan, DIANATools	progestin and adipoQ receptor family member 8	4,766610723	$3,55x10^{-09}$
PIK3C2B	miRDB, DIANATools	phosphatidylinositol-4-phosphate 3-kinase catalytic subunit type 2 beta	2,003493348	0,000744783
PLXNB1	miRDB, TargetScan	plexin B1	2,493540546	$3,99x10^{-08}$
QSOX1	TargetScan, DIANATools	quiescin sulfhydryl oxidase 1	3,229100916	$1,63x10^{-14}$
SLC38A11	TargetScan, DIANATools	solute carrier family 38 member 11	133,2806107	$1,63x10^{-05}$
SYS1	miRDB, TargetScan	SYS1 golgi trafficking protein	2,792039005	$2,66x10^{-10}$
TMEM115	TargetScan, DIANATools	transmembrane protein 115	2,85004976	$1,58x10^{-09}$

Table 3:9 Putative Targets of mir362-3p.

Gene	Found In	Gene Name	RNASeq Fold Change	RNASeq p-val
DUSP10	miRDB, TargetScan, DIANATools	dual specificity phosphatase 10	2,632720003	$6,02x10^{-06}$
ERI3	miRDB, TargetScan, DIANATools	ERI1 exoribonuclease family member 3	2,20098667	$2,10x10^{-05}$

HHIP	miRDB, TargetScan, DIANATools	hedgehog interacting protein	3,424168775	$2{,}46 \times 10^{-08}$
PCDHAC1	miRDB, TargetScan, DIANATools	protocadherin alpha subfamily C, 1	5,797900504	0,001316118
RNF19B	miRDB, TargetScan, DIANATools	ring finger protein 19B	3,098003779	$2{,}68 \times 10^{-12}$
SHB	miRDB, TargetScan, DIANATools	SH2 domain containing adaptor protein B	2,982501377	$4{,}46 \times 10^{-11}$
ABCG1	miRDB, DIANATools	ATP binding cassette subfamily G member 1	29,73584867	$3{,}56 \times 10^{-85}$
AQP3	miRDB, DIANATools	aquaporin 3 (Gill blood group)	622,1864056	$1{,}78 \times 10^{-287}$
ATP6V0B	miRDB, DIANATools	ATPase H+ transporting V0 subunit b	2,81504006	$4{,}32 \times 10^{-09}$
BEX4	miRDB, DIANATools	brain expressed X-linked 4	2,523382812	0,009952669
BMF	TargetScan, DIANATools	Bcl2 modifying factor	2,567488556	0,001605867
C6orf106	miRDB, DIANATools	-	2,231385729	0,000000208
CADPS2	miRDB, DIANATools	calcium dependent secretion activator 2	21,9014889	0,011267482
CD59	miRDB, DIANATools	CD59 molecule (CD59 blood group)	2,127079464	0,00000134
CHRM3	TargetScan, DIANATools	cholinergic receptor muscarinic 3	9,346223666	0,022740379
FAH	miRDB, DIANATools	fumarylacetoacetate hydrolase	2,075647663	0,0000256
FAM174A	miRDB, DIANATools	family with sequence similarity 174 member A	2,206288907	0,00000974
GOLGA7B	miRDB, DIANATools	golgin A7 family member B	4,083529531	$7{,}07 \times 10^{-09}$
GRIK2	miRDB, DIANATools	glutamate ionotropic receptor kainate type subunit 2	29,73651584	0,000150112
HOXC10	miRDB, DIANATools	homeobox C10	3,993067752	$3{,}77 \times 10^{-09}$
LHX9	miRDB, DIANATools	LIM homeobox 9	8,660774978	0,0000585
MOB3C	miRDB, DIANATools	MOB kinase activator 3C	3,823759934	$4{,}23 \times 10^{-14}$

NFASC	miRDB, DIANATools	neurofascin	4,156607063	0,010114104
NTHL1	miRDB, DIANATools	nth like DNA glycosylase 1	3,376016331	$1{,}63 \times 10^{-09}$
PANX2	miRDB, TargetScan	pannexin 2	2,96768246	$1{,}91 \times 10^{-09}$
PELI2	miRDB, DIANATools	pellino E3 ubiquitin protein ligase family member 2	2,565103465	0,000212956
PLCXD3	miRDB, DIANATools	phosphatidylinositol specific phospholipase C X domain containing 3	3,778045559	0,000000043
PRR7	miRDB, DIANATools	proline rich 7, synaptic	2,263473652	0,00000544
RNF144B	miRDB, DIANATools	ring finger protein 144B	4,838492736	0,000000215
RORA	miRDB, DIANATools	RAR related orphan receptor A	2,572975342	0,032023499
SH3TC2	miRDB, DIANATools	SH3 domain and tetratricopeptide repeats 2	11,40254688	$2{,}09 \times 10^{-10}$
SLC1A4	miRDB, DIANATools	solute carrier family 1 member 4	2,419950425	$8{,}25 \times 10^{-08}$
SOX17	miRDB, DIANATools	SRY-box transcription factor 17	3,131066583	0,001399339
STX1B	miRDB, DIANATools	syntaxin 1B	2,668505713	0,000219094
THRB	TargetScan, DIANATools	thyroid hormone receptor beta	2,527325204	0,0006638
TNFAIP8L3	TargetScan, DIANATools	TNF alpha induced protein 8 like 3	2,386517521	0,034737928
USF2	TargetScan, DIANATools	upstream transcription factor 2, c-fos interacting	4,074562197	$2{,}28 \times 10^{-19}$
ZER1	miRDB, TargetScan	zyg-11 related cell cycle regulator	2,691801229	$4{,}34 \times 10^{-10}$

Table 3:10 Putative Targets of mir210-5p.

Gene	Found In	Gene Name	RNASeq Fold Change	RNASeq p-val
AKT3	miRDB, TargetScan, DIANATools	AKT serine/threonine kinase 3	0,426745105	$2{,}17 \times 10^{-05}$
BICD2	miRDB, TargetScan, DIANATools	BICD cargo adaptor 2	0,480928366	0,000426519

MED13L	miRDB, TargetScan, DIANATools	mediator complex subunit 13L	0,247557326	$1,58x10^{-08}$
RAB3B	miRDB, TargetScan, DIANATools	RAB3B, member RAS oncogene family	0,371049126	$6,15x10^{-09}$
RIMS4	miRDB, TargetScan, DIANATools	regulating synaptic membrane exocytosis 4	0,002979899	$9,19x10^{-08}$
ADAM11	miRDB, TargetScan	ADAM metallopeptidase domain 11	0,246166308	$2,31x10^{-06}$
ARHGEF39	miRDB, TargetScan	Rho guanine nucleotide exchange factor 39	0,127100161	$1,20x10^{-24}$
ATP2B3	miRDB, TargetScan	ATPase plasma membrane Ca2+ transporting 3	0,027134737	0,023370557
BTG2	miRDB, TargetScan	BTG anti-proliferation factor 2	0,275307572	$1,66x10^{-07}$
CDK13	miRDB, TargetScan	cyclin dependent kinase 13	0,341946959	$5,17x10^{-06}$
CNIH2	miRDB, TargetScan	cornichon family AMPA receptor auxiliary protein 2	0,203118245	0,007825376
COTL1	miRDB, TargetScan	coactosin like F-actin binding protein 1	0,376414725	$8,82x10^{-11}$
CRIM1	miRDB, TargetScan	cysteine rich transmembrane BMP regulator 1	0,229116683	$1,91x10^{-08}$
CRISPLD2	miRDB, TargetScan	cysteine rich secretory protein LCCL domain containing 2	0,160004517	$2,29x10^{-06}$
DCBLD2	miRDB, TargetScan	discoidin, CUB and LCCL domain containing 2	0,180721383	$5,43x10^{-22}$
DENND5B	miRDB, TargetScan	DENN domain containing 5B	0,177394543	$1,23x10^{-14}$
ELOVL2	miRDB, TargetScan	ELOVL fatty acid elongase 2	0,11766031	$1,47x10^{-20}$
EP300	miRDB, TargetScan	E1A binding protein p300	0,503147878	0,004573975
FAM161A	miRDB, TargetScan	FAM161 centrosomal protein A	0,132114688	0,01253123

FAM167A	miRDB, TargetScan	family with sequence similarity 167 member A	0,20383803	$1,23x10^{-11}$
FLRT2	miRDB, TargetScan	fibronectin leucine rich transmembrane protein 2	0,004522164	$1,17x10^{-07}$
FOXJ1	miRDB, TargetScan	forkhead box J1	0,021535982	0,009960177
FSD1L	miRDB, TargetScan	fibronectin type III and SPRY domain containing 1 like	0,104453926	$6,13x10^{-10}$
GNAZ	miRDB, TargetScan	G protein subunit alpha z	0,3126332	0,000136957
GNL3L	miRDB, TargetScan	G protein nucleolar 3 like	0,477594495	$1,96x10^{-05}$
GRAMD1C	miRDB, TargetScan	GRAM domain containing 1C	0,015381992	0,002281892
HIPK1	miRDB, TargetScan	homeodomain interacting protein kinase 1	0,32039004	$7,75x10^{-08}$
ICOSLG	TargetScan, DIANATools	inducible T cell costimulator ligand	0,187646848	0,019388118
KCNA7	miRDB, TargetScan	potassium voltage-gated channel subfamily A member 7	0,027265796	0,023934417
KMT2C	miRDB, TargetScan	lysine methyltransferase 2C	0,323004268	$1,61x10^{-05}$
LINGO1	miRDB, TargetScan	leucine rich repeat and Ig domain containing 1	0,053306718	$2,82x10^{-22}$
LYL1	miRDB, TargetScan	LYL1 basic helix-loop-helix family member	0,257382485	0,024665475
MEX3A	miRDB, TargetScan	mex-3 RNA binding family member A	0,227409343	$3,50x10^{-11}$
PDE7A	miRDB, TargetScan	phosphodiesterase 7A	0,266285393	$1,40x10^{-09}$
PDS5A	miRDB, TargetScan	PDS5 cohesin associated factor A	0,286572884	$1,04x10^{-09}$
PID1	miRDB, TargetScan	phosphotyrosine interaction domain containing 1	0,163350562	$7,25x10^{-10}$
PIK3R1	miRDB, TargetScan	phosphoinositide-3-kinase regulatory subunit 1	0,321926173	$1,30x10^{-06}$
PPP6R3	miRDB, TargetScan	protein phosphatase 6 regulatory subunit 3	0,354807412	$1,30x10^{-08}$

PPTC7	miRDB, TargetScan	protein phosphatase targeting COQ7	0,328595721	$2,90x10^{-08}$
PRKCQ	miRDB, TargetScan	protein kinase C theta	0,488266231	0,002338308
RNF207	miRDB, TargetScan	ring finger protein 207	0,462865313	$8,21x10^{-05}$
SCML2	miRDB, TargetScan	Scm polycomb group protein like 2	0,105338629	$1,49x10^{-18}$
SDK2	miRDB, TargetScan	sidekick cell adhesion molecule 2	0,480225911	0,032305672
SH3BP4	miRDB, TargetScan	SH3 domain binding protein 4	0,42431969	$7,42x10^{-08}$
SHQ1	miRDB, TargetScan	SHQ1, H/ACA ribonucleoprotein assembly factor	0,351377613	$9,78x10^{-08}$
SLC30A3	miRDB, TargetScan	solute carrier family 30 member 3	0,250373375	$1,01x10^{-05}$
SLC7A11	miRDB, TargetScan	solute carrier family 7 member 11	0,253559358	$2,02x10^{-17}$
SLC8A1	miRDB, TargetScan	solute carrier family 8 member A1	0,121014644	0,00101227
SPTLC2	miRDB, TargetScan	serine palmitoyltransferase long chain base subunit 2	0,497089186	$2,03x10^{-05}$
SRSF6	miRDB, TargetScan	serine and arginine rich splicing factor 6	0,470810285	$1,63x10^{-06}$
STXBP5	miRDB, TargetScan	syntaxin binding protein 5	0,267842352	$4,07x10^{-09}$
TFCP2L1	miRDB, TargetScan	transcription factor CP2 like 1	0,198889975	$4,34x10^{-06}$
TIAM1	miRDB, TargetScan	TIAM Rac1 associated GEF 1	0,011357041	0,000483039
TMEM107	miRDB, TargetScan	transmembrane protein 107	0,450447351	0,000296921
TNRC6C	miRDB, TargetScan	trinucleotide repeat containing adaptor 6C	0,369731557	0,008081365
TRERF1	miRDB, TargetScan	transcriptional regulating factor 1	0,482056282	0,000409169
USP46	miRDB, TargetScan	ubiquitin specific peptidase 46	0,357017073	$2,49x10^{-05}$
USP49	miRDB, TargetScan	ubiquitin specific peptidase 49	0,303335902	$7,13x10^{-05}$

ZDHHC22	miRDB, TargetScan	zinc finger DHHC-type palmitoyltransferase 22	0,049169235	0,024890276
ZFX	miRDB, TargetScan	zinc finger protein X-linked	0,234395805	$6{,}80 \times 10^{-13}$
ZNF597	miRDB, TargetScan	zinc finger protein 597	0,464687487	0,030499868

Table 3:11 Putative Targets of mir210-3p.

Gene	Found In	Gene Name	RNASeq Fold Change	RNASeq p-val
E2F3	miRDB, TargetScan, DIANATools	E2F transcription factor 3	0,216469591	$1{,}35 \times 10^{-11}$
DENND6A	miRDB, TargetScan	DENN domain containing 6A	0,339779391	$7{,}67 \times 10^{-06}$
DIMT1	miRDB, TargetScan	DIMT1 rRNA methyltransferase and ribosome maturation factor	0,361438353	$6{,}65 \times 10^{-10}$
GPD1L	miRDB, TargetScan	glycerol-3-phosphate dehydrogenase 1 like	0,43254228	$1{,}16 \times 10^{-05}$
KMT2D	miRDB, TargetScan	lysine methyltransferase 2D	0,414471772	$5{,}16 \times 10^{-05}$
NR1D2	miRDB, DIANATools	nuclear receptor subfamily 1 group D member 2	0,376113699	$2{,}65 \times 10^{-06}$
SCARA3	miRDB, TargetScan	scavenger receptor class A member 3	0,407098037	$1{,}05 \times 10^{-08}$

Chapter 4:
CONCLUSION

Drug resistance and cancer dormancy are the two main causes of cancer deaths from untreated metastases. Therefore, understanding cancer dormancy at the molecular level is crucial for saving lives and opening new horizons in treatments. It is as important to understand the molecular functioning of dormancy as to identify these cells, which can remain undivided for many years in patients who are thought to have healed medically, by imaging methods. Unfortunately, currently used imaging technologies are insufficient in this regard. Despite this undeniable importance of dormancy, research is very limited and remains focused on some tumor subtypes. Molecular and rigorous studies have focused especially on molecules originating from breast cancer and the microenvironment.

Lung cancer ranks first and second in the world in terms of frequency in men and women, respectively. However, lung cancer metastases are not included in the clinical and academic literature in parallel with their frequency. On the other hand, many studies on the lung consist of tumors of other organs that have metastasized secondary to the lung. Under all these circumstances, the importance of lung cancer metastasis, recurrence and dormancy research is clear.

In this study, the creation of a 2D and 3D in vitro cell culture model using NSCLC cells and the discovery and confirmation of lung cancer signature miRNAs with multiple omics analyses using this model and the genetic manipulation of miRNAs to be discovered in line with cell biology and bioinformatics analysis. It is aimed to examine the behavior of dormant cells and identify possible target genes using online tools in the dormancy model.

In this context, this study has the feature of being the first comprehensive study in Turkey and the world, in which results containing more than one omics analysis will be revealed. In line with the studies briefly summarized above, the dormancy model of NSCLC A549 cells was successfully established with the 3D in vitro commercial Matrigel cell culture method and targeted multi-omics analyzes were carried out with the help of this model. As a result of omics analyzes, mRNA, miRNA, gene, protein, and dozens of candidate molecules related to dormancy were discovered.

Within the scope of the study, further analyzes were carried out by focusing on these candidate molecules, especially those known to have never been or little studied before.

As a result of mirSeq analysis, it was revealed that 4 miRNAs were up-regulated and 40 miRNAs were down-regulated in dormant cells compared to proliferative cells. These miRNAs from mirSeq were confirmed in the dormancy model. Both pairs (5p and 3p) of miRNAs, if any, were tested. Confirmed miRNAs paralleling the mirSeq was carefully selected for further analysis. Of the 4 miRNAs that appear to be up-regulated in mirSeq analysis, only 2 confirmed significantly changed. To examine the effect of these two up-regulated miRNAs, on the dormancy model, it was aimed to delete these genes in cells. For this, the CRISPR/CAS9 system was preferred. However, due to the lack of the appropriate PAM sequence in the sequence of mir-1290, only the mir-210 gene was focused on among the up-regulated miRNAs. Mir-210 has been associated with many cellular events in the literature. It plays an important regulatory role in the cell cycle, DNA damage repair, immune system and inflammation, angiogenesis, metabolism, macrophage regulation, and T cell differentiation and stimulation (Hui et al. 2020). However, its role in cancer dormancy is not yet known.

Due to the small number of up-regulated miRNAs, preliminary target gene analysis was performed for all of them. As a result of this analysis, possible genes associated with cancer, cell cycle, cell growth, migration, metastasis and invasion in the literature were selected, and the changes in expression levels within the dormancy model were tested. Within the scope of informatics analysis, the online tool (TargetScan) and RNASeq and Proteomic results obtained from dormant cells were used. Genes obtained from the Online Tool were compared with RNASeq and proteomic results. Since miRNAs generally cause suppression of target gene expression levels, the focus has been on genes that down-regulated in mRNA and protein levels.

There were no significant changes among the selected genes based on the results, except for CAPZA1. CAPZA1 is among the possible targets of mir-1290 and mir-181a-2 and has roles in cancer migration and invasion, according to the literature (Eigentler et al., 2020; Che et al., 2018; Kang et al., 2017; Qian et al. et al., 2016). The focus was not on the CAPZA1 gene, as both mir-181a-2 did not change significantly when tested in the dormancy model by qPCR, and mir-1290 couldn't work in the CRISPR/CAS9 system.

However, the fact that mir-1290 is the most up-regulated miRNA in this dormancy system makes it a very large potential dormancy-associated miRNA candidate. If a

system other than the CRISPR/CAS9 system is used (eg sponge system), it is very valuable to examine its effect on this system.

The down-regulated miRNAs, known to have never been or little studied before due to a large number of declining miRNAs, were first tested in the dormancy system. Among the selected miRNAs, it was confirmed that mir-130b, mir-362, mir-374, mir-2278, mir-1304, mir-190, mir-301a, and mir-138-2 were significantly decreased. Almost all of the qPCR results were parallel with the mirSeq results. The most decreased miRNAs were selected for further analysis (mir-301a, mir-190, and mir-362). For the testing of down-regulated miRNAs in the system, it was first aimed to produce A549 clones that overexpress these miRNAs. The overexpression vector of mir-301 has been ordered but has not reached this working period, so the focus is on mir-362 and mir-190.

In the literature, mir-362 has been associated with cell growth inhibition and metastasis in glioblastomas (Shi et al. 2020), invasion and cell growth inhibition in colorectal cancer (Wan et al. 2019), and aberrant expression inducing metastasis in lung cancer (Luo et al. 2018). But its role in cancer dormancy is not yet known. Interestingly, up-regulation of mir-190 has been reported to induce long-term dormancy in growing glioblastomas and osteosarcomas (N. et al. 2013). In our system, mir-190 was significantly reduced in the dormancy condition of A549 lung cancer cells. In another study, mir-190 associated with tumor dormancy was shown to be a potential circulating miRNA marker in metastatic breast cancer (Papadaki et al. 2019). Due to our results' inverse overlap with the literature, mir-190 was chosen for further analysis. Mir-190 overexpression A549 cells were created, but no significant morphological change was detected in this dormancy model when cultured in Matrigel and observed for 14 days (Data is not shown). Of the down-regulated miRNAs, only mir-362 was focused.

The genetic manipulations for both miRNAs were successfully performed. No significant difference was observed in the growth of cells under normal cell culture conditions compared to WT cells. However, the cells behaved differently from WT cells under 3D cell culture conditions (dormancy model).

It was observed that both different clones of MIR362 observed disruptions in spheroid formation. Cell colonies formed a regular and tight structure in WT cells, while scattered non-tight structures were observed in MIR362 overexpressing cells. On the other hand, when MIR210 was deleted from the cells, it was observed that the cells observed disruption in spheroid formation as well. Cells were smaller than WT cells, and

even dead cell-like structures were observed. In this case, it can be considered that both miRNAs are critically important in dormancy. In order to better understand the effects of these miRNAs on the dormancy behavior of cells, target genes and the pathways in which these genes are involved are of critical importance. Informative analyzes reveal possible target genes.

Uncovering the expression level changes in these genes in the dormancy condition and how the genetic manipulations in these genes affect the behavior of cells in the dormancy condition may play a role in elucidating the dormancy-related pathways. Moreover, examining the behavior of these clones obtained in vivo when injected into mice will provide a much different perspective to these results.

As a result, miRNAs obtained in many studies have been indirectly associated with dormancy. Of course, dormancy-related miRNAs in the obtained literature contribute to understanding the mechanism of cancer dormancy, but they are insufficient. In the optimized dormancy model, mirSeq was performed directly from the dormant cells. As a result of this analysis, manipulating miRNAs and miRNAs that differ in dormancy behavior in the same model can potentially be associated with dormancy. With the development of in vitro and in vivo models of cancer dormancy, elucidating the mechanisms underlying cancer dormancy, finding new therapeutic targets, detecting dormant cells in the clinic and developing treatment methods for dormant cells, understanding the mechanisms of cancer recurrence are very important for the course of the disease and the survival of patients.

BIBLIOGRAPHY

Adam, Alejandro P., Ajish George, Denis Schewe, Paloma Bragado, Bibiana V. Iglesias, Aparna C. Ranganathan, Antonis Kourtidis, Douglas S. Conklin, and Julio A. Aguirre-Ghiso. 2009. "Computational Identification of a P38 SAPK-Regulated Transcription Factor Network Required for Tumor Cell Quiescence." *Cancer Research*. doi: 10.1158/0008-5472.CAN-08-3820.

Aguirre-Ghiso, J. A., D. Liu, A. Mignatti, K. Kovalski, and L. Ossowski. 2001. "Urokinase Receptor and Fibronectin Regulate the ERKMAPK to P38MAPK Activity Ratios That Determine Carcinoma Cell Proliferation or Dormancy in Vivo." *Molecular Biology of the Cell*. doi: 10.1091/mbc.12.4.863.

Aguirre-Ghiso, Julio A. 2007. "Models, Mechanisms and Clinical Evidence for Cancer Dormancy." *Nature Reviews Cancer*.

Aguirre-Ghiso, Julio A., Yeriel Estrada, David Liu, and Liliana Ossowski. 2003. "ERK^{MAPK} Activity as a Determinant of Tumor Growth and Dormancy; Regulation by P38^{SAPK}" *Cancer Research*.

Aguirre-Ghiso, Julio A., Liliana Ossowski, and Sarah K. Rosenbaum. 2004. "Green Fluorescent Protein Tagging of Extracellular Signal-Regulated Kinase and P38 Pathways Reveals Novel Dynamics of Pathway Activation during Primary and Metastatic Growth." *Cancer Research*. doi: 10.1158/0008-5472.CAN-04-0113.

Aguirre Ghiso, Julio A. 2002. "Inhibition of FAK Signaling Activated by Urokinase Receptor Induces Dormancy in Human Carcinoma Cells in Vivo." *Oncogene*. doi: 10.1038/sj.onc.1205342.

Akkoc, Yunus, Nesibe Peker, Arzu Akcay, and Devrim Gozuacik. 2021. "Autophagy and Cancer Dormancy." *Frontiers in Oncology*.

Aqbi, Hussein F., Liliya Tyutyunyk-Massey, Rebecca C. Keim, Savannah E. Butler, Theresa Thekkudan, Supriya Joshi, Timothy M. Smith, Dipankar Bandyopadhyay, Michael O. Idowu, Harry D. Bear, Kyle K. Payne, David A. Gewirtz, and Masoud H. Manjili. 2018. "Autophagy-Deficient Breast Cancer Shows Early Tumor Recurrence and Escape from Dormancy." *Oncotarget*. doi: 10.18632/oncotarget.25197.

Axe, Elizabeth L., Simon A. Walker, Maria Manifava, Priya Chandra, H. Llewelyn

Roderick, Anja Habermann, Gareth Griffiths, and Nicholas T. Ktistakis. 2008. "Autophagosome Formation from Membrane Compartments Enriched in Phosphatidylinositol 3-Phosphate and Dynamically Connected to the Endoplasmic Reticulum." *Journal of Cell Biology*. doi: 10.1083/jcb.200803137.

Backer, Jonathan M. 2008. "The Regulation and Function of Class III PI3Ks: Novel Roles for Vps34." *Biochemical Journal*.

Barkan, Dalit, Hynda Kleinman, Justin L. Simmons, Holly Asmussen, Anil K. Kamaraju, Mark J. Hoenorhoff, Zi Yao Liu, Sylvain V. Costes, Edward H. Cho, Stephen Lockett, Chand Khanna, Ann F. Chambers, and Jeffrey E. Green. 2008. "Inhibition of Metastatic Outgrowth from Single Dormant Tumor Cells by Targeting the Cytoskeleton." *Cancer Research*. doi: 10.1158/0008-5472.CAN-07-6849.

Barkan, Dalit, Lara H. El Touny, Aleksandra M. Michalowski, Jane Ann Smith, Isabel Chu, Anne Sally Davis, Joshua D. Webster, Shelley Hoover, R. Mark Simpson, Jack Gauldie, and Jeffrey E. Green. 2010. "Metastatic Growth from Dormant Cells Induced by a Col-I-Enriched Fibrotic Environment." *Cancer Research*. doi: 10.1158/0008-5472.CAN-09-2356.

Barth, Sandra, Danielle Glick, and Kay F. Macleod. 2010. "Autophagy: Assays and Artifacts." *Journal of Pathology*.

La Belle Flynn, Alyssa, Benjamin C. Calhoun, Arishya Sharma, Jenny C. Chang, Alexandru Almasan, and William P. Schiemann. 2019. "Autophagy Inhibition Elicits Emergence from Metastatic Dormancy by Inducing and Stabilizing Pfkfb3 Expression." *Nature Communications*. doi: 10.1038/s41467-019-11640-9.

Bennett, Dorothy C., Linda A. Peachey, Helga Durbin, and Philip S. Rudland. 1978. "A Possible Mammary Stem Cell Line." *Cell*. doi: 10.1016/0092-8674(78)90104-6.

Besson, Arnaud, Mark Gurian-West, Xueyan Chen, Karen S. Kelly-Spratt, Christopher J. Kemp, and James M. Roberts. 2006. "A Pathway in Quiescent Cells That Controls P27Kip1 Stability, Subcellular Localization, and Tumor Suppression." *Genes and Development*. doi: 10.1101/gad.1384406.

Bleau, Anne Marie, Carolina Zandueta, Miriam Redrado, Susana Martínez-Canarias, Leyre Larzábal, Luis M. Montuenga, Alfonso Calvo, and Fernando Lecanda. 2015. "Sphere-Derived Tumor Cells Exhibit Impaired Metastasis by a Host-Mediated Quiescent Phenotype." *Oncotarget*. doi: 10.18632/oncotarget.4803.

Bliss, Sarah A., Garima Sinha, Oleta A. Sandiford, Lisa M. Williams, Daniel J. Engelberth, Khadidiatou Guiro, Leidy L. Isenalumhe, Steven J. Greco, Seda Ayer, Margarette Bryan, Rakesh Kumar, Nicholas M. Ponzio, and Pranela Rameshwar. 2016. "Mesenchymal Stem Cell-Derived Exosomes Stimulate Cycling Quiescence and Early Breast Cancer Dormancy in Bone Marrow." *Cancer Research*. doi: 10.1158/0008-5472.CAN-16-1092.

Borgen, Elin, Maria C. Rypdal, Maria Soledad Sosa, Anne Renolen, Ellen Schlichting, Per E. Lønning, Marit Synnestvedt, Julio A. Aguirre-Ghiso, and Bjørn Naume. 2018. "NR2F1 Stratifies Dormant Disseminated Tumor Cells in Breast Cancer Patients." *Breast Cancer Research*. doi: 10.1186/s13058-018-1049-0.

Boyerinas, Benjamin, Maya Zafrir, Ali E. Yesilkanal, Trevor T. Price, Elizabeth M. Hyjek, and Dorothy A. Sipkins. 2013. "Adhesion to Osteopontin in the Bone Marrow Niche Regulates Lymphoblastic Leukemia Cell Dormancy." *Blood*. doi: 10.1182/blood-2012-12-475483.

Bragado, Paloma, Yeriel Estrada, Falguni Parikh, Sarah Krause, Carla Capobianco, Hernan G. Farina, Denis M. Schewe, and Julio A. Aguirre-Ghiso. 2013. "TGF-B2 Dictates Disseminated Tumour Cell Fate in Target Organs through TGF-β-RIII and P38α/β Signalling." *Nature Cell Biology*. doi: 10.1038/ncb2861.

Braun, Stephan, Florian D. Vogl, Bjørn Naume, Wolfgang Janni, Michael P. Osborne, R. Charles Coombes, Günter Schlimok, Ingo J. Diel, Bernd Gerber, Gerhard Gebauer, Jean-Yves Pierga, Christian Marth, Daniel Oruzio, Gro Wiedswang, Erich-Franz Solomayer, Günther Kundt, Barbara Strobl, Tanja Fehm, George Y. C. Wong, Judith Bliss, Anne Vincent-Salomon, and Klaus Pantel. 2005. "A Pooled Analysis of Bone Marrow Micrometastasis in Breast Cancer." *New England Journal of Medicine*. doi: 10.1056/nejmoa050434.

Buczacki, Simon J. A., Semiramis Popova, Emma Biggs, Chrysa Koukorava, Jon Buzzelli, Louis Vermeulen, Lee Hazelwood, Hayley Francies, Mathew J. Garnett, and Douglas J. Winton. 2018. "Itraconazole Targets Cell Cycle Heterogeneity in Colorectal Cancer." *Journal of Experimental Medicine*. doi: 10.1084/jem.20171385.

Cai, Yimei, Xiaomin Yu, Songnian Hu, and Jun Yu. 2009. "A Brief Review on the Mechanisms of MiRNA Regulation." *Genomics, Proteomics and Bioinformatics*.

Chaffer, Christine L., Beatriz P. San Juan, Elgene Lim, and Robert A. Weinberg. 2016.

"EMT, Cell Plasticity and Metastasis." *Cancer and Metastasis Reviews*. doi: 10.1007/s10555-016-9648-7.

Chen, Yuhao, and Xiaowei Wang. 2020. "MiRDB: An Online Database for Prediction of Functional MicroRNA Targets." *Nucleic Acids Research*. doi: 10.1093/nar/gkz757.

Cheng, Yan, Xingcong Ren, William N. Hait, and Jin Ming Yang. 2013. "Therapeutic Targeting of Autophagy in Disease: Biology and Pharmacology." *Pharmacological Reviews*.

Cianfanelli, Valentina, Claudia Fuoco, Mar Lorente, Maria Salazar, Fabio Quondamatteo, Pier Federico Gherardini, Daniela De Zio, Francesca Nazio, Manuela Antonioli, Melania D'Orazio, Tatjana Skobo, Matteo Bordi, Mikkel Rohde, Luisa Dalla Valle, Manuela Helmer-Citterich, Christine Gretzmeier, Joern Dengjel, Gian Maria Fimia, Mauro Piacentini, Sabrina Di Bartolomeo, Guillermo Velasco, and Francesco Cecconi. 2015. "AMBRA1 Links Autophagy to Cell Proliferation and Tumorigenesis by Promoting C-Myc Dephosphorylation and Degradation." *Nature Cell Biology*. doi: 10.1038/ncb3072.

Crea, Francesco, Nur Ridzwan Nur Saidy, Colin C. Collins, and Yuzhuo Wang. 2015. "The Epigenetic/Noncoding Origin of Tumor Dormancy." *Trends in Molecular Medicine*.

Dai, Yafei, Lujuan Wang, Jingqun Tang, Pengfei Cao, Zhaohui Luo, Jun Sun, Abraha Kiflu, Buqing Sai, Meili Zhang, Fan Wang, Guiyuan Li, and Juanjuan Xiang. 2016. "Activation of Anaphase-Promoting Complex by P53 Induces a State of Dormancy in Cancer Cells against Chemotherapeutic Stress." *Oncotarget*. doi: 10.18632/oncotarget.8172.

Damen, Maartje P. F., Jacco van Rheenen, and Colinda L. G. J. Scheele. 2021. "Targeting Dormant Tumor Cells to Prevent Cancer Recurrence." *FEBS Journal*.

Darzynkiewicz, Zbigniew, Gloria Juan, and Edward F. Srour. 2004. "Differential Staining of DNA and RNA." *Current Protocols in Cytometry / Editorial Board, J. Paul Robinson, Managing Editor ... [et Al.]*. doi: 10.1002/0471142956.cy0703s30.

Demicheli, Romano, Marco Fornili, Federico Ambrogi, Kristin Higgins, Jessamy A. Boyd, Elia Biganzoli, and Chris R. Kelsey. 2012. "Recurrence Dynamics for Non-Small-Cell Lung Cancer: Effect of Surgery on the Development of Metastases." *Journal of Thoracic Oncology*. doi: 10.1097/JTO.0b013e31824a9022.

Deng, Xiaobing, Daina Z. Ewton, and Eileen Friedman. 2009. “Mirk Dyrk1B Maintains the Viability of Quiescent Pancreatic Cancer Cells by Reducing Levels of Reactive Oxygen Species.” *Cancer Research*. doi: 10.1158/0008-5472.CAN-08-2903.

Dey-Guha, Ipsita, Cleidson P. Alves, Albert C. Yeh, Salony, Xavier Sole, Revati Darp, and Sridhar Ramaswamy. 2015. “A Mechanism for Asymmetric Cell Division Resulting in Proliferative Asynchronicity.” *Molecular Cancer Research*. doi: 10.1158/1541-7786.MCR-14-0474.

Díaz-Troya, Sandra, María Esther Pérez-Pérez, Francisco J. Florencio, and José L. Crespo. 2008. “The Role of TOR in Autophagy Regulation from Yeast to Plants and Mammals.” *Autophagy*.

Dongre, Anushka, and Robert A. Weinberg. 2019. “New Insights into the Mechanisms of Epithelial–Mesenchymal Transition and Implications for Cancer.” *Nature Reviews Molecular Cell Biology*.

Drageset, Vilde, Jahn M. Nesland, Bjorn Erikstein, Eva Skovlund, Hilde Sommer, Gun Anker, Erik Wist, Steinar Lundgren, Jonas Bergh, and Gunnar Kvalheim. 2006. “Monitoring of Disseminated Tumor Cells in Bone Marrow in High-Risk Breast Cancer Patients Treated with High-Dose Chemotherapy.” *International Journal of Cancer*. doi: 10.1002/ijc.21709.

Dunn, Gavin P., Lloyd J. Old, and Robert D. Schreiber. 2004. “The Immunobiology of Cancer Immunosurveillance and Immunoediting.” *Immunity*.

Eskelinen, Eeva Liisa. 2005. “Maturation of Autophagic Vacuoles in Mammalian Cells.” *Autophagy*.

Fares, Jawad, Mohamad Y. Fares, Hussein H. Khachfe, Hamza A. Salhab, and Youssef Fares. 2020. “Molecular Principles of Metastasis: A Hallmark of Cancer Revisited.” *Signal Transduction and Targeted Therapy*.

Farrar, J. D., K. H. Katz, J. Windsor, G. Thrush, R. H. Scheuermann, J. W. Uhr, and N. E. Street. 1999. “Cancer Dormancy. VII. A Regulatory Role for CD8+ T Cells and IFN-Gamma in Establishing and Maintaining the Tumor-Dormant State.” *Journal of Immunology (Baltimore, Md. : 1950)*.

Finnegan, Emily F., and Amy E. Pasquinelli. 2013. “MicroRNA Biogenesis: Regulating the Regulators.” *Critical Reviews in Biochemistry and Molecular Biology*.

Folkman, Judah, and Raghu Kalluri. 2004. “Cancer without Disease.” *Nature*.

Friedman, Robin C., Kyle Kai How Farh, Christopher B. Burge, and David P. Bartel.

2009. “Most Mammalian MRNAs Are Conserved Targets of MicroRNAs.” *Genome Research*. doi: 10.1101/gr.082701.108.

Furuichi, Yoshiyuki, Kumiko Goi, Takeshi Inukai, Hiroki Sato, Atsushi Nemoto, Kazuya Takahashi, Koshi Akahane, Kinuko Hirose, Hiroko Honna, Itaru Kuroda, Xiaochun Zhang, Keiko Kagami, Yasuhide Hayashi, Kenichi Harigaya, Shinpei Nakazawa, and Kanji Sugita. 2007. “Fms-like Tyrosine Kinase 3 Ligand Stimulation Induces MLL-Rearranged Leukemia Cells into Quiescence Resistant to Antileukemic Agents.” *Cancer Research*. doi: 10.1158/0008-5472.CAN-07-0105.

Galluzzi, Lorenzo, José Manuel Bravo-San Pedro, Beth Levine, Douglas R. Green, and Guido Kroemer. 2017. “Pharmacological Modulation of Autophagy: Therapeutic Potential and Persisting Obstacles.” *Nature Reviews Drug Discovery*.

Galvao, Rui Pedro, Anita Kasina, Robert S. McNeill, Jordan E. Harbin, Oded Foreman, Roel G. W. Verhaak, Akiko Nishiyama, C. Ryan Miller, and Hui Zong. 2014. “Transformation of Quiescent Adult Oligodendrocyte Precursor Cells into Malignant Glioma through a Multistep Reactivation Process.” *Proceedings of the National Academy of Sciences of the United States of America*. doi: 10.1073/pnas.1414389111.

Gao, Hua, Goutam Chakraborty, Ai Ping Lee-Lim, Konstantinos J. Mavrakis, Hans Guido Wendel, and Filippo G. Giancotti. 2014. “Forward Genetic Screens in Mice Uncover Mediators and Suppressors of Metastatic Reactivation.” *Proceedings of the National Academy of Sciences of the United States of America*. doi: 10.1073/pnas.1403234111.

Gao, Hua, Goutam Chakraborty, Ai Ping Lee-Lim, Qianxing Mo, Markus Decker, Alin Vonica, Ronglai Shen, Edi Brogi, Ali H. Brivanlou, and Filippo G. Giancotti. 2012. “The BMP Inhibitor Coco Reactivates Breast Cancer Cells at Lung Metastatic Sites.” *Cell*. doi: 10.1016/j.cell.2012.06.035.

Gao, Xiao Lei, Min Zheng, Hao Fan Wang, Lu Ling Dai, Xiang Hua Yu, Xiao Yang, Xin Pang, Li Li, Mei Zhang, Sha Sha Wang, Jing Biao Wu, Ya Jie Tang, Xin Hua Liang, and Ya Ling Tang. 2019. “NR2F1 Contributes to Cancer Cell Dormancy, Invasion and Metastasis of Salivary Adenoid Cystic Carcinoma by Activating CXCL12/CXCR4 Pathway.” *BMC Cancer*. doi: 10.1186/s12885-019-5925-5.

Ghajar, Cyrus M., Héctor Peinado, Hidetoshi Mori, Irina R. Matei, Kimberley J.

Evason, Hélène Brazier, Dena Almeida, Antonius Koller, Katherine A. Hajjar, Didier Y. R. Stainier, Emily I. Chen, David Lyden, and Mina J. Bissell. 2013. “The Perivascular Niche Regulates Breast Tumour Dormancy.” *Nature Cell Biology*. doi: 10.1038/ncb2767.

Giuriato, Sylvie, Sandra Ryeom, Alice C. Fan, Pavan Bachireddy, Ryan C. Lynch, Matthew J. Rioth, Jan Van Riggelen, Andrew M. Kopelman, Emmanuelle Passegué, Flora Tang, Judah Folkman, and Dean W. Felsher. 2006. “Sustained Regression of Tumors upon MYC Inactivation Requires P53 or Thrombospondin-1 to Reverse the Angiogenic Switch.” *Proceedings of the National Academy of Sciences of the United States of America*. doi: 10.1073/pnas.0608017103.

Gozuacik, Devrim, Yunus Akkoc, Deniz Gulfem Ozturk, and Muhammed Kocak. 2017. “Autophagy-Regulating MicroRNAs and Cancer.” *Frontiers in Oncology*. doi: 10.3389/fonc.2017.00065.

Gozuacik, Devrim, and Adi Kimchi. 2004. “Autophagy as a Cell Death and Tumor Suppressor Mechanism.” *Oncogene*.

Graves, Paul, and Yan Zeng. 2012. “Biogenesis of Mammalian MicroRNAs: A Global View.” *Genomics, Proteomics and Bioinformatics*.

Gupta, Anu, Srirupa Roy, Alexander J. F. Lazar, Wei Lien Wang, John C. McAuliffe, David Reynoso, James McMahon, Takahiro Taguchi, Giuseppe Floris, Maria Debiec-Rychter, Patrick Schoffski, Jonathan A. Trent, Jayanta Debnath, and Brian P. Rubin. 2010. “Autophagy Inhibition and Antimalarials Promote Cell Death in Gastrointestinal Stromal Tumor (GIST).” *Proceedings of the National Academy of Sciences of the United States of America*. doi: 10.1073/pnas.1000248107.

Hadfield, Geoffrey. 1954. “The Dormant Cancer Cell.” *British Medical Journal*. doi: 10.1136/bmj.2.4888.607.

Hager, Jean C., Gloria H. Heppner, Wayne Stanley, Anne M. Richardson, and Suzanne Fligiel. 1981. “Characterization of a Variant-Producing Tumor Cell Line from a Heterogeneous Strain BALB/CfC3H Mouse Mammary Tumor.” *Cancer Research*.

Hall, Carolyn, Savitri Krishnamurthy, Ashutosh Lodhi, Anirban Bhattacharyya, Amber Anderson, Henry Kuerer, Isabelle Bedrosian, Balraj Singh, and Anthony Lucci. 2012. “Disseminated Tumor Cells Predict Survival after Neoadjuvant Therapy in Primary Breast Cancer.” *Cancer*. doi: 10.1002/cncr.26202.

Hanahan, D., and R. A. Weinberg. 2011. “Hallmarks of Cancer: The Next Generation -

PIIS0092867411001279.Pdf." *Cell*.

Hanahan, Douglas. 2022. "Hallmarks of Cancer: New Dimensions." *Cancer Discovery*.

Hanahan, Douglas, and Robert A. Weinberg. 2000. "The Hallmarks of Cancer." *Cell*.

Harper, Kathryn L., Maria Soledad Sosa, David Entenberg, Hedayatollah Hosseini, Julie F. Cheung, Rita Nobre, Alvaro Avivar-Valderas, Chandandaneep Nagi, Nomeda Girnius, Roger J. Davis, Eduardo F. Farias, John Condeelis, Christoph A. Klein, and Julio A. Aguirre-Ghiso. 2016. "Mechanism of Early Dissemination and Metastasis in Her2+ Mammary Cancer." *Nature*. doi: 10.1038/nature20609.

He, Bei Ping, Jian Jun Wang, Xian Zhang, Yan Wu, Miao Wang, Boon Huat Bay, and Alex Yuang Chi Chang. 2006. "Differential Reactions of Microglia to Brain Metastasis of Lung Cancer." *Molecular Medicine*. doi: 10.2119/2006-00033.He.

Hess, Kenneth R., Gauri R. Varadhachary, Sarah H. Taylor, Wei Wei, Martin N. Raber, Renato Lenzi, and James L. Abbruzzese. 2006. "Metastatic Patterns in Adenocarcinoma." *Cancer*. doi: 10.1002/cncr.21778.

Holmgren, Lars, Michael S. O'reilly, and Judah Folkman. 1995. "Dormancy of Micrometastases: Balanced Proliferation and Apoptosis in the Presence of Angiogenesis Suppression." *Nature Medicine*. doi: 10.1038/nm0295-149.

Holtzhausen, Alisha, Christelle Golzio, Tam How, Yong Hun Lee, William P. Schiemann, Nicholas Katsanis, and Gerard C. Blobe. 2014. "Novel Bone Morphogenetic Protein Signaling through Smad2 and Smad3 to Regulate Cancer Progression and Development." *FASEB Journal*. doi: 10.1096/fj.13-239178.

Hui, Xu, Hisham Al-Ward, Fahmi Shaher, Chun Yang Liu, and Ning Liu. 2020. "The Role of MiR-210 in the Biological System: A Current Overview." *Human Heredity*.

Hüsemann, Yves, Jochen B. Geigl, Falk Schubert, Piero Musiani, Manfred Meyer, Elke Burghart, Guido Forni, Roland Eils, Tanja Fehm, Gert Riethmüller, and Christoph A. Klein. 2008. "Systemic Spread Is an Early Step in Breast Cancer." *Cancer Cell*. doi: 10.1016/j.ccr.2007.12.003.

Ichimura, Yoshinobu, Takayoshi Kirisako, Toshifumi Takao, Yoshinori Satomi, Yasutsugu Shimonishi, Naotada Ishihara, Noboru Mizushima, Isei Tanida, Eiki Kominami, Mariko Ohsumi, Takeshi Noda, and Yoshinori Ohsumi. 2000. "A Ubiquitin-like System Mediates Protein Lipidation." *Nature*. doi: 10.1038/35044114.

Indraccolo, Stefano, Laura Stievano, Sonia Minuzzo, Valeria Tosello, Giovanni Esposito, Erich Piovan, Rita Zamarchi, Luigi Chieco-Bianchi, and Alberto Amadori. 2006. “Interruption of Tumor Dormancy by a Transient Angiogenic Burst within the Tumor Microenvironment.” *Proceedings of the National Academy of Sciences of the United States of America*. doi: 10.1073/pnas.0506200103.

Janni, Wolfgang, Florian D. Vogl, Gro Wiedswang, Marit Synnestvedt, Tanja Fehm, Julia Jückstock, Elin Borgen, Brigitte Rack, Stephan Braun, Harald Sommer, Erich Solomayer, Klaus Pantel, Jahn Nesland, Klaus Friese, and Bjørn Naume. 2011. “Persistence of Disseminated Tumor Cells in the Bone Marrow of Breast Cancer Patients Predicts Increased Risk for Relapse - A European Pooled Analysis.” *Clinical Cancer Research*. doi: 10.1158/1078-0432.CCR-10-2515.

Jemal, Ahmedin, Melissa M. Center, Carol DeSantis, and Elizabeth M. Ward. 2010. “Global Patterns of Cancer Incidence and Mortality Rates and Trends.” *Cancer Epidemiology Biomarkers and Prevention*.

Kabeya, Yukiko, Noboru Mizushima, Akitsugu Yamamoto, Satsuki Oshitani-Okamoto, Yoshinori Ohsumi, and Tamotsu Yoshimori. 2004. “LC3, GABARAP and GATE16 Localize to Autophagosomal Membrane Depending on Form-II Formation.” *Journal of Cell Science*. doi: 10.1242/jcs.01131.

Karrison, Theodore G., Donald J. Ferguson, and Paul Meier. 1999. “Dormancy of Mammary Carcinoma after Mastectomy.” *Journal of the National Cancer Institute*. doi: 10.1093/jnci/91.1.80.

Khaled, Annette R., Dmitry V. Bulavin, Christina Kittipatarin, Wen Qing Li, Michelle Alvarez, Kyungjae Kim, Howard A. Young, Albert J. Fornace, and Scott K. Durum. 2005. “Cytokine-Driven Cell Cycling Is Mediated through Cdc25A.” *Journal of Cell Biology*. doi: 10.1083/jcb.200409099.

Kienast, Yvonne, Louisa Von Baumgarten, Martin Fuhrmann, Wolfgang E. F. Klinkert, Roland Goldbrunner, Jochen Herms, and Frank Winkler. 2010. “Real-Time Imaging Reveals the Single Steps of Brain Metastasis Formation.” *Nature Medicine*. doi: 10.1038/nm.2072.

Kim, Ryung S., Alvaro Avivar-Valderas, Yeriel Estrada, Paloma Bragado, Maria Soledad Sosa, Julio A. Aguirre-Ghiso, and Jeffrey E. Segall. 2012. “Dormancy Signatures and Metastasis in Estrogen Receptor Positive and Negative Breast Cancer.” *PLoS ONE*. doi: 10.1371/journal.pone.0035569.

Klionsky, Daniel J. 2007. “Autophagy: From Phenomenology to Molecular Understanding in Less than a Decade.” *Nature Reviews Molecular Cell Biology*.

Kobayashi, Hirotoshi, Hidetaka Mochizuki, Kenichi Sugihara, Takayuki Morita, Kenjiro Kotake, Tatsuo Teramoto, Shingo Kameoka, Yukio Saito, Keiichi Takahashi, Kazuo Hase, Masatoshi Oya, Koutarou Maeda, Takashi Hirai, Masao Kameyama, Kazuo Shirouzu, and Tetsuichiro Muto. 2007. “Characteristics of Recurrence and Surveillance Tools after Curative Resection for Colorectal Cancer: A Multicenter Study.” *Surgery*. doi: 10.1016/j.surg.2006.07.020.

Koebel, Catherine M., William Vermi, Jeremy B. Swann, Nadeen Zerafa, Scott J. Rodig, Lloyd J. Old, Mark J. Smyth, and Robert D. Schreiber. 2007. “Adaptive Immunity Maintains Occult Cancer in an Equilibrium State.” *Nature*. doi: 10.1038/nature06309.

Korpal, Manav, Esther S. Lee, Guohong Hu, and Yibin Kang. 2008. “The MiR-200 Family Inhibits Epithelial-Mesenchymal Transition and Cancer Cell Migration by Direct Targeting of E-Cadherin Transcriptional Repressors ZEB1 and ZEB2.” *Journal of Biological Chemistry*. doi: 10.1074/jbc.C800074200.

Kundu, M., and C. B. Thompson. 2005. “Macroautophagy versus Mitochondrial Autophagy: A Question of Fate?” *Cell Death and Differentiation*. doi: 10.1038/sj.cdd.4401780.

Lambert, Arthur W., Diwakar R. Pattabiraman, and Robert A. Weinberg. 2017. “Emerging Biological Principles of Metastasis.” *Cell*.

Lazova, Rossitza, Robert L. Camp, Vincent Klump, Summar F. Siddiqui, Ravi K. Amaravadi, and John M. Pawelek. 2012. “Punctate LC3B Expression Is a Common Feature of Solid Tumors and Associated with Proliferation, Metastasis, and Poor Outcome.” *Clinical Cancer Research*. doi: 10.1158/1078-0432.CCR-11-1282.

Leclercq, Mickael, Abdoulaye Baniré Diallo, and Mathieu Blanchette. 2017. “Prediction of Human MiRNA Target Genes Using Computationally Reconstructed Ancestral Mammalian Sequences.” *Nucleic Acids Research*. doi: 10.1093/nar/gkw1085.

Lee, Han Na, Mi Suk Jeong, and Se Bok Jang. 2021. “Molecular Characteristics of Amyloid Precursor Protein (App) and Its Effects in Cancer.” *International Journal of Molecular Sciences*.

Di Leva, Gianpiero, and Carlo M. Croce. 2013. “MiRNA Profiling of Cancer.” *Current Opinion in Genetics and Development*.

Lewis, Benjamin P., Christopher B. Burge, and David P. Bartel. 2005. “Conserved Seed Pairing, Often Flanked by Adenosines, Indicates That Thousands of Human Genes Are MicroRNA Targets.” *Cell*.

Lin, Shuibin, and Richard I. Gregory. 2015. “MicroRNA Biogenesis Pathways in Cancer.” *Nature Reviews Cancer*.

Litchfield, Lacey M., Krista A. Riggs, Alyson M. Hockenberry, Laura D. Oliver, Katelyn G. Barnhart, Jian Cai, William M. Pierce, Margarita M. Ivanova, Paula J. Bates, Savitri N. Appana, Susmita Datta, Piotr Kulesza, Jean McBryan, Leonie S. Young, and Carolyn M. Klinge. 2012. “Identification and Characterization of Nucleolin as a COUP-TFII Coactivator of Retinoic Acid Receptor β Transcription in Breast Cancer Cells.” *PLoS ONE*. doi: 10.1371/journal.pone.0038278.

Litovchick, Larisa, Laurence A. Florens, Selene K. Swanson, Michael P. Washburn, and James A. Decaprio. 2011. “DYRK1A Protein Kinase Promotes Quiescence and Senescence through DREAM Complex Assembly.” *Genes and Development*. doi: 10.1101/gad.2034211.

Lu, Zhen, Robert Z. Luo, Yiling Lu, Xuhui Zhang, Qinghua Yu, Shilpi Khare, Seiji Kondo, Yasuko Kondo, Yinhua Yu, Gordon B. Mills, Warren S. L. Liao, and Robert C. Bast. 2008. “The Tumor Suppressor Gene ARHI Regulates Autophagy and Tumor Dormancy in Human Ovarian Cancer Cells.” *Journal of Clinical Investigation*. doi: 10.1172/JCI35512.

Luo, Dan, Zheng Zhang, Zhao Zhang, Jia Yue Li, Jian Cui, Wen Pu Shi, Xi Wen Dong, Lin Yuan, Peng Lin, Zhi Nan Chen, Hui Jie Bian, and Zi Ling Wang. 2018. “Aberrant Expression of Mir-362 Promotes Lung Cancer Metastasis through Downregulation of SEMA3A.” *Journal of Immunology Research*. doi: 10.1155/2018/1687097.

Luo, Meng, Jin Fan Li, Qi Yang, Kun Zhang, Zhan Wei Wang, Shu Zheng, and Jiao Jiao Zhou. 2020. “Stem Cell Quiescence and Its Clinical Relevance.” *World Journal of Stem Cells*. doi: 10.4252/wjsc.v12.i11.1307.

Lwin, Tint, Lori A. Hazlehurst, Sophie Dessureault, Raymond Lai, Wenlong Bai, Eduardo Sotomayor, Lynn C. Moscinski, William S. Dalton, and Jianguo Tao. 2007. “Cell Adhesion Induces P27Kip1-Associated Cell-Cycle Arrest through

down-Regulation of the SCFSkp2 Ubiquitin Ligase Pathway in Mantle-Cell and Other Non-Hodgkin B-Cell Lymphomas." *Blood*. doi: 10.1182/blood-2006-11-060350.

MacKie, Rona M., Robin Reid, and Brian Junor. 2003. "Fatal Melanoma Transferred in a Donated Kidney 16 Years after Melanoma Surgery." *New England Journal of Medicine*. doi: 10.1056/nejm200302063480620.

Maeda, Ryo, Junji Yoshida, Tomoyuki Hishida, Keiju Aokage, Mitsuyo Nishimura, Yutaka Nishiwaki, and Kanji Nagai. 2010. "Late Recurrence of Non-Small Cell Lung Cancer More than 5 Years after Complete Resection: Incidence and Clinical Implications in Patient Follow-Up." *Chest*. doi: 10.1378/chest.09-2361.

Magbanua, Mark Jesus M., Eduardo V. Sosa, Ritu Roy, Lauren E. Eisenbud, Janet H. Scott, Adam Olshen, Dan Pinkel, Hope S. Rugo, and John W. Park. 2013. "Genomic Profiling of Isolated Circulating Tumor Cells from Metastatic Breast Cancer Patients." *Cancer Research*. doi: 10.1158/0008-5472.CAN-11-3017.

Malladi, Srinivas, Danilo G. MacAlinao, Xin Jin, Lan He, Harihar Basnet, Yilong Zou, Elisa De Stanchina, and Joan Massagué. 2016. "Metastatic Latency and Immune Evasion through Autocrine Inhibition of WNT." *Cell*. doi: 10.1016/j.cell.2016.02.025.

Marlow, Rebecca, Gabriella Honeth, Sara Lombardi, Massimiliano Cariati, Sonya Hessey, Aikaterini Pipili, Veronica Mariotti, Bharath Buchupalli, Katie Foster, Dominique Bonnet, Agamemnon Grigoriadis, Pranela Rameshwar, Anand Purushotham, Andrew Tutt, and Gabriela Dontu. 2013. "A Novel Model of Dormancy for Bone Metastatic Breast Cancer Cells." *Cancer Research*. doi: 10.1158/0008-5472.CAN-13-0991.

Matsuzawa, Akio, Yasutaka Takeda, Mutsumi Narita, and Hideki Ozawa. 1991. "Survival of Leukemic Cells in a Dormant State Following Cyclophosphamide-induced Cure of Strongly Immunogenic Mouse Leukemia (DL811)." *International Journal of Cancer*. doi: 10.1002/ijc.2910490227.

Mauri, Marta, Marieluise Kirchner, Reuven Aharoni, Camilla Ciolli Mattioli, David Van Den Bruck, Nadya Gutkovitch, Vengamanaidu Modepalli, Matthias Selbach, Yehu Moran, and Marina Chekulaeva. 2017. "Conservation of MiRNA-Mediated Silencing Mechanisms across 600 Million Years of Animal Evolution." *Nucleic Acids Research*. doi: 10.1093/nar/gkw792.

McGrath, Julie, Louis Panzica, Ryan Ransom, Henry G. Withers, and Irwin H. Gelman. 2019. “Identification of Genes Regulating Breast Cancer Dormancy in 3D Bone Endosteal Niche Cultures.” *Molecular Cancer Research*. doi: 10.1158/1541-7786.MCR-18-0956.

Medina, Ricardo, Sayyed K. Zaidi, Chang Gong Liu, Janet L. Stein, Andre J. VanWijnen, Carlo M. Croce, and Gary S. Stein. 2008. “MicroRNAs 221 and 222 Bypass Quiescence and Compromise Cell Survival.” *Cancer Research*. doi: 10.1158/0008-5472.CAN-07-6754.

Miga, Karen H., Yulia Newton, Miten Jain, Nicolas Altemose, Huntington F. Willard, and E. James Kent. 2014. “Centromere Reference Models for Human Chromosomes X and y Satellite Arrays.” *Genome Research*. doi: 10.1101/gr.159624.113.

Mizushima, Noboru. 2007. “Autophagy: Process and Function.” *Genes and Development*.

Mizushima, Noboru, and Daniel J. Klionsky. 2007. “Protein Turnover via Autophagy: Implications for Metabolism.” *Annual Review of Nutrition*.

Mizushima, Noboru, and Masaaki Komatsu. 2011. “Autophagy: Renovation of Cells and Tissues.” *Cell*.

Mizushima, Noboru, Takeshi Noda, and Yoshinori Ohsumi. 1999. “Apg16p Is Required for the Function of the Apg12p-Apg5p Conjugate in the Yeast Autophagy Pathway.” *EMBO Journal*. doi: 10.1093/emboj/18.14.3888.

Mortensen, Monika, Elizabeth J. Soilleux, Gordana Djordjevic, Rebecca Tripp, Michael Lutteropp, Elham Sadighi-Akha, Amanda J. Stranks, Julie Glanville, Samantha Knight, Sten Eirik W. Jacobsen, Kamil R. Kranc, and Anna Katharina Simon. 2011. “The Autophagy Protein Atg7 Is Essential for Hematopoietic Stem Cell Maintenance.” *Journal of Experimental Medicine*. doi: 10.1084/jem.20101145.

Moses, Blake S., Rebecca Evans, William L. Slone, Debbie Piktel, Ivan Martinez, Michael D. Craig, and Laura F. Gibson. 2016. “Bone Marrow Microenvironment Niche Regulates MiR-221/222 in Acute Lymphoblastic Leukemia.” *Molecular Cancer Research*. doi: 10.1158/1541-7786.MCR-15-0474.

Mowers, E. E., M. N. Sharifi, and K. F. Macleod. 2017. “Autophagy in Cancer Metastasis.” *Oncogene*.

Müller, Volkmar, Nicole Stahmann, Sabine Riethdorf, Thomas Rau, Tanja Zabel,

Alexander Goetz, Fritz Jänicke, and Klaus Pantel. 2005. “Circulating Tumor Cells in Breast Cancer: Correlation to Bone Marrow Micrometastases, Heterogeneous Response to Systemic Therapy and Low Proliferative Activity.” *Clinical Cancer Research*. doi: 10.1158/1078-0432.CCR-04-2469.

N., Almog, Briggs C., Beheshti A., Ma L., Wilkie K.P., Rietman E., and Hlatky L. 2013. “Transcriptional Changes Induced by the Tumor Dormancy-Associated MicroRNA-190.” *Transcription*.

Naumov, George N., Lars A. Akslen, and Judah Folkman. 2006. “Role of Angiogenesis in Human Tumor Dormancy: Animal Models of the Angiogenic Switch.” *Cell Cycle*.

Naumov, George N., Elise Bender, David Zurakowski, Soo Young Kang, David Sampson, Evelyn Flynn, Randolph S. Watnick, Oddbjorn Straume, Lars A. Akslen, Judah Folkman, and Nava Almog. 2006. “A Model of Human Tumor Dormancy: An Angiogenic Switch from the Nonangiogenic Phenotype.” *Journal of the National Cancer Institute*. doi: 10.1093/jnci/djj068.

Naumov, George N., Judah Folkman, and Oddbjorn Straume. 2009. “Tumor Dormancy Due to Failure of Angiogenesis: Role of the Microenvironment.” *Clinical and Experimental Metastasis*. doi: 10.1007/s10585-008-9176-0.

Naumov, George N., Ian C. MacDonald, Pascal M. Weinmeister, Nancy Kerkvliet, Kishore V. Nadkarni, Sylvia M. Wilson, Vincent L. Morris, Alan C. Groom, and Ann F. Chambers. 2002. “Persistence of Solitary Mammary Carcinoma Cells in a Secondary Site: A Possible Contributor to Dormancy.” *Cancer Research*.

Ng, Marie, Michael K. Freeman, Thomas D. Fleming, Margaret Robinson, Laura Dwyer-Lindgren, Blake Thomson, Alexandra Wollum, Ella Sanman, Sarah Wulf, Alan D. Lopez, Christopher J. L. Murray, and Emmanuela Gakidou. 2014. “Smoking Prevalence and Cigarette Consumption in 187 Countries, 1980-2012.” *JAMA - Journal of the American Medical Association*. doi: 10.1001/jama.2013.284692.

Nieto, M. Angela. 2002. “The Snail Superfamily of Zinc-Finger Transcription Factors.” *Nature Reviews Molecular Cell Biology*.

Nishikawa, Shimpei, Dyah Laksmi Dewi, Hideshi Ishii, Masamitsu Konno, Naotsugu Haraguchi, Yoshihiro Kano, Takahito Fukusumi, Katsuya Ohta, Yuko Noguchi, Miyuki Ozaki, Daisuke Sakai, Taroh Satoh, Yuichiro Doki, and Masaki Mori.

2012. “Transcriptomic Study of Dormant Gastrointestinal Cancer Stem Cells.” *International Journal of Oncology*. doi: 10.3892/ijo.2012.1531.

O’Reilly, Michael S., Lars Holmgren, Catherine Chen, and Judah Folkman. 1996. “Angiostatin Induces and Sustains Dormancy of Human Primary Tumors in Mice.” *Nature Medicine*. doi: 10.1038/nm0696-689.

Oikawa, Akihiro, Hideto Takahashi, Hiroichi Ishikawa, Koichi Kurishima, Katsunori Kagohashi, and Hiroaki Satoh. 2012. “Application of Conditional Probability Analysis to Distant Metastases from Lung Cancer.” *Oncology Letters*. doi: 10.3892/ol.2011.535.

Ornelas, Argentina, Christopher R. McCullough, Zhen Lu, Niki M. Zacharias, Lindsay E. Kelderhouse, Joshua Gray, Hailing Yang, Brian J. Engel, Yan Wang, Weiqun Mao, Margie N. Sutton, Pratip K. Bhattacharya, Robert C. Bast, and Steven W. Millward. 2016. “Induction of Autophagy by ARHI (DIRAS3) Alters Fundamental Metabolic Pathways in Ovarian Cancer Models.” *BMC Cancer*. doi: 10.1186/s12885-016-2850-8.

Paik, Paul K., Ronglai Shen, Helen Won, Natasha Rekhtman, Lu Wang, Camelia S. Sima, Arshi Arora, Venkatraman Seshan, Marc Ladanyi, Michael F. Berger, and Mark G. Kris. 2016. “Next-Generation Sequencing of Stage IV Squamous Cell Lung Cancers Reveals an Association of PI3K Aberrations and Evidence of Clonal Heterogeneity in Patients with Brain Metastases.” *Cancer Discovery*. doi: 10.1158/2159-8290.CD-14-1129.

Pankiv, Serhiy, Terje Høyvarde Clausen, Trond Lamark, Andreas Brech, Jack Ansgar Bruun, Heidi Outzen, Aud Øvervatn, Geir Bjørkøy, and Terje Johansen. 2007. “P62/SQSTM1 Binds Directly to Atg8/LC3 to Facilitate Degradation of Ubiquitinated Protein Aggregates by Autophagy*[S].” *Journal of Biological Chemistry*. doi: 10.1074/jbc.M702824200.

Pantel, Klaus, Ruud H. Brakenhoff, and Burkhard Brandt. 2008. “Detection, Clinical Relevance and Specific Biological Properties of Disseminating Tumour Cells.” *Nature Reviews Cancer*.

Papadaki, Chara, Giannis Stoupis, Leuteris Tsalikis, Alexia Monastirioti, Maria Papadaki, Neofytos Maliotis, Michalis Stratigos, Georgios Mastrostamatis, Dimitrios Mavroudis, and Sofia Agelaki. 2019. “Circulating MiRNAs as a Marker of Metastatic Disease and Prognostic Factor in Metastatic Breast Cancer.”

Oncotarget. doi: 10.18632/oncotarget.26629.

Parker, Amelia L., and Thomas R. Cox. 2020. "The Role of the ECM in Lung Cancer Dormancy and Outgrowth." *Frontiers in Oncology*.

Peart, Teresa, Yudith Ramos Valdes, Rohann J. M. Correa, Elena Fazio, Monique Bertrand, Jacob McGee, Michel Préfontaine, Akira Sugimoto, Gabriel E. DiMattia, and Trevor G. Shepherd. 2015. "Intact LKB1 Activity Is Required for Survival of Dormant Ovarian Cancer Spheroids." *Oncotarget*. doi: 10.18632/oncotarget.4211.

Pixberg, C. F., K. Raba, F. Müller, B. Behrens, E. Honisch, D. Niederacher, H. Neubauer, T. Fehm, W. Goering, W. A. Schulz, P. Flohr, G. Boysen, M. Lambros, J. S. De Bono, W. T. Knoefel, C. Sproll, N. H. Stoecklein, and R. P. L. Neves. 2017. "Analysis of DNA Methylation in Single Circulating Tumor Cells." *Oncogene*. doi: 10.1038/onc.2016.480.

Ramamoorthi, Ganesan, Krithika Kodumudi, Corey Gallen, Nadia Nocera Zachariah, Amrita Basu, Gabriella Albert, Amber Beyer, Colin Snyder, Doris Wiener, Ricardo L. B. Costa, and Brian J. Czerniecki. 2022. "Disseminated Cancer Cells in Breast Cancer: Mechanism of Dissemination and Dormancy and Emerging Insights on Therapeutic Opportunities." *Seminars in Cancer Biology*.

Ren, Dong, Yuhu Dai, Qing Yang, Xin Zhang, Wei Guo, Liping Ye, Shuai Huang, Xu Chen, Yingrong Lai, Hong Du, Chuyong Lin, Xinsheng Peng, and Libing Song. 2019. "Wnt5a Induces and Maintains Prostate Cancer Cells Dormancy in Bone." *Journal of Experimental Medicine*. doi: 10.1084/jem.20180661.

Riihimäki, M., A. Hemminki, M. Fallah, H. Thomsen, K. Sundquist, J. Sundquist, and K. Hemminki. 2014. "Metastatic Sites and Survival in Lung Cancer." *Lung Cancer*. doi: 10.1016/j.lungcan.2014.07.020.

Risson, Emma, Ana Rita Nobre, Veronique Maguer-Satta, and Julio A. Aguirre-Ghiso. 2020. "The Current Paradigm and Challenges Ahead for the Dormancy of Disseminated Tumor Cells." *Nature Cancer* 1(7):672–80. doi: 10.1038/s43018-020-0088-5.

Sadasivam, Subhashini, and James A. DeCaprio. 2013. "The DREAM Complex: Master Coordinator of Cell Cycle-Dependent Gene Expression." *Nature Reviews Cancer*.

Saftig, Paul, Wouter Beertsen, and Eeva Liisa Eskelinen. 2008. "LAMP-2: A Control Step Fot Phagosome and Autophagosome Maturation." *Autophagy*. doi: 10.4161/auto.5724.

Santa, Francesca De, Ilaria Iosue, Alberto Del Rio, and Francesco Fazi. 2012. "MicroRNA Biogenesis Pathway as a Therapeutic Target for Human Disease and Cancer." *Current Pharmaceutical Design*. doi: 10.2174/13816128130413.

Schardt, Julian A., Manfred Meyer, Claudia H. Hartmann, Falk Schubert, Oleg Schmidt-Kittler, Christine Fuhrmann, Bernhard Polzer, Marco Petronio, Roland Eils, and Christoph A. Klein. 2005. "Genomic Analysis of Single Cytokeratin-Positive Cells from Bone Marrow Reveals Early Mutational Events in Breast Cancer." *Cancer Cell*. doi: 10.1016/j.ccr.2005.08.003.

Schmit, Fabienne, Michael Korenjak, Mirijam Mannefeld, Kathrin Schmitt, Claudia Franke, Björn Von Eyss, Sladjana Gagrica, Frank Hänel, Alexander Brehm, and Stefan Gaubatz. 2007. "LINC, a Human Complex That Is Related to PRB-Containing Complexes in Invertebrates Regulates the Expression of G2/M Genes." *Cell Cycle*. doi: 10.4161/cc.6.15.4512.

Semenza, Gregg L. 2003. "Targeting HIF-1 for Cancer Therapy." *Nature Reviews Cancer*.

Sharma, Sambad, Xinhong Pei, Fei Xing, Shih Ying Wu, Kerui Wu, Abhishek Tyagi, Dan Zhao, Ravindra Deshpande, Marco Gabriel Ruiz, Ravi Singh, Feng Lyu, and Kounosuke Watabe. 2021. "Regucalcin Promotes Dormancy of Prostate Cancer." *Oncogene*. doi: 10.1038/s41388-020-01565-9.

Sharma, Sambad, Fei Xing, Yin Liu, Kerui Wu, Neveen Said, Radhika Pochampally, Yusuke Shiozawa, Hui Kuan Lin, K. C. Balaji, and Kounosuke Watabe. 2016. "Secreted Protein Acidic and Rich in Cysteine (Sparc) Mediates Metastatic Dormancy of Prostate Cancer in Bone." *Journal of Biological Chemistry*. doi: 10.1074/jbc.M116.737379.

Shi, H. Z., D. N. Wang, L. N. Ma, and H. Zhu. 2020. "MicroRNA-362 Inhibits Cell Growth and Metastasis in Glioblastoma by Targeting MAPK1." *European Review for Medical and Pharmacological Sciences*. doi: 10.26355/eurrev_202009_22834.

Shiao, Stephen L., A. Preethi Ganesan, Hope S. Rugo, and Lisa M. Coussens. 2011. "Immune Microenvironments in Solid Tumors: New Targets for Therapy." *Genes and Development*. doi: 10.1101/gad.169029.111.

Shibue, Tsukasa, and Robert A. Weinberg. 2009. "Integrin B1-Focal Adhesion Kinase Signaling Directs the Proliferation of Metastatic Cancer Cells Disseminated in the Lungs." *Proceedings of the National Academy of Sciences of the United States of*

America. doi: 10.1073/pnas.0904227106.

Shih, David J. H., Naema Nayyar, Ivanna Bihun, Ibiayi Dagogo-Jack, Corey M. Gill, Elisa Aquilanti, Mia Bertalan, Alexander Kaplan, Megan R. D'Andrea, Ugonma Chukwueke, Franziska Maria Ippen, Christopher Alvarez-Breckenridge, Nicholas D. Camarda, Matthew Lastrapes, Devin McCabe, Ben Kuter, Benjamin Kaufman, Matthew R. Strickland, Juan Carlos Martinez-Gutierrez, Deepika Nagabhushan, Magali De Sauvage, Michael D. White, Brandyn A. Castro, Kaitlin Hoang, Andrew Kaneb, Emily D. Batchelor, Sun Ha Paek, Sun Hye Park, Maria Martinez-Lage, Anna S. Berghoff, Parker Merrill, Elizabeth R. Gerstner, Tracy T. Batchelor, Matthew P. Frosch, Ryan P. Frazier, Darrell R. Borger, A. John Iafrate, Bruce E. Johnson, Sandro Santagata, Matthias Preusser, Daniel P. Cahill, Scott L. Carter, and Priscilla K. Brastianos. 2020. "Genomic Characterization of Human Brain Metastases Identifies Drivers of Metastatic Lung Adenocarcinoma." *Nature Genetics*. doi: 10.1038/s41588-020-0592-7.

Shiozawa, Yusuke, Elisabeth A. Pedersen, Lalit R. Patel, Anne M. Ziegler, Aaron M. Havens, Younghun Jung, Jingcheng Wang, Stephanie Zalucha, Robert D. Loberg, Kenneth J. Pienta, and Russell S. Taichman. 2010. "GAS6/AXL Axis Regulates Prostate Cancer Invasion, Proliferation, and Survival in the Bone Marrow Niche." *Neoplasia*. doi: 10.1593/neo.91384.

Siegel, Rebecca L., Kimberly D. Miller, and Ahmedin Jemal. 2020. "Cancer Statistics, 2020." *CA: A Cancer Journal for Clinicians*. doi: 10.3322/caac.21590.

Simonsen, Anne, and Sharon A. Tooze. 2009. "Coordination of Membrane Events during Autophagy by Multiple Class III PI3-Kinase Complexes." *Journal of Cell Biology*.

Solakoglu, Oender, Christine Maierhofer, Georgia Lahr, Elisabeth Breit, Peter Scheunemann, Isabella Heumos, Uwe Pichlmeier, Günter Schlimok, Ralph Oberneder, Manfred W. Köllermann, Jens Köllermann, Michael R. Speicher, and Klaus Pantel. 2002. "Heterogeneous Proliferative Potential of Occult Metastatic Cells in Bone Marrow of Patients with Solid Epithelial Tumors." *Proceedings of the National Academy of Sciences of the United States of America*. doi: 10.1073/pnas.042372199.

Sosa, María Soledad, Paloma Bragado, and Julio A. Aguirre-Ghiso. 2014. "Mechanisms of Disseminated Cancer Cell Dormancy: An Awakening Field." *Nature Reviews*

Cancer.

Sosa, Maria Soledad, Falguni Parikh, Alexandre Gaspar Maia, Yeriel Estrada, Almudena Bosch, Paloma Bragado, Esther Ekpin, Ajish George, Yang Zheng, Hung Ming Lam, Colm Morrissey, Chi Yeh Chung, Eduardo F. Farias, Emily Bernstein, and Julio A. Aguirre-Ghiso. 2015. "NR2F1 Controls Tumour Cell Dormancy via SOX9- and RARβ-Driven Quiescence Programmes." *Nature Communications*. doi: 10.1038/ncomms7170.

Spiliotaki, Maria, Dimitris Mavroudis, Kyriaki Kapranou, Harris Markomanolaki, Galatea Kallergi, Filippos Koinis, Kostas Kalbakis, Vassilis Georgoulias, and Sofia Agelaki. 2014. "Evaluation of Proliferation and Apoptosis Markers in Circulating Tumor Cells of Women with Early Breast Cancer Who Are Candidates for Tumor Dormancy." *Breast Cancer Research*. doi: 10.1186/s13058-014-0485-8.

Taichman, Russell S., Lalit R. Patel, Rachel Bedenis, Jingcheng Wang, Savannah Weidner, Taibriana Schumann, Kenji Yumoto, Janice E. Berry, Yusuke Shiozawa, and Kenneth J. Pienta. 2013. "GAS6 Receptor Status Is Associated with Dormancy and Bone Metastatic Tumor Formation." *PLoS ONE*. doi: 10.1371/journal.pone.0061873.

Teng, Michele W. L., Jeremy B. Swann, Catherine M. Koebel, Robert D. Schreiber, and Mark J. Smyth. 2008. "Immune-Mediated Dormancy: An Equilibrium with Cancer." *Journal of Leukocyte Biology*. doi: 10.1189/jlb.1107774.

Thai, Alesha A., Benjamin J. Solomon, Lecia V. Sequist, Justin F. Gainor, and Rebecca S. Heist. 2021. "Lung Cancer." *The Lancet*.

Tiram, Galia, Ehud Segal, Adva Krivitsky, Rony Shreberk-Hassidim, Shiran Ferber, Paula Ofek, Taturo Udagawa, Liat Edry, Noam Shomron, Maayan Roniger, Batsheva Kerem, Yuval Shaked, Sarit Aviel-Ronen, Iris Barshack, Marcelo Calderón, Rainer Haag, and Ronit Satchi-Fainaro. 2016. "Identification of Dormancy-Associated MicroRNAs for the Design of Osteosarcoma-Targeted Dendritic Polyglycerol Nanopolyplexes." *ACS Nano*. doi: 10.1021/acsnano.5b06189.

Uhr, Jonathan W., and Klaus Pantel. 2011. "Controversies in Clinical Cancer Dormancy." *Proceedings of the National Academy of Sciences of the United States of America*. doi: 10.1073/pnas.1106613108.

Vera-Ramirez, Laura, Suman K. Vodnala, Ryan Nini, Kent W. Hunter, and Jeffrey E.

Green. 2018. “Autophagy Promotes the Survival of Dormant Breast Cancer Cells and Metastatic Tumour Recurrence.” *Nature Communications*. doi: 10.1038/s41467-018-04070-6.

Vlachos, Ioannis S., Maria D. Paraskevopoulou, Dimitra Karagkouni, Georgios Georgakilas, Thanasis Vergoulis, Ilias Kanellos, Ioannis Laertis Anastasopoulos, Sofia Maniou, Konstantina Karathanou, Despina Kalfakakou, Athanasios Fevgas, Theodore Dalamagas, and Artemis G. Hatzigeorgiou. 2015. “DIANA-TarBase v7.0: Indexing More than Half a Million Experimentally Supported MiRNA:MRNA Interactions.” *Nucleic Acids Research*. doi: 10.1093/nar/gku1215.

Wahid, Fazli, Adeeb Shehzad, Taous Khan, and You Young Kim. 2010. “MicroRNAs: Synthesis, Mechanism, Function, and Recent Clinical Trials.” *Biochimica et Biophysica Acta - Molecular Cell Research*.

Wan, Jin’e, Jian Yang, Cuixia Qiao, Xiaomei Sun, Aiting Di, Lize Zhang, Dandan Wang, and Gang Zhao. 2019. “MicroRNA-362 Inhibits Cell Proliferation and Invasion by Directly Targeting Six1 in Colorectal Cancer.” *Yonsei Medical Journal*. doi: 10.3349/ymj.2019.60.5.414.

Washington, M. N., G. Suh, A. F. Orozco, M. N. Sutton, H. Yang, Y. Wang, W. Mao, S. Millward, A. Ornelas, N. Atkinson, W. Liao, R. C. Bast, and Z. Lu. 2015. “ARHI (DIRAS3)-Mediated Autophagy-Associated Cell Death Enhances Chemosensitivity to Cisplatin in Ovarian Cancer Cell Lines and Xenografts.” *Cell Death and Disease*. doi: 10.1038/cddis.2015.208.

Watson, Katrina L., Robert A. Jones, Anthony Bruce, and Roger A. Moorehead. 2018. “The MiR-200b/200a/429 Cluster Prevents Metastasis and Induces Dormancy in a Murine Claudin-Low Mammary Tumor Cell Line.” *Experimental Cell Research*. doi: 10.1016/j.yexcr.2018.04.024.

Weaver, V. M., O. W. Petersen, F. Wang, C. A. Larabell, P. Briand, C. Damsky, and M. J. Bissell. 1997. “Reversion of the Malignant Phenotype of Human Breast Cells in Three- Dimensional Culture and in Vivo by Integrin Blocking Antibodies.” *Journal of Cell Biology*. doi: 10.1083/jcb.137.1.231.

Weidberg, Hilla, Elena Shvets, and Zvulun Elazar. 2011. “Biogenesis and Cargo Selectivity of Autophagosomes.” *Annual Review of Biochemistry*. doi: 10.1146/annurev-biochem-052709-094552.

Weinhold, Kent J., Lester T. Goldstein, and E. Frederick Wheelock. 1979. “The Tumor

Dormant State: Quantitation of L5178Y Cells and Host Immune Responses during the Establishment and Course of Dormancy in Syngeneic DBA/2 Mice*." *Journal of Experimental Medicine*. doi: 10.1084/jem.149.3.732.

White, Donald E., Natasza A. Kurpios, Dongmei Zuo, John A. Hassell, Sandra Blaess, Ulrich Mueller, and William J. Muller. 2004. "Targeted Disruption of B1-Integrin in a Transgenic Mouse Model of Human Breast Cancer Reveals an Essential Role in Mammary Tumor Induction." *Cancer Cell*. doi: 10.1016/j.ccr.2004.06.025.

Winton, Timothy, Robert Livingston, David Johnson, James Rigas, Michael Johnston, Charles Butts, Yvon Cormier, Glenwood Goss, Richard Inculet, Eric Vallieres, Willard Fry, Drew Bethune, Joseph Ayoub, Keyue Ding, Lesley Seymour, Barbara Graham, Ming-Sound Tsao, David Gandara, Kenneth Kesler, Todd Demmy, and Frances Shepherd. 2005. "Vinorelbine plus Cisplatin vs. Observation in Resected Non–Small-Cell Lung Cancer." *New England Journal of Medicine*. doi: 10.1056/nejmoa043623.

Xie, Zhiping, and Daniel J. Klionsky. 2007. "Autophagosome Formation: Core Machinery and Adaptations." *Nature Cell Biology*.

Yang, Annan, N. V. Rajeshkumar, Xiaoxu Wang, Shinichi Yabuuchi, Brian M. Alexander, Gerald C. Chu, Daniel D. Von Hoff, Anirban Maitra, and Alec C. Kimmelman. 2014. "Autophagy Is Critical for Pancreatic Tumor Growth and Progression in Tumors with P53 Alterations." *Cancer Discovery*. doi: 10.1158/2159-8290.CD-14-0362.

Yeh, Albert C., and Sridhar Ramaswamy. 2015. "Mechanisms of Cancer Cell Dormancy-Another Hallmark of Cancer?" *Cancer Research*.

Yorimitsu, T., and D. J. Klionsky. 2005. "Autophagy: Molecular Machinery for Self-Eating." *Cell Death and Differentiation*.

Yu-Lee, Li Yuan, Guoyu Yu, Yu Chen Lee, Song Chang Lin, Jing Pan, Tianhong Pan, Kai Jie Yu, Bin Liu, Chad J. Creighton, Jaime Rodriguez-Canales, Pamela A. Villalobos, Ignacio I. Wistuba, Eulalia de Nadal, Francesc Posas, Gary E. Gallick, and Sue Hwa Lin. 2018. "Osteoblast-Secreted Factors Mediate Dormancy of Metastatic Prostate Cancer in the Bone via Activation of the TGFbRIII–P38MAPK–PS249/ T252RB Pathway." *Cancer Research*. doi: 10.1158/0008-5472.CAN-17-1051.

Yumoto, Kenji, Matthew R. Eber, Jingcheng Wang, Frank C. Cackowski, Ann M.

Decker, Eunsohl Lee, Ana Rita Nobre, Julio A. Aguirre-Ghiso, Younghun Jung, and Russell S. Taichman. 2016. “Axl Is Required for TGF-B2-Induced Dormancy of Prostate Cancer Cells in the Bone Marrow.” *Scientific Reports*. doi: 10.1038/srep36520.

Zou, Peng, Hiroki Yoshihara, Kentaro Hosokawa, Ikue Tai, Kaori Shinmyozu, Fujiko Tsukahara, Yoshiro Maru, Keiko Nakayama, Keiichi I. Nakayama, and Toshio Suda. 2011. “P57 Kip2 and P27 Kip1 Cooperate to Maintain Hematopoietic Stem Cell Quiescence through Interactions with Hsc70.” *Cell Stem Cell*. doi: 10.1016/j.stem.2011.07.003.